N 70 30992

NASA TECHNICAL TRANSLATION

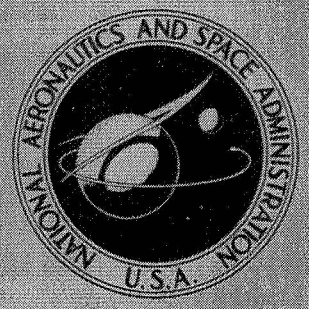

NASA TT F-618

NASA TT F-618

CASE FILE
COPY

STUDIES OF AURORAE AND UPPER ATMOSPHERE BY RADIOPHYSICAL METHODS

by Ye. A. Ponomarev and Ye. F. Vershinin

IGY Series No. 15, "Nauka" Press
Moscow, 1967

NATIONAL AERONAUTICS AND SPACE ADMINISTRATION • WASHINGTON, D. C. • JUNE 1970

NASA TT F-618

STUDIES OF AURORAE AND UPPER ATMOSPHERE BY RADIOPHYSICAL METHODS

By Ye. A. Ponomarev and Ye F. Vershinin

Translation of: "Issledovaniye polyarnykh siyaniy i verkhney atmosfery radiofizicheskimi metodami."
IGY Series No. 15, "Nauka" Press, Moscow, 1967

NATIONAL AERONAUTICS AND SPACE ADMINISTRATION

For sale by the Clearinghouse for Federal Scientific and Technical Information
Springfield, Virginia 22151 – CFSTI price $3.00

ABSTRACT: The work presents the results of a study of sporadic ionization zones associated with aurora and ultralow frequency radio emission in the auroral zone. The work has two parts. Each part begins with a short summary. The first part suggests a physical model of the ray arc of aurorae. Further, on the basis of parameters calculated according to that model the study of conditions of origination of diffusion quasineutral waves in the auroral plasma is carried out. These waves are assumed to cause the diffusion of the ultrashort wave signals. The radar equipment is described which was used to observe radio reflections from the zones of sporadic ionization in 1964-1965 in Yakutsk. Major results of these observations are given. The second part describes the equipment which carried out observations of continuous ultrashort emission in 1962-1965 in the Tiksi Bay region. A classification is given of an ultrashort emission, as well as the description of the connection between each type of emission and other geophysical phenomena. The work also provides an evaluation of the energy flow of the ultralow frequency in several frequency bands and gives suggestions about the nature of isolated sound bursts.

Editor-in-Chief
Doctor of Physical-Mathematical Sciences
G.S. Ivanov-Kholodnyy

PREFACE

Aurorae are possibly the brightest manifestation of solar corpuscular activity. Carried by intrusions of fast electrons into relatively dense layers of the Earth's atmosphere, they are to a certain degree an extreme case of the ionospheric state in which the action of secondary corpuscular agents is especially prominent. Here it is not difficult to separate a small number of basic factors determining the overall pattern of the phenomenon, which in turn allows considering the problems connected with the conditions in aurorae in an arrangement near the conditions of laboratory physics. This circumstance and also the genetic connection with other phenomena of the ionospheric-magnetic complex permit us to explain the growing interest which geophysicists have shown toward the problem of aurorae since the time of Shtermer.

Methodologically the entire problem may be arbitrarily divided into three areas which, at the present time, may still exist rather independently.

(1) The nature of auroral electrons; the mechanism of the transmission of energy from the solar wind to active electrons of the magnetosphere; processes of interaction of various types of electromagnetic emission with fast electrons of the magnetosphere.

(2) Physical conditions in the aurorae; the balance of ionization, energy and matter in the region of the aurorae; investigation of chemical reactions and processes of excitation; radiation of ionospheric current systems in the auroral zone.

(3) Morphology, dynamics and space-time regularities.

This study was completed in the spirit of the second area of study, where the question of the nature of fast electrons or of ionospheric electromotive force does not appear, but the physical characteristics of these agents are assumed to be known from experiments. Thus we considered as a basic problem the establishment of connections between known parameters of the electron stream and emf on the one hand, and several observable characteristics of the auroral ionosphere on the other, as well as the communication of new facts and discussion of methodological and technical questions.

In fact, this problem was solved only within the limits of those extremely modest resources which made a group of radiophysical methods available to the Auroral Laboratory of the Institute of Cosmophysical Studies and Aeronomia of the Yakutsk Branch of the

Siberian Department of the Academy of Sciences USSR [1].

The authors take this opportunity to express their thanks to chief radio technician V.D. Shvetsov, the builder and creater of radar equipment which worked excellently; to Engineer S.P. Val'kov and radio technician Yu.P. Nikitin, who developed a complex of original recording instruments for investigation of ultralow frequency (ULF) measurement; to Engineer M.F. Khoroshev; to laboratory assistant V.I. Shapayev; and to student A.M. Makrygin, who took part in observations and analyzing materials. We are also extremely indebted to the group of scientists at the Tiksi Polar Laboratory, to the colleagues of the polar station at Muosty Island, of the Tiksi Radiometry Center and Optic Observatory of the Arctic and Antarctic Scientific Research Institute for their kind hospitality and constant help in conducting the expeditionary studies.

TABLE OF CONTENTS

I. STUDY OF AURORAL IONIZATION WITH RADAR METHODS

Equipment and Observation Methods

Investigations of the regions of auroral ionization began in 1947. /7* There are two methods of active radiosonde auroral inhomogeneities. In the first method the radar principle is used; the signal is emitted by a pulse transmitter in the form of a short message, and it is picked up by a receiver which is usually on the same antenna. This method is called one-position or radar (R-method). The other method is based on reception of a scattered signal from a transmitting station by one or several receivers, located a certain distance from the transmitting station. This method is called the two- (or multi-) position or the corresponding method (C-method). Both methods have their advantages and disadvantages and supplement each other well, which is visually apparent from the following comparative table.

ADVANTAGES OF THE R-METHOD	DISADVANTAGES OF THE C-METHOD
Possibility of accurate position determination of reflection regions	Impossibility of accurate position determination of reflection regions
Possibility of performing circular scanning	Impossibility of performing circular scanning
Relatively great freedom from interference	Relatively small freedom from interference
Simple organization of observations	Complicated organization of observations
High operativity	Lower operativity than the R-method
DISADVANTAGES OF THE R-METHOD	**ADVANTAGES OF THE C-METHOD**
Great difficulty in investigating high-frequency signal	Possibility of detailed investigation of fadings

---

* Numbers in the margin indicate pagination in the foreign text.

fading (for frequencies above the repetition frequencies)	High sensitivity obtainable
Lower sensitivity attainable, all other conditions being equal	Arrangement of the experiment in a form closer to radio communication practice than by the R-method
Difficulty of sounding at several frequencies	Possibility of utilizing the operation of broadcast and departmental stations

From the given comparison it is apparent that in setting up experiments for studying auroral ionization it is necessary to apply both methods simultaneously, especially considering the phenomena of radio wave scattering from different sides, since forward scattering and backscattering, although related, are actually different phenomena.

Figures 1 and 2 present generalized block-diagrams typical of the R- and C-methods.

Let us give a short characterization of several typical experimental problems.

(1) The investigation of the time distribution of scattered signal amplitudes (frequency of the appearance of reflections) may be performed by means of both methods. The usual observation system is as follows: the transmitting station or radar operate in definite cycles, switching on the transmitter every 5 or 15 minutes, or continuously (around-the-clock or at definite hours of the day). The fact of the appearance of the signal is fixed, and sometimes even its amplitude is set on a conventional scale: for example, reflections with a signal-to-noise ratio (1.5-3) are evaluated as Number 1, a ratio (3-10) as Number 2 and higher as Number 3. Then the cases of signal appearance (or a definite number of reflections) are added according to the hours of the day for various seasons of the year. For example, such a type of data analysis may be found in [2]. /8

(2) The investigation of the space distribution of reflections is easily performed by radar with a rotating antenna having a plan position indicator (PPI). Analysis is carried out on the basis of photographs with regard to the resolving power of the radar equipment in distance and azimuth. An example of such an analysis may be found in [3]. If the radar has a split radiation pattern in the vertical plane and is provided with a goniometer, then it is also possible to experimentally determine the position angle of a reflecting object and then, at a certain distance, to find its altitude. The accuracy of these measurements, for example for a P-8 radar station with signal amplitudes greater than 5 (on the signal-to-noise scale), may be reduced to 5% if the ODS-type reflection is sufficiently quiet. An example of similar measurements may be found in [4].

(3) The amplitudes of the scattered signal may be measured using both methods. With the R-method, measurements are somewhat more complicated and less accurate. Their technique will be described below. Accurate measurements may be made using the C-method by comparing a detected and smoothed signal with the signals of a standard generator by the riometer method or the comparator method. It is necessary to note that R- and C-methods will give different characteristics even in the case of simultaneous measurement of the same region. /9

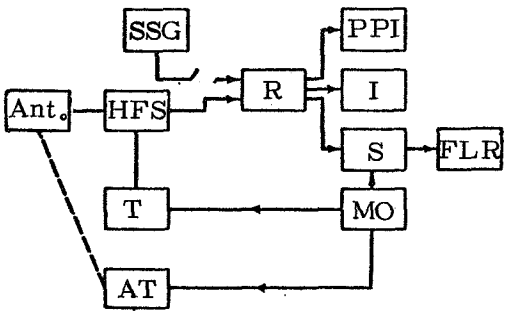

Fig. 1. Block-Diagram of Equipment for Radar Study of Auroral Ionization Regions. Ant. - Antenna; HFS - High-Frequency Switch; R - Receiver; T - Transmitter; I - Amplitude-Range Indicator; PPI - Plan Position Indicator; S - Selector; MO - Master Oscillator; AT - Artificial Target; FLR - Field Level Recorder; SSG - Standard-Signal Generator.

(4) For measurements of rapid variations of a scattered signal the C-method is more applicable. The detected signal may be recorded on magnetic tape and analyzed by a sonograph [5] or directly from the detector output onto an appropriate spectroanalyzer. A correlometer may be used for this purpose. Then it is not difficult to translate the obtained autocorrelation function into the spectral power density. The correlation method allows us to investigate fading even with the aid of radar. In this case fading frequencies below the repetition frequency may be registered with the aid of pulse recording on a loop oscillograph, and frequencies greater than the repetition frequency may be measured by correlation of a coded (doubled or tripled) radar pulse.

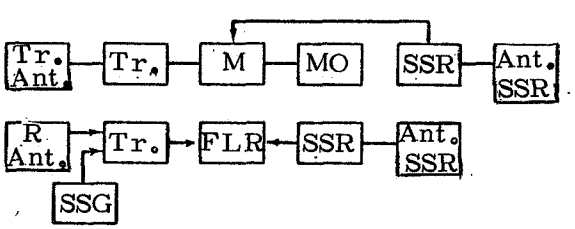

Fig. 2. Block-Diagram of the Two-Position Equipment for Radiosonde Observation of Auroral Ionization Regions (C-Method). Ant. (Tr., R.) - Transmitting and Receiving Antennas; M - Modulator; SSR - Synchronized Signal Receiver; Ant. SSR - Antenna for Synchronized Signal Receiver; Remaining Abbreviations Same As in Figure 1.

(5) Measurement of scattered signal polarization is more conveniently accomplished by the C-method. Usually, reception is accomplished on crossed antennas. The main difficulty is not only identifying the radiation patterns, but also having polarized antennas receive different signals from the same area of the radio reflecting regions. In experiments known to the authors this case has never been thoroughly considered.

It is possible to perform recording by directly photographing the screen of an oscillograph or analyzing video signals from both crossed antennas on an analog computer.

(6) Measurement of drifts may be easily made on radar equipment by means of sufficiently frequent photographing of the PPI. With the presence of a coherent pulse attachment it is possible to measure radial velocities by the Doppler method. The Doppler method also allows investigating radial velocities (both drifting and disordered) by the C-method.

(7) Mutual tie-in, calibration of measurements and measurements at many frequencies. In the overwhelming majority of cases calibration of both pulse equipment and equipment operating on a continuous cycle is accomplished by using standard-signal generators (SSG). In the case of the C-method this is completely admissible if the receiver has a sufficiently broad band pass, since fading modulation of a scattered signal reaches 6 and possibly 10 kHz; the receiver band must be no narrower than 12-15 kHz.

For the R-method the best calibration method is to compute measurements on an artificial target. Application in the given case of calibration based on SSG's is connected with the introduction of corrections which are difficult to take into account. In these cases, when there is a suspicion that the antenna parameters may deviate from the calculated parameters, this especially concerns multi-element yagi antennas, and it is completely necessary to carry out an investigation of the radiation patterns of the antennas (in the case of the C-method, for both the receiver and the transmitter). Measurement of the radar pattern may conveniently be taken using low-power transmitters which can be launched on weather balloons.

Simultaneous surveillance of reflection regions at various frequencies provides very rich experimental material and permits solving a number of questions which are impossible or difficult to answer by any other method. In particular, this method is very convenient for measuring characteristic dimensions of inhomogeneities and scattering radio signals [4-8].

Extensive application of the multiple-sounding method is hindered by significant technical and methodological difficulties connected with its realization. In particular, it is difficult to obtain complete identity of antenna diagrams and complete assurance of the fact that scattered waves at various frequencies originate in the same region of space. /10

Table 1 includes some data on radar stations used for surveillance of auroral ionization regions.

From the table it is apparent that the equipment used at various stations is very far from identical, and it is very difficult to directly compare results of measurements made by different investigators.

TABLE 1

Station Position	Frequency, MHz	Pulse Power, kW	Pulse Duration, sec	Antenna Gain	Receiver Sensitivity, W
Switzerland...	30	100	40	8	3.10^{-14}
	41.0	3	120	8	10^{-16}
Dikson (USSR).	50	50	10	10	10^{-14}
Saskatoon (Canada)....	56	50	60	20	5.10^{-13}
Manchester (England)...	72	10	40	90	2.10^{-14}
Yakutsk (USSR)	73	90	8	30	3.10^{-15}
College (Alaska)....	106	100	100	120	10^{-13}
	398	60	400-900	4000	10^{-16}

Space-Time Distribution of Radio Reflections and Their Connection with Magnetic-Ionospheric and Auroral Activity

Many studies have been dedicated to the space and time distribution of radio reflections, including several surveys [5, 9, 10]. The present state of the question may be summarized in the following way.

(1) Scattering of UHF and SHF radio waves is observed in the auroral and subauroral zones, in the polar cap and on the equator in the electrojet regions.

(2) In the northern hemisphere the overwhelming majority of radio reflections for stations of the auroral and subauroral zones take place from the north; in the south they occur from the south.

(3) Radio reflecting regions are distributed so that they approximately satisfy the Chapman conditions for a real magnetic field. The appearance of radio reflections is also connected with magnetic activity, which creates the impression that the alternating magnetic field, caused by the flow of ionospheric current, necessarily changes the angle of force lines of the constant field until these conditions are satisfied [10].

(4) The distribution of radio reflections during the day has three maxima in the auroral zone (morning, evening and night), two maxima in the subauroral zone (evening and night [5]) and one maxima in the electrojet region (day). Day reflections at all stations of the auroral-subauroral zone are rare.

(5) The probability of the appearance of radio reflections on the average increases with an increase in magnetic field disturbances [8, 11, 12] (Fig. 3).

A detailed investigation led to the discovery, however, that this connection is rather complicated, and at different stations it appears differently in details. For example, for Yakutsk [13] 82% of reflections are connected with negative bays and only 18% with positive ones, the latter appearing predominantly in the evening hours. A detailed phenomenological description of the connection between these phenomena is given in [10]. The author of this report is inclined to the opinion, first substantiated in [14], that the system of ionospheric currents may distort the local constant magnetic field so that the Chapman reflection conditions are satisfied. Evidently this factor plays a certain sometimes dominant role in the formation of reflections, but in no case is there an alternative for ensuring the appearance of radio reflections from those points in space where the Chapman conditions are not fulfilled with a purely geometric treatment, although they may be satisfied with regard to corrections for refraction [15, 16]. Both effects may be separated since they are described by different functions of magnetic disturbances. It is more difficult to calculate the third, probably most important factor, the formation of the very structure of radio reflecting regions, which may be connected with the existence of an electric field in the auroral plasma. This question will be discussed in detail below. In [3, 17] a statistical dependence of the mean reflection distance and the maximum azimuth on the degree of magnetic field disturbance was also found.

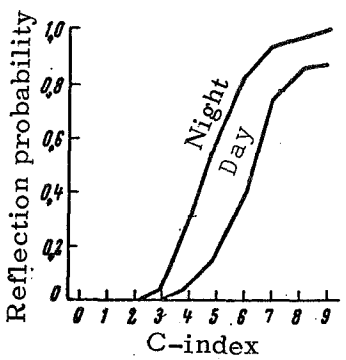

Fig. 3. Dependence Between the Probability of the Appearance of Radio Reflections and Magnetic Activity According to the C-Index [9].

(6) There are too few data characterizing the state of the ionosphere in a region of intense scattering of ultrashort wave signals to establish a clear concept of ionospheric characteristics in regions reflecting ultrashort waves. However, indirect data (the connection of ionospheric parameters with visually observable luminescence, data on the scattering of ultrashort wave signals on paths where, near the assumed reflection point, there was an ionospheric station) show that the appearance of luminescences at the zenith of an ionospheric station is accompanied by a definite type of sporadic ionization (E_{sa}), or complete absorption in the ionosphere. The E_{sa} ionization never appears during the daytime, but it may be present even when visible forms of luminescences are not detected. The E_{sa} is characterized by very large electron density gradients and may be grouped around discrete levels at altitudes of 100, 105, 111, 117 and 129 km. There are no data allowing us to

consider that the mean electron concentration in E_{sa} may be anomalously high (much greater than $3\text{-}10^5$ or 10^6) [18-21].

(7) Extremely little investigation of the connection between position of radio reflections and position of visible forms of aurorae has been carried out to date. In 1959 a series of observations of this kind was organized in Tiksi [22], but inaccurate knowledge of the radiation pattern of the radar equipment did not permit a satisfactory judgement to be made on the results, although the position of the visible forms was fixed fairly accurately with the aid of a movie camera. In the other case [4], the antenna diagram was well known but the observations of luminescences were made visually. In both cases, however, the results proved the same: it was established that radio reflection takes place from inhomogeneous, weakly-reflecting areas, especially from the edges of ray bands, from inhomogeneities and depressions in active homogeneous bands, and more rarely from quiet bands of moderate intensity. Very bright luminescences and very quiet arcs of small mobility and separate rays usually do not give reflections. There are grounds to consider that strong reflections also take place from the lower edge of active ray bands.

Study of Auroral Fading, Scintillation of Radio Sources in the Auroral Zone, Polarization of Ultrashort Frequency Radio Emission and Comments on Refraction

The problem of the spectrum of auroral fading is very important for understanding the scattering processes, and in this sense it is /12 one of the cardinal problems. The entire fading spectrum from the lowest to the highest frequencies is of interest. The low-frequency and high-frequency fadings behave differently, and it is possible to assume that these phenomena are caused by different factors. High-frequency fadings are of particular interest and were experimentally investigated in a number of studies [5, 23-26]. General conclusions may be stated as follows:

(a) a scattered signal undergoes fadings whose frequency spectrum extends from fractions of a Hz to several kHz;

(b) it is noted that with an increase in the frequency of the sounding signal the maximum fading frequency also increases;

(c) the frequency spectrum of the reflected signal power is not continuous, on the contrary it usually shows a discrete structure;

(d) no connection between the amplitude of the scattered signal type of reflection and the nature of fading seems to be detected.

The local fading frequencies (period 1-30 sec) are apparently connected with a change in the total reflectance of scattering re-

gions and are caused by a change in the position of the scattering region relative to the radar (or receiver-transmitter stations in the C-method), and also by a change in the mean electron density connected with a change in the ionizing agent. Intermediate frequencies (1-30 Hz) are possibly connected with the relative motion of large blocks of ionization, with the lifespan of scattering structures and with polarization fading. Finally, the high frequencies (30 Hz-10 kHz) may be connected with small-scale motions in the reflection region. Very high frequencies, fadings and the line-band pattern of the power spectrum of the reflected signal lead to the thought that scattering by elements of wave structures moving at great phase velocities takes place here. The type of frequency power spectrum contradicts Booker's assumption [42] of signal scattering by small, weak, uncorrelated inhomogeneities.

Experiments on translucence of sporadic ionization regions by discrete (point) sources of galactic radio emission are closely related to the problem of fading frequencies and scattered signal structures. As noted in [27], scintillation of a radio source in the constellation Signus at frequencies of 33 and 150 MHz are subject to simple laws. Rapid and especially intense scintillations arise with the passage of radio emission through the E_s region. The duration of rapid scintillations is 5-10 minutes, the maximum occurring in the winter months. The distribution of amplitudes before the appearance of rapid scintillation is a Rayleigh distribution; during rapid scintillation it is Gaussian.

One of the causes of reflected radio signal fading in the case of an antenna operating with linear polarization may be a change in the area of radio signal polarization upon reflection; i.e., the appearance of polarized fading (in essence, an equipment phenomenon). It is possible to foresee this circumstance in the construction of radio zones and to exclude it in the case of crossed receiving antennas. According to certain data [5, 28, 29], depolarization of a scattered signal is always observed to be of a disordered nature and sometimes reaches large values ($\sim$60%). In Booker's opinion [21], on the other hand, the appearance of depolarization is an exceptionally rare phenomenon. We made an attempt to measure depolarization by the R-method at Tiksi in 1958 at a frequency of 72 MHz. In this case, marked depolarization of the signal (> 20%) was not detected. /13
It is necessary to note that the lack of success there might have been due to a different antenna radiation pattern with horizontal and vertical polarization.

Calculations presented in [15] indicate that for frequencies of 70-100 MHz, Faraday rotation of the polarization plane during surveillance of luminescences under normal conditions will be sufficient to create noticeable depolarization of the reflected signal.

We do not know of any experimental study on the refraction of ultrashort waves in the auroral zone, although such experiments might be set up, for example, by receiving signals from low-flying (180-200 km) satellites or rockets. In this situation, an attempt

to evaluate the influence of refraction in the case of auroral ultrashort wave propagation by calculation on the basis of electron concentration data in the auroral ionosphere is especially important. Such evaluations [8, 15, 16, 30] are in good agreement with each other and indicate that refraction introduces a substantial error into determination of the position angle. Even at frequencies of ~ 100 MHz this error may reach 10-15%. It is necessary to take tropospheric refraction into account as well. Instances of anomalously far reception of signals from satellites (at distances up to 3200 km behind the horizon at 212 MHz [31]) attest to the importance of considering both factors.

Physical Conditions in Aurorae and Radio Reflecting Regions

This problem may be boldly called one of the central problems involving aurorae. Very many studies are dedicated to this problem. Let us recall the basic facts which have been established, of which there are not too many at the present time.

(1) Aurorae are caused by powerful electron currents with energies in the area of several keV. The energy flux of fast electrons causing No. 1, 2 and 3 luminescences is equal in order of magnitude to 1, 10 and 100 erg/cm^2·sec, respectively. In anomalously bright aurorae the energy flux may evidently reach even several thousand erg/cm^2·sec.

(2) The radiation energy of aurorae is basically concentrated in the infrared region. In a No. 3 aurora the total radiant energy flux reaches ~18.0 erg/cm^2·sec [32]: in the ultraviolet region (λ < 3000 Å) the energy flux is equal to 4.7 erg/cm^2·sec; in the visible spectrum (3000 Å < λ < 6500 Å) it is approximately 1.6 erg/cm^2·sec; and in the infrared it is 11.7 erg/cm^2·sec.

(3) At the present time there is still no single opinion on what amount of energy of the electron stream is converted directly into heat and what amount is radiated.

Chamberlain [32] considers that the basic amount (around 85%) is given off as light and only 15% is directly converted to heat. In this study we maintain the opposite point of view, and consider that ~ 6/7-9/10 of the energy of the electron stream is converted to heat. If the latter assumption is true, electron streams may cause a substantial increase in not only the electron temperature but also the temperature of the heavy components (ions + neutral particles) in an intense auroral region.

(4) Spectrointerferometric temperature measurements in aurorae indicate that such heating actually does take place. An evaluation performed according to the broadening of the red line of oxygen yielded a temperature of around 3500° [33] in a red, high-altitude, type A aurora. Later experiments on infrasonic wave

recording also indicate this [34]. Maeda [35, 36] considers that infrasonic waves are caused by pulse heating of the ionosphere with electron currents in the auroral zone. The basic mechanism of energy transmission from an electron stream to atoms and ions in the /14
atmosphere is considered to be oxygen dissociation with a subsequent association in the case of a triple collision, when the third particle may remove some of the energy after being liberated as a result of association. In the case of electron streams on the order of 10^{12} $cm^{-2} \cdot sec^{-1}$, this mechanism ensures the liberation of 10^{-7} $erg/cm^3 \cdot sec$ heat at an altitude of 100 km [37].

Interaction of the fast electron stream with the ionosphere increases evenly with intense heating of the electron component of the auroral plasma. This will take place partially due to the residual energy of secondary electrons arising upon ionization, partially due to inelastic collisions of the second type, and finally in cases of triple collisions with recombination and association. It is clear that the mechanisms of energy transmission from an electric field to an electron gas will act more effectively than the mechanism proposed by Maeda, and the basic amount of energy will be transmitted exactly to the electron component of the plasma. This leads to various results, depending on the magnitude of the energy introduced into the plasma. When the power density of energy sources connected with the dissipation of the electron stream is small, a simple elevation of the electron gas temperature takes place and a difference arises: the electron temperature minus the temperature of the heavy components of the plasma. Electrons begin to slowly heat the heavy gas. If the power density of the energy sources is so high that the electron gas is heated to a temperature of 8000-10,000°, a significant number of electrons will then be able to excite a low energy level of atoms and molecules; for example, emission of oxygen (6300 Å) and nitrogen (5200 Å) where the excitation potentials are 1.96 and 2.35 eV, respectively. In this case we note that an anomalous increase of these emissions is actually observed [38]. For such periods we must also record a great infrared excess and the presence of thermal radio emission [32].

To the best of our knowledge, no direct measurements of electron temperature in aurorae have been made. However, for a quiet ionosphere such measurements were conducted on rockets with the aid of Langmuir probes [39]. It proved to be the case that the electron temperature at the level of the *E* layer in Churchill (69° N. lat.) was 500-700° higher than in Michikava (29° N. lat.); on Wallops Island (49° N. lat.) it was only 100° higher than in Michikava. According to other data obtained with the same method, the night electron temperature at altitudes of 90-120 km during a comparatively quiet period was equal to 600° K and the day temperature 800-1000° K [40].

(5) Often discussion has arisen around the question on the amount of electron concentration in aurorae, in particular when attempts were made to rehabilitate the hypothesis of critical reflection.

At the present time we may consider it established that in regions where radio reflections are formed the electron concentration usually does not exceed several units$\cdot 10^5 \cdot cm^{-3}$ [41], and only in rare cases does it attain values of greater orders of magnitude. It is clear that no conceivable ionization mechanisms could create the electron concentration necessary for critical reflection of signals at frequencies of 1300 MHz [42]. Although it is possible to assume critical reflections at frequencies of 30-50 MHz in exceptional cases, the general mechanism of radio reflections must be the scattering of weak, small inhomogeneities.

We shall introduce several evaluations of the relative variation of electron concentration. Booker [42] considers that the relative elevation of electron concentration in an inhomogeneity $(\Delta n/n) \sim 10^{-4}$-$3 \cdot 10^{-3}$ and that the absolute value is $\Delta n \sim 500$ cm^{-3}. According to the calculations of V.I. Pogorelov [43] the absolute value is $\Delta n \sim 10^5 \cdot cm^{-3}$, and $\Delta n/n$ may reach tens of percents. In the opinion of V.I. Dovger [4], the relative electron concentration in inhomogeneities may reach 10%, but more frequently it is 1-2%. Wickersham [44], interpreting ionospheric inhomogeneities as acoustic waves, /15 comes to the conclusion that for effective scattering it is sufficient that $\Delta n/n$ be on the order of 0.3%. It is necessary to note that all these calculations are highly arbitrary, and we can only speak precisely of evaluations by referring to order of magnitude.

(6) Evaluations of the recombination coefficient made by various methods for the night polar ionosphere and auroral regions also contained large discrepancies (from several units$\cdot 10^{-9}$ [45] to several units$\cdot 10^{-7}$ cm$^3 \cdot$sec^{-1} [46]). Evidently the value of the effective recombination coefficient yielded by direct recombination processes is near 10^{-8} cm$^3 \cdot$sec^{-1} for the E layer [47].[1]

(7) Ionospheric currents in the auroral regions may have a double influence on the formation of reflections: in the first place, they may change the inclination of force lines so that the Chapman conditions are satisfied (or inversely, they may destroy them); and in the second place, the electric field of auroral currents leads to drift motions of electrons and ions and to liberation of Joule heat. The relative success of the first aspect of explaining the connection between magnetic disturbances and the appearance of radio reflections achieved in [10, 48] somewhat inhibited the development of ideas in the second direction. However, in connection with the progress in explaining the scattering power of the equatorial layer E_s, in the region of the equatorial electrojet, where a purely geometric interpretation of the action of ionospheric current cannot be applied, this question again became timely. At the present time the task may be formulated in the following way: is the presence of current (electric field) in the region of

[1] In the E region it is necessary to use the value $(3\text{-}10) \cdot 10^{-8}$ cm$^3 \cdot$sec^{-1} (editor's note).

reflection formation a necessary condition for the appearance of scattering structures?

The experiment with radiosonde observation of the equatorial region E_s related to the electrojet indicates that the answer to this question must be positive.

The total current in the aurora may be rather positively evaluated based on the data of magnetic observatories. The difficulty ends in the fact that total current does not enter equations describing the state of ionospheric plasma, but rather values of current density or of electric field strength. The latter parameters are rather difficult to determine in a well-defined way since the total cross section of the ionospheric current and its distribution along the section are not known. Recently these difficulties were overcome to a certain degree [49]. Values of the area covered by the current were evaluated as $3 \cdot 10^{13}$-10^{14} cm^2, current density 10^{-10} A/cm^2 and field strength 10^7 CGS units. Although these evaluations are very indefinite and are based on the introduction of supplementary assumptions, it is possible to consider that further improvement of the method will make this process sufficiently accurate.

Comments on Theories Explaining the Appearance of Small-Scale Ionospheric Inhomogeneities

At the present time, we assume three types of mechanisms for the appearance of small-scale inhomogeneities in the E_s layer to which ultrashort wave and ultrahigh frequency scattering may be attributed:

(1) turbulent and thermal fluctuations of electron concentration, by which it would be possible to explain noncoherent scattering of radio waves;

(2) fluctuations of electron concentration in the various types of waves (acoustic, magnetoacoustic, neutral diffusion, etc.), by which it would be possible to explain the appearance of quasicoherent scattering;

(3) fluctuations of electron concentration within a fast electron stream when it penetrates the ionospheric plasma; such fluctu- /16
ations, of the plasmatic oscillation type, may arise in the case of a double-stage instability.

The hypothesis that scattering takes place on turbulent inhomogeneities of ionization located in auroral regions was advanced by Booker [31]. The success of the theory of tropospheric scattering made such a hypothesis especially tempting, and the initial successes in explaining many characteristics of reflections from auroral ionization regions gave rise to hopes that this theory might prove to be exhaustive. The same views on the nature of auroral radio

reflections were maintained by Chamberlain [32], V.I. Dovger [4] and others. Pogorelov [48] introduced certain improvements into Booker's original proposal, and Egeland [5] generalized it to the case of more complex scattering elements: triple-axis ellipsoids.

However, with the accumulation of experimental material it proved to be the case that the model of scattering centers (small, weak, disordered fluctuations of electron concentration) was incapable of explaining many facts (cf. § II). At the same time, SHF emission at frequencies of 1000-1300 MHz is scattered noncoherently and possibly originates from thermal fluctuations of electron concentration or from plasma waves [42].

The hypothesis that wave processes in the *E* layer may be responsible for the formation of inhomogeneity systems is considered in a number of studies. Although almost all studies are basically dedicated to the explanation of the mechanism of ultrashort wave scattering in the equatorial layer E_s, connected with the electrojet, it is possible to consider that these investigations will give serious interest to the theory of auroral scattering inhomogeneities.

"Wave" hypotheses on the formation of inhomogeneities may be divided into two groups. In the first group we shall include studies based on an assumption that inhomogeneities are caused by the appearance of acoustic waves, the excitation mechanism of which most often remains hypothetical [5, 52]. It is necessary to note that the connections between E_s and tropospheric phenomena (hurricanes, cyclones and thunderstorms) noted by many authors may receive a real explanation in this way. The leading idea of the second group of hypotheses consists in using the known nature of plasma to display instability toward many types of disturbances (drift, ionization recombination, beam, etc.). A rather large number of studies primarily on the theory of the equatorial layer E_s [53-59] have already been dedicated to this very promising concept which was formulated in the last two years.

II. PHYSICAL CONDITIONS IN THE AURORAL IONOSPHERE

Here a new definition is introduced: the auroral ionosphere, /17 by which we designate that region of the ionosphere where the action of electron streams plays the decisive role in the energy and ionization balance. A more accurate definition of the auroral ionosphere as a medium with a definite set of basic parameters, including:

N - neutral particle concentration,
μ - molecular weight,
H - magnetic field strength,
n_e - electron concentration,
n_i - ion concentration,
T_e - kinetic temperature of electrons,
T_i - kinetic temperature of ions,
α - effective recombination coefficient,
$\sum_j \omega_{sj}$ - total power density of energy sources,
$\sum_j \omega_{rj}$ - total power density of energy discharges,

is given by a system of equations connecting these parameters. Some of the parameters listed above, namely neutral particle concentration, molecular weight, magnetic field strength, kinetic temperature of the heavy particle gas and the effective recombination coefficient, will be considered to be independent of the action of the electron stream. The task will consist of expressing the remaining dependent ionospheric parameters by independent parameters and by parameters of the electron stream.

Energy Balance of the Auroral Ionosphere

The energy balance of the auroral ionosphere has a number of characteristics which sharply distinguish processes of energy exchange in the auroral plasma from the energy balance of a nocturnal, undisturbed ionosphere in the high latitudes. The basic energy source for the auroral ionosphere is probably energy dissipating from the electron stream. A certain amount of this energy is converted to light. Evidently the energy fraction of the original stream converting to radiation is from 1/7 to 1/15 of the total

energy flux for No. 3 aurorae.[2] On the basis of available data, a more accurate evaluation is difficult to make.

According to the observations of MacIlvaine [60], the effective conversion of primary electron energy into light energy in the visible region totals approximately 0.2% with a possible error by a factor of two. The emission intensity in the infrared region is /18
20-30 times greater than in the visible region [32]. Thus the total light output may amount to several percent (5-8% for No. 3 aurorae and up to 10-12% for even weaker aurorae). In the remainder of this study we shall consider that, on the average, 10% of the energy of the electron stream is converted to light energy. In calculation this amounts to 3.5 eV per one act of ionization. A primary electron usually expends around 19 eV on ionization with dissociation and excitation of nitrogen or oxygen molecules [61]. On the average a secondary electron carries away approximately 8 eV. The dissociation energy and kinetic energy capable of being removed by heavy particles after dissociation on the average amounts to around 5.5 eV; evidently, not more than 0.5 eV is necessary per portion of kinetic energy.

Thus the electron gas receives around 2/3 of the 35 eV which are necessary for each act of ionization (bearing in mind that stationarity is always maintained and that energy removed for dissociation, ionization and excitation is partially converted to electron gas in the case of reversible processes; i.e., by inelastic collisions of the second type). It is important for us to know what amount of energy of an electron stream is finally converted to heat.

Here we may be completely satisfied by the assumption that almost the entire 35 eV expended by a fast electron for each act of ionization goes to heating the electron gas.

Electrons of the auroral plasma expend some radiation energy in the case of free-free transition. In rare cases, when the electron temperature rises to 8000-10,000°, losses due to excitation by electron collision begin to play a certain role, but most of the energy is transmitted by the electron gas to the heavy particle gas, which is a practically unlimited energy reservoir and "refrigerator". Joule losses of electron current, usually increasing in the *E* layer at those times when an optical aurora appears, may provide a significant contribution to the energy balance.

According to Chamberlain [32], approximately 5 eV of each 35 eV per act of ionization changes into heat, and approximately 30 eV is given off as light.

---

[2] The brightness of aurorae is usually designated by roman numerals on a three-point scale. In this report, we will use Arabic numerals in order to introduce designations for the aurorae of intermediate brightnesses (No. 2.5).

In other words, Chamberlain accepts the value 85% for the total light output and not the 10% which we consider. The great value of total light output contradicts the measurements of MacIlvaine or, indeed, requires assumptions that in the infrared region of the spectrum there is radiated not 20-30 times more energy than in the visible spectrum, but approximately 500 times more.

Thus, if we designate the power density of the energy sources for an electron gas by w_{se} and charges by w_{re} then, ignoring the influence of heat conductivity and for the time being not considering Joule heat, we obtain:

$$\operatorname{div} I_\varepsilon = w_{se} = 6m_e \frac{kn_e\nu_{eN}}{m_N}(T_e - T_N). \tag{1}$$

Considering that the arrival of heat to the electron gas is equal to the outflow of energy from the electron gas to the heavy gas due to the "gradientless" heat conductivity [75], we may write:

$$\operatorname{div} I_\varepsilon = \frac{6d_{eN}k(T_e - T_N)}{m_N}, \tag{2}$$

where $d_{eN} = m_e \nu_{eN}$. In (1) and (2) the following symbols are used: ν_{eN} is the number of collisions per second of a plasma electron with heavy particles; d_{eN} is the coefficient of friction between the electron gas and the heavy particle gas.

We have already noted that we consider the energy capacity of a heavy gas to be infinitely great. This is only approximately true. The amount of energy contained per cm^3 of a medium at a temperature of 300° K and a concentration 10^{13} cm^{-3} is approximately 0.4 erg/cm^3. The power density of the energy sources, connected with the dissipation of energy of an electron stream as we shall see below, does not exceed 10^{-5} $erg/cm^3 \cdot sec$. Consequently, approximately 10^{-4} sec is needed for the temperature of the heavy gas to be significantly changed in any way. It is necessary to note that at altitudes of 150 km, for instance, where $N \sim 10^{11}$ cm^{-3}, this requires several minutes, and our assumption naturally loses validity. Since in the following discussion we shall limit ourselves to altitudes up to 130 km and time intervals of up to 10 min, the approximation of a "neutral thermostat" will be satisfactory for us. Formula (2) may be used for calculating the electron temperature in the case where the left-hand side of it is known to us, let us say, from rocket measurements. For example, when a rocket was launched into the arc of a visible aurora, which was accomplished on February 25, 1958 at 5 hrs 48 min 32 sec UT in the area of Fort Churchill [60], the total energy of an electron stream was measured as a function of altitude. Assuming that during the rocket flight the energy of the electron stream did not essentially change (it is possible to judge this by the symmetry of the curve of the energy flux density obtained on the ascending and descending branches of the rocket motion), we may evaluate div I_ε and then, using an approximation of

/19

the "neutral thermostat", to calculate the course of electron temperature with altitude, assuming that the temperature of the heavy component is constant and equal to 400° K. The results of such a calculation are given in Table 2.

TABLE 2

Height h, km	Energy Flux Density I, erg/cm^2·sec	Divergence of Energy Flux Density $\frac{dI}{dh}$, erg/cm^3·sec	Electron Concentration n_e, cm^{-3}	Electron Temperature T_e, °K
124	60			
118,4	30	$5,4\cdot10^{-5}$	$8,8\cdot10^{5}$	$1,7\cdot10^{3}$
114,0	1,6	$6,5\cdot10^{-5}$	$2,2\cdot10^{6}$	$3,1\cdot10^{3}$
110,7	0,7	$2,8\cdot10^{-6}$	$1,6\cdot10^{6}$	$1,7\cdot10^{3}$
107,6	0,16	$1,7\cdot10^{-6}$	$1,8\cdot10^{6}$	$1,1\cdot10^{3}$
105,0	0,10	$2,5\cdot10^{-7}$	$1,4\cdot10^{6}$	$5,2\cdot10^{2}$
102,6	0,075	$1,0\cdot10^{-7}$	$9,8\cdot10^{5}$	$4,6\cdot10^{2}$
100,6	0,060	$7,5\cdot10^{-8}$	$8,6\cdot10^{5}$	$4,4\cdot10^{2}$
99,0	0,050	$6,8\cdot10^{-8}$	$8,0\cdot10^{5}$	$4,3\cdot10^{2}$
97,7	0,044	$4,6\cdot10^{-8}$	$7,4\cdot10^{5}$	$4,2\cdot10^{2}$
96,1	0,037	$4,4\cdot10^{-8}$	$7,0\cdot10^{5}$	$4,2\cdot10^{2}$

The aurora into which the rocket was launched was apparently a No. 3 ray arc. The lower edge of the luminescence was located at an altitude of around 110 km. The calculated course of the electron temperature has a maximum of approximately 3000° K at an altitude of 114 km. The flux density of energy sources at this altitude also has a maximum equal to $6.5\cdot10^{-5}$ erg/cm^3·sec. The electron concentration for calculations of temperature (T_e) was calculated from the condition

$$w_{ee} = \alpha n_e^2 \widetilde{\Delta\varepsilon}, \qquad (3)$$

where α is the recombination coefficient; n_e of the electron concentration; $\Delta\widetilde{\varepsilon}$ the amount of energy capable of being transmitted to the electron gas of the ionospheric plasma in the case of one act of ionization. Here it is assumed that the process is stationary.

The obtained distribution of electron concentration with altitude indicates a monotonously increasing passage up to an altitude of 118 km, where $n_e \approx 8.8\cdot10^{6}$ cm^{-3}. /20

Uniting (2) and (3) we obtain the formula

$$\alpha n_e^2 \widetilde{\Delta\varepsilon} = \frac{6 d_{eN} k (T_e - T_N)}{m_N}, \qquad (4)$$

which allows us to determine the course of electron temperature according to the known ionization distribution (certainly within the limits of the above-mentioned assumptions).

Although the approximation of the "neutral thermostat" and the assumption that inelastic collisions are the basic mechanism for the transmission of energy from the electron stream to the ionospheric plasma, are rather rough (as is the assumption of stationarity), they make it possible to formulate a closed problem for determining the physical parameters of the auroral ionosphere (T_e, w_{se}, I_ε) as a function of values usually accessible to direct determinations (n_e, N, α).

Thus, within the assumed limitations, a model of the auroral ionosphere may be constructed, for example, as indicated above. In fact, it will evidently be more convenient to proceed not from the known distribution of electron concentration (with a subsequent calculation of the distribution function of primary electrons according to energies, etc.), but from generalized energy spectra of primary electrons. The selection of such a method is connected with the fact that we can indicate a completely defined limited number of such spectral types, while to separate definite types of electron concentration distributions for the auroral ionosphere is difficult.

Model of the Ray Arc of an Aurora

Let us assume that on the basis of experiments we know the energy distribution for the energy flux density of fast electrons. Such data may be obtained, for example, by rocket sounding of aurora [60]. Then, knowing the law by which a primary electron is braked in the atmosphere, it is possible to find the energy distribution for the flux density of electron energy at any level of the ionosphere if the angular distribution of primary electrons is known.

The braking of fast electrons upon penetration into the atmosphere is basically determined by ionization losses (here and subsequently we are considering electrons with energies of 1-15 keV). The braking force in this case may be presented in the form [62]:

$$\frac{d\varepsilon}{dh} = -\frac{NA}{\cos\nu} \frac{\ln b\varepsilon}{\varepsilon}, \qquad (5)$$

where A is the coefficient $2\pi e^4 z = 2.33 \cdot 10^{-36}$ erg$^2 \cdot$cm^{-2};
b is the coefficient $8\pi/\tau v_0 h z = 2.72 \cdot 10^{10}$ erg^{-1} = $4.37 \cdot 10^{-2}$ eV^{-1};
e is the electron charge;

z is the atomic weight of atmospheric particles;
N is the concentration of atmospheric particles;
τ is the coefficient characterized by the natural velocities of atoms in the medium (for air, $\tau = 6.02$);
v_0 is the Riedberg frequency;
h is the Planck constant;
ϑ is the pitch angle;
ε is particle energy;
dh is a path length element read along a force line.

The braking force described by (5) is inversely proportional to the energy of a fast electron and also depends on the logarithm of energy, but this dependence is slight, and we may consider $\ln b\varepsilon$ to be a constant value and designate it by L. In extreme cases, with a change of energy from 1 to 15 keV, L changes from 3.77 to 6.48; i.e., by 1.7 times (we shall accept $L = 5$). Then from (1) we find /21

$$\varepsilon^2 = \varepsilon_n^2 - \frac{A\Gamma L}{\cos \upsilon}, \tag{6}$$

where $\Gamma = \int N dh$ indicates the reduced atmospheric thickness. Since calculations are conducted for the auroral zone where the inclination of magnetic force lines is great, a path element (dh) is read along the vertical. We shall designate the initial energy of an electron by ε_n. We shall further assume that the energy flux density of fast electrons at infinity has the form

$$I = I_0 \exp(-\varepsilon_n/\varepsilon_0). \tag{7}$$

According to [60], electrons actually have an exponential distribution based on auroral energies, which may be identified as a ray band, where ε_0 in the above-mentioned experiment has a value equal to 5 keV.

We shall consider that the exponential spectrum is characteristic of all ray-type aurorae and that ray aurorae on different number scales are distinguished only by electron stream intensity, and not by spectral distribution. Conditionally we shall attribute to No. 3 aurorae an energy flux connected with primary electrons in the energy band from 1-15 keV at 100 erg/cm^2·sec and an altitude of 133 km. Then for No. 2 and No. 1 aurorae we obtain, respectively, 10 erg/cm^2·sec and 1 erg/cm^2·sec. The strongest No. 4 aurorae are caused by electrons with an energy flux also assumed conditionally to be 1000 erg/cm^2·sec. Such an energy classification approximately corresponds to the accepted photometric classification, wherein No. 1, 2, 3 and 4 aurorae give fluxes of 1, 10, 100 and 1000 kilorayleighs at the 5577 Å line.

After passing through a thickness Γ_j the primary electron energy will be partially expended by ionizing collisions. In the energy range from ε to $\varepsilon + d\varepsilon$ at a depth Γ_j particles will fall with various

initial energies depending on the pitch angle. To simplify, we shall consider that the angular distribution of primary particles is isotropic at infinity. It is clear that this will be most true after the electrons have penetrated a certain thickness of matter. In order to find an expression for $I(\varepsilon,\Gamma)$, it is necessary to integrate (3) over all pitch angles with regard to (2); i.e., to find the integral[3]

$$I(\varepsilon\Gamma)=\frac{1}{\pi}\int_0^{\pi} I_0\exp\left[-\frac{\sqrt{\varepsilon^2+A\Gamma Z/\cos v}}{\varepsilon_0}\right]d\vartheta. \tag{8}$$

To find an expression for the integral by known functions is apparently difficult, but bearing in mind that a high degree of accuracy is not needed from the result, it is possible to limit ourselves to an approximate expression for (8). Indeed, the solution of the cone from which particles may arrive at the given level Γ_j is determined by the expression

$$\vartheta_{cr}=\arccos\frac{A\Gamma_j L}{\varepsilon_n^2}. \tag{9}$$

Consequently for (8) we have the approximate expression: /22

$$I(\varepsilon\Gamma_j)=\frac{I_0}{\pi}\exp\left[\frac{\sqrt{\varepsilon^2+A\Gamma_j L}}{\varepsilon_0}\right]-\arccos\frac{A\Gamma_j L}{\varepsilon^2+A\Gamma_j L}. \tag{10}$$

For the initial level we select an altitude above which the thickness will be less than the critical thickness for electron energies of 1 keV and a pitch angle equal to zero. In our model this corresponds to an altitude of 133 km (Table 3).

The results of calculating the energy flux density as a function of altitude are given in Table 4. The electron concentration and the electron temperature calculated for this same model (for No. 1, 1.5, 2.5 aurorae) are given in Table 5.

As mentioned above,

$$w_{se}=\frac{\partial I}{\partial h}, \tag{11}$$

and the electron concentration was found from condition (3):

$$n_e=\sqrt{\frac{w_{se}}{\alpha\widetilde{\Delta\varepsilon}}}. \tag{12}$$

The electron temperature was determined by a numerical solution

[3] The problem was solved more accurately in the studies of Reese: Planet. Space Sci., Vol. 11, p. 1209, 1963; Vol. 12, p. 722, 1964 (author's note).

TABLE 3

Primary Electron Energy ε_n, keV	Electron Penetration Altitude h (km)	Particle Concentration N, cm^{-3}	No. of Particles in Column Γ, cm^{-2}
1	133	$4{,}5 \cdot 10^{11}$	$3{,}4 \cdot 10^{17}$
2	124	10^{12}	$1{,}15 \cdot 10^{18}$
3	118,4	$2{,}0 \cdot 10^{12}$	$2{,}4 \cdot 10^{18}$
4	114	$3{,}0 \cdot 10^{12}$	$3{,}9 \cdot 10^{18}$
5	110,7	$5{,}0 \cdot 10^{12}$	$5{,}6 \cdot 10^{18}$
6	107,6	$7{,}2 \cdot 10^{12}$	$7{,}8 \cdot 10^{18}$
7	105,0	$9{,}6 \cdot 10^{12}$	10^{19}
8	102,6	$1{,}3 \cdot 10^{13}$	$1{,}3 \cdot 10^{19}$
9	100,6	$1{,}64 \cdot 10^{13}$	$1{,}61 \cdot 10^{19}$
10	99,0	$1{,}85 \cdot 10^{13}$	$1{,}95 \cdot 10^{19}$
11	97,7	$2{,}4 \cdot 10^{13}$	$2{,}35 \cdot 10^{19}$
12	96,1	$3{,}3 \cdot 10^{13}$	$2{,}75 \cdot 10^{19}$
13	95,7	$4{,}0 \cdot 10^{13}$	$3{,}2 \cdot 10^{19}$
14	94,2	$4{,}6 \cdot 10^{13}$	$3{,}6 \cdot 10^{19}$
15	93,4	$4{,}9 \cdot 10^{13}$	$4{,}1 \cdot 10^{19}$

TABLE 4

Altitude h, km	Relative Energy Flux Density I/I_0	Divergence of Energy Flux Density $\frac{\partial}{\partial h}\left(\frac{I}{I_0}\right)$
133	1	$3{,}5 \cdot 10^{-7}$
124	0,683	$3{,}8 \cdot 10^{-7}$
118,4	0,473	$2{,}6 \cdot 10^{-7}$
114	0,365	$2{,}5 \cdot 10^{-7}$
110,7	0,283	$2{,}4 \cdot 10^{-7}$
107,6	0,210	$1{,}7 \cdot 10^{-7}$
105,0	0,166	$2 \cdot 10^{-7}$
102,6	0,118	$1{,}7 \cdot 10^{-7}$
100,6	0,084	$1{,}2 \cdot 10^{-7}$
99,0	0,065	$1{,}2 \cdot 10^{-7}$
97,7	0,045	$1{,}3 \cdot 10^{-7}$
96,1	0,029	$1{,}3 \cdot 10^{-7}$
95,1	0,016	$7{,}6 \cdot 10^{-8}$
94,2	0,009	$5{,}7 \cdot 10^{-8}$
93,4	0,0035	$4{,}0 \cdot 10^{-8}$

(1) with the condition that the assumption of "neutral thermostat" is correct and that the temperature of the neutral component is constant and equal to 400° K. Figure 4 is given as an illustration; there the curves $n_e(h)$, $T_e(h)$ and $\omega_{se}(h)$ are drawn for a No. 2.5 ray arc.

A characteristic feature of the distribution flux density as a function of altitude for all three cases is the almost strict constancy of ω_{se}. At altitudes from 105 to 133 km this value varies only by a factor of 1.7. If the "light output" is approximately constant, then the surface brightness of an aurora in the altitude range under consideration must be maintained unchanged. This circumstance does not contradict the known fact of the significant elongation of rays in ray arcs along the vertical. The electron concentration in all cases steadily increases, and from 93 to 133 /23
km it is increased by approximately one order of magnitude. The electron concentration in No. 2.5 aurorae reaches a maximum value corresponding to the critical frequency 20 MHz and evidently is somewhat overstated. Probably this is connected with the fact that in the energy range from 1-3 keV there are indeed fewer primary electrons than given by extrapolation of the exponential distribu-

tion.[4] It is necessary to note that during intense aurorae in the zenith above an ionosphere station, reflections from the layers are usually not observed due to the intense absorption below the E layer; therefore it is difficult to evaluate the amount of divergence.

Analysis of the high-altitude electron temperature distribution also leads to the conclusion that in intense aurorae at high altitudes, overstated electron temperature values are obtained. The cause may be the same as in the case with overstated electron concentration; i.e., an incorrect extrapolation of the exponential distribution for the electron energy flux as a function of their energy in the low-energy region of the spectrum [60]. It is clear that even in the case of No. 2.5-3 ray arcs, electron temperatures of 7000-10,000° must lead to the appearance of infrared band excitation by means of the collision between thermal electrons, which must cause a sharp emission "excess" in the infrared region. It is impossible to completely deny such a possibility, since in a number of cases of high-altitude, red, type A aurorae an anomolous infrared and thermal radioemission evidently took place [32, 63]. Another characteristic of the curves $T_e(h)$ is the slight dependence of the electron temperature at low altitudes on the energy flux density of primary electrons. Considering the above-mentioned data, we must be careful in applying results obtained with our models for elevations greater than 120 km.

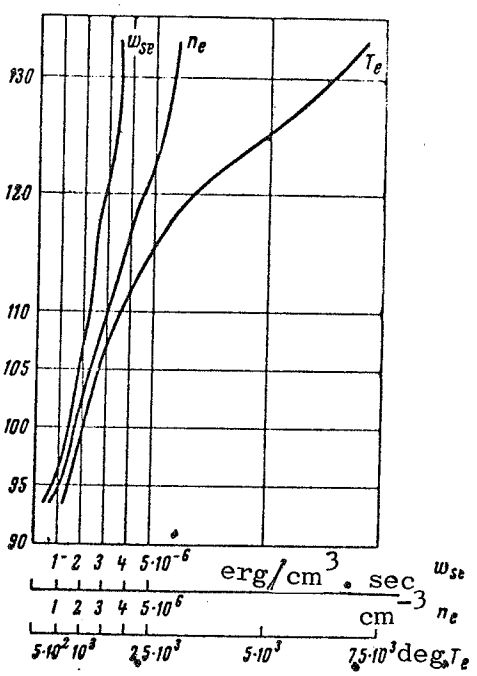

Fig. 4. Physical Conditions in No. 2.5 Ray Arcs.

Below we shall deal with an investigation of the mechanism of scattering center formation in ray forms of aurorae, although analogous results evidently may be obtained even for homogeneous arcs. Probably homogeneous arcs are caused by almost monochromatic electron streams. In the remainder of this study, the calculation method and the general physical picture will have much in common with the cases considered.

[4] Also the use of understated values of α' led to the overstatement n_e (editor's note).

TABLE 5

No. 1

/24

ε_n, keV	Altitude h, km	Electron Temperature T_e, °K	Electric Field (Critical) E_{cr}, CGSU	Critical Phase Velocity v'_T, cm/sec	Critical Wavelength λ_2, cm	Minimum Wavelength λ_{min}, cm	Maximum Electric Field E_{max}, CGSU
1	2	3	4	5	6	7	8
1	133	$2{,}52\cdot10^3$	$5{,}4\cdot10^{-6}$	$3{,}64\cdot10^2$	$1{,}12\cdot10^3$	$2{,}32\cdot10^2$	$5{,}22\cdot10^{-5}$
2	124	$1{,}48\cdot10^3$	$4{,}3\cdot10^{-6}$	$5{,}67\cdot10^2$	$9{,}9\cdot10^2$	$1{,}88\cdot10^2$	$4{,}8\cdot10^{-5}$
3	118,4	$1{,}17\cdot10^3$	$3{,}6\cdot10^{-6}$	$7{,}50\cdot10^2$	$7{,}8\cdot10^2$	$1{,}3\cdot10^2$	$4{,}32\cdot10^{-5}$
4	114	$1{,}01\cdot10^3$	$3{,}3\cdot10^{-6}$	$9{,}27\cdot10^2$	$7{,}34\cdot10^2$	$1{,}16\cdot10^2$	$4{,}15\cdot10^{-5}$
5	110,7	$8{,}23\cdot10^2$	$2{,}8\cdot10^{-6}$	$1{,}26\cdot10^3$	$7{,}04\cdot10^2$	10^2	$3{,}95\cdot10^{-5}$
6	107,6	$7{,}3\cdot10^2$	$2{,}73\cdot10^{-6}$	$1{,}57\cdot10^3$	$6{,}4\cdot10^2$	91,7	$3{,}83\cdot10^{-5}$
7	105,0	$6{,}7\cdot10^2$	$2{,}6\cdot10^{-6}$	$1{,}91\cdot10^3$	$6{,}34\cdot10^2$	85,7	$3{,}75\cdot10^{-5}$
8	102,6	$6{,}2\cdot10^2$	$2{,}40\cdot10^{-6}$	$2{,}32\cdot10^3$	$6{,}2\cdot10^2$	81,0	$3{,}67\cdot10^{-5}$
9	100,6	$5{,}7\cdot10^2$	$2{,}32\cdot10^{-6}$	$2{,}71\cdot10^3$	$5{,}9\cdot10^2$	76,0	$3{,}6\cdot10^{-5}$
10	99,0	$5{,}5\cdot10^2$	$2{,}26\cdot10^{-6}$	$2{,}92\cdot10^3$	$5{,}9\cdot10^2$	74,0	$3{,}57\cdot10^{-5}$
11	97,7	$5{,}4\cdot10^2$	$2{,}19\cdot10^{-6}$	$3{,}04\cdot10^3$	$5{,}9\cdot10^2$	73,0	$3{,}56\cdot10^{-5}$
12	96,1	$5{,}1\cdot10^2$	$2{,}15\cdot10^{-6}$	$4{,}66\cdot10^3$	$5{,}8\cdot10^2$	70,0	$3{,}5\cdot10^{-5}$
13	95,1	$4{,}7\cdot10^2$	$2{,}05\cdot10^{-6}$	$5{,}27\cdot10^3$	$5{,}6\cdot10^2$	66,0	$3{,}43\cdot10^{-5}$
14	94,2	$4{,}7\cdot10^2$	$2{,}01\cdot10^{-6}$	$5{,}90\cdot10^3$	$5{,}5\cdot10^2$	65,0	$3{,}47\cdot10^{-5}$
15	93,4	$4{,}5\cdot10^2$	$1{,}98\cdot10^{-6}$	$6{,}13\cdot10^3$	$5{,}5\cdot10^2$	64,0	$3{,}39\cdot10^{-5}$

/25

Phase Velocity v_{ph}, cm/sec	Maximum Fading Frequency f_{max}, Hz	Electron Concentration n_e, cm^{-3}	Minimum Ion Current Density $j_{i\,min}$, CGSU	Minimum Electron Current Density $j_{e\,min}$, CGSU	Maximum Ion Current Density $j_{i\,max}$, CGSU	Maximum Electron Current Density $j_{e\,max}$, CGSU
9	10	11	12	13	14	15
$3{,}96\cdot10^3$	34	$1{,}15\cdot10^6$	$2{,}12\cdot10^3$	0,437	$2{,}05\cdot10^4$	4,23
$6{,}75\cdot10^3$	74	$1{,}04\cdot10^6$	$6{,}87\cdot10^2$	0,52	$7{,}67\cdot10^3$	6,57
$9{,}93\cdot10^3$	153	$7{,}83\cdot10^5$	$2{,}17\cdot10^2$	0,60	$2{,}58\cdot10^3$	7,2
$1{,}3\cdot10^4$	223	$6{,}85\cdot10^5$	$1{,}15\cdot10^2$	0,675	$1{,}45\cdot10^3$	8,47
$1{,}89\cdot10^4$	380	$6{,}3\cdot10^5$	53,7	0,79	$7{,}58\cdot10^2$	11,2
$2{,}49\cdot10^4$	545	$5{,}15\cdot10^5$	30	0,854	$4{,}22\cdot10^2$	12,2
$3{,}13\cdot10^4$	730	$4{,}61\cdot10^5$	19,2	0,925	$2{,}77\cdot10^2$	13,7
$4\cdot10^4$	990	$3{,}9\cdot10^5$	11,1	0,945	$1{,}68\cdot10^2$	14,8
$4{,}72\cdot10^4$	1240	$3{,}04\cdot10^5$	6,62	0,860	$1{,}05\cdot10^2$	13,3
$5{,}18\cdot10^4$	1400	$2{,}87\cdot10^5$	5,37	0,810	85	13,7
$6{,}4\cdot10^4$	1760	$2{,}8\cdot10^5$	4,12	1,01	66,7	16,5
$8{,}75\cdot10^4$	2500	$8{,}61\cdot10^5$	2,62	1,30	42,7	21,7
$1{,}00\cdot10^5$	3000	$1{,}93\cdot10^5$	1,51	1,06	25,4	17,7
$1{,}13\cdot10^5$	3500	$1{,}59\cdot10^5$	1,07	0,985	18,2	16,7
$1{,}19\cdot10^5$	3720	$1{,}26\cdot10^5$	0,785	0,805	13,4	13,7

TABLE 5 (cont.)

No. 1.5

ε_n, keV	Altitude h, km	Electron Temperature T_e, °K	Electric Field (Critical) E_{cr}, CGSU	Critical Phase Velocity v'_T, cm/sec	Critical Wavelength λ_2, cm	Minimum Wavelength λ_{min}, cm
1	2	3	4	5	6	7
1	133	$3{,}5\cdot10^3$	$6{,}47\cdot10^{-6}$	$5{,}1\cdot10^2$	$1{,}3\cdot10^3$	$2{,}96\cdot10^3$
2	124	$2{,}3\cdot10^3$	$5{,}25\cdot10^{-6}$	$7{,}5\cdot10^2$	$10{,}5\cdot10^3$	$2{,}16\cdot10^3$
3	118,4	$1{,}58\cdot10^3$	$4{,}23\cdot10^{-6}$	10^3	$8{,}95\cdot10^2$	$1{,}63\cdot10^3$
4	114	$1{,}33\cdot10^3$	$3{,}88\cdot10^{-6}$	$1{,}26\cdot10^3$	$8{,}24\cdot10^2$	$1{,}44\cdot10^3$
5	110,7	$1{,}10\cdot10^3$	$3{,}55\cdot10^{-6}$	$1{,}76\cdot10^3$	$7{,}55\cdot10^2$	$1{,}25\cdot10^3$
6	107,6	$9{,}5\cdot10^2$	$3{,}21\cdot10^{-6}$	$2{,}11\cdot10^3$	$7{,}15\cdot10^2$	$1{,}11\cdot10^3$
7	105,0	$8{,}3\cdot10^2$	$2{,}93\cdot10^{-6}$	$2{,}42\cdot10^3$	$6{,}8\cdot10^2$	$1{,}06\cdot10^3$
8	102,6	$7{,}4\cdot10^2$	$2{,}74\cdot10^{-6}$	$2{,}89\cdot10^3$	$6{,}5\cdot10^2$	9,23
9	100,6	$6{,}8\cdot10^2$	$2{,}59\cdot10^{-6}$	$3{,}3\cdot10^3$	$6{,}3\cdot10^2$	81,6
10	99,0	$6{,}4\cdot10^2$	$2{,}52\cdot10^{-6}$	$3{,}5\cdot10^3$	$6{,}1\cdot10^2$	82,6
11	97,7	$6{,}1\cdot10^2$	$2{,}43\cdot10^{-6}$	$4{,}12\cdot10^3$	$6{,}0\cdot10^2$	7,96
12	96,1	$5{,}6\cdot10^2$	$2{,}37\cdot10^{-6}$	$5{,}32\cdot10^3$	$5{,}65\cdot10^2$	75,0
13	95,1	$5{,}21\cdot10^2$	$2{,}25\cdot10^{-6}$	$5{,}95\cdot10^3$	$5{,}5\cdot10^2$	71,2
14	94,2	$4{,}96\cdot10^2$	$2{,}12\cdot10^{-6}$	$6{,}46\cdot10^3$	$5{,}5\cdot10^2$	68,4
15	93,4	$4{,}80\cdot10^2$	$2{,}08\cdot10^{-6}$	$6{,}65\cdot10^3$	$5{,}5\cdot10^2$	67,0

Maximum Electric Field E_{max}, CGSU	Phase Velocity v_{ph}, cm/sec	Electron Concentration n_e, cm^{-3}	Minimum Ion Current Density $j_{i\,min}$, CGSU	Minimum Electron Current Density $j_{e\,min}$, CGSU	Maximum Ion Current Density $j_{i\,max}$, CGSU	Maximum Electron Current Density $j_{e\,max}$, CGSU
8	9	10	11	12	13	14
$5{,}67\cdot10^{-5}$	$5{,}02\cdot10^3$	$2\cdot10^6$	$3{,}13\cdot10^3$	1,08	$2{,}74\cdot10^4$	9,47
$5{,}1\cdot10^{-5}$	$8{,}2\cdot10^3$	$1{,}8\cdot10^6$	$1{,}45\cdot10^3$	1,42	$1{,}41\cdot10^4$	13,8
$4{,}65\cdot10^{-5}$	$1{,}24\cdot10^4$	$1{,}36\cdot10^6$	$4{,}48\cdot10^2$	1,43	$4{,}83\cdot10^3$	15,7
$4{,}45\cdot10^{-5}$	$1{,}56\cdot10^4$	$1{,}2\cdot10^6$	$2{,}36\cdot10^2$	1,58	$2{,}71\cdot10^3$	18,2
$4{,}25\cdot10^{-5}$	$2{,}37\cdot10^4$	$1{,}1\cdot10^6$	$1{,}19\cdot10^2$	2,01	$1{,}43\cdot10^3$	24,1
$4{,}1\cdot10^{-5}$	$3{,}05\cdot10^4$	$8{,}9\cdot10^5$	61,3	1,98	$7{,}85\cdot10^2$	25,3
$3{,}96\cdot10^{-5}$	$3{,}8\cdot10^4$	$7{,}32\cdot10^5$	2,01	2,03	$5{,}03\cdot10^2$	27,2
$3{,}84\cdot10^{-5}$	$4{,}72\cdot10^4$	$6{,}75\cdot10^5$	21,8	2,03	$3{,}05\cdot10^2$	28,6
$3{,}76\cdot10^{-5}$	$5{,}37\cdot10^4$	$5{,}26\cdot10^5$	12,8	1,83	$1{,}86\cdot10^2$	26,6
$3{,}71\cdot10^{-5}$	$6{,}40\cdot10^4$	$4{,}57\cdot10^5$	10,4	1,80	$1{,}53\cdot10^2$	26,6
$3{,}67\cdot10^{-5}$	$7{,}05\cdot10^4$	$4{,}88\cdot10^5$	7,94	2,11	$1{,}2\cdot10^2$	32,0
$3{,}59\cdot10^{-5}$	$9{,}27\cdot10^4$	$4{,}52\cdot10^5$	5,0	2,61	75,5	39,5
$3{,}52\cdot10^{-5}$	$1{,}07\cdot10^5$	$3{,}34\cdot10^5$	2,88	2,13	45,5	33,3
$3{,}48\cdot10^{-5}$	$1{,}2\cdot10^5$	$2{,}75\cdot10^5$	1,95	1,87	32,0	30,7
$3{,}44\cdot10^{-5}$	$1{,}25\cdot10^5$	$2{,}18\cdot10^5$	1,42	1,52	23,6	25,1

TABLE 5 (cont.)

No. 2.5

ε_n, keV	Altitude h, km	Electron Temperature T_e, °K	Electric Field (Critical) E_{cr}, CGSU	Critical Phase Velocity v'_T, cm/sec	Critical Wavelength λ_2, cm	Minimum Wavelength λ_{min}, cm
1	2	3	4	5	6	7
1	133	$7 \cdot 10^3$	$9{,}25 \cdot 10^{-6}$	$1{,}03 \cdot 10^3$	$1{,}82 \cdot 10^3$	$5 \cdot 10^2$
2	124	$4{,}1 \cdot 10^3$	$6{,}98 \cdot 10^{-6}$	$1{,}33 \cdot 10^3$	$1{,}41 \cdot 10^3$	$2{,}64 \cdot 10^2$
3	118,4	$2{,}9 \cdot 10^3$	$5{,}85 \cdot 10^{-6}$	$1{,}88 \cdot 10^3$	$1{,}19 \cdot 10^3$	$2{,}62 \cdot 10^2$
4	114	$2{,}4 \cdot 10^3$	$5{,}32 \cdot 10^{-6}$	$2{,}32 \cdot 10^3$	$1{,}08 \cdot 10^3$	$2{,}22 \cdot 10^2$
5	110,7	$1{,}9 \cdot 10^3$	$4{,}68 \cdot 10^{-6}$	$3{,}04 \cdot 10^3$	$9{,}77 \cdot 10^2$	$1{,}88 \cdot 10^2$
6	107,6	$1{,}6 \cdot 10^3$	$4{,}3 \cdot 10^{-6}$	$3{,}68 \cdot 10^3$	$8{,}94 \cdot 10^2$	$1{,}58 \cdot 10^2$
7	105,0	$1{,}4 \cdot 10^3$	$3{,}96 \cdot 10^{-6}$	$4{,}24 \cdot 10^3$	$8{,}48 \cdot 10^2$	$1{,}44 \cdot 10^2$
8	102,6	$1{,}2 \cdot 10^3$	$3{,}65 \cdot 10^{-6}$	$4{,}88 \cdot 10^3$	$8{,}1 \cdot 10^2$	$1{,}33 \cdot 10^2$
9	100,6	$1{,}05 \cdot 10^3$	$3{,}5 \cdot 10^{-6}$	$5{,}52 \cdot 10^3$	$7{,}2 \cdot 10^2$	$1{,}2 \cdot 10^2$
10	99,0	$9{,}8 \cdot 10^2$	$3{,}24 \cdot 10^{-6}$	$5{,}68 \cdot 10^3$	$7{,}2 \cdot 10^2$	$1{,}15 \cdot 10^2$
11	97,7	$9 \cdot 10^2$	$3{,}1 \cdot 10^{-6}$	$6{,}35 \cdot 10^3$	$7{,}0 \cdot 10^2$	$1{,}09 \cdot 10^2$
12	96,1	$8 \cdot 10^2$	$2{,}96 \cdot 10^{-6}$	$8{,}17 \cdot 10^3$	$6{,}5 \cdot 10^2$	98
13	91,1	$7 \cdot 10^2$	$2{,}14 \cdot 10^{-6}$	$8{,}37 \cdot 10^3$	$6{,}35 \cdot 10^2$	88
14	94,2	$6{,}5 \cdot 10^2$	$2{,}53 \cdot 10^{-6}$	$8{,}53 \cdot 10^3$	$6{,}16 \cdot 10^2$	82
15	93,4	$6{,}0 \cdot 10^2$	$2{,}41 \cdot 10^{-6}$	$8{,}7 \cdot 10^3$	$6{,}0 \cdot 10^2$	79

Maximum Electric Field E_{max} CGSU	Phase Velocity v_{ph}, cm/sec	Electron Concentration n_e, cm^{-3}	Minimum Ion Current Density $j_{i\,min}$, CGSU	Minimum Electron Current Density $j_{e\,min}$, CGSU	Maximum Ion Current Density $j_{i\,max}$, CGSU	Maximum Electron Current Density $j_{e\,max}$, CGSU
8	9	10	11	12	13	14
$6{,}75 \cdot 10^{-5}$	$8{,}43 \cdot 10^3$	$6 \cdot 10^6$	$1{,}9 \cdot 10^4$	6,55	$1{,}39 \cdot 10^5$	47,8
$5{,}9 \cdot 10^{-5}$	$1{,}27 \cdot 10^4$	$5{,}4 \cdot 10^6$	$5{,}8 \cdot 10^3$	7,52	$4{,}9 \cdot 10^4$	63,8
$5{,}31 \cdot 10^{-5}$	$1{,}91 \cdot 10^4$	$4{,}18 \cdot 10^6$	$1{,}84 \cdot 10^3$	8,0	$1{,}67 \cdot 10^4$	72,7
$5{,}16 \cdot 10^{-5}$	$2{,}52 \cdot 10^4$	$3{,}6 \cdot 10^6$	$9{,}62 \cdot 10^2$	8,72	$9{,}33 \cdot 10^3$	84,7
$4{,}86 \cdot 10^{-5}$	$3{,}54 \cdot 10^4$	$3{,}3 \cdot 10^6$	$4{,}72 \cdot 10^2$	10,4	$4{,}91 \cdot 10^3$	108
$4{,}66 \cdot 10^{-5}$	$4{,}53 \cdot 10^4$	$2{,}7 \cdot 10^6$	$2{,}45 \cdot 10^2$	10,3	$2{,}66 \cdot 10^3$	112
$4{,}5 \cdot 10^{-5}$	$5{,}45 \cdot 10^4$	$2{,}4 \cdot 10^6$	$1{,}51 \cdot 10^2$	10,6	$1{,}72 \cdot 10^3$	112
$4{,}33 \cdot 10^{-5}$	$6{,}53 \cdot 10^4$	$2 \cdot 10^6$	86,8	10,0	$1{,}03 \cdot 10^3$	122
$4{,}19 \cdot 10^{-5}$	$7{,}35 \cdot 10^4$	$1{,}6 \cdot 10^6$	52,2	9,17	$6{,}26 \cdot 10^2$	110
$4{,}10 \cdot 10^{-5}$	$8 \cdot 10^4$	$1{,}5 \cdot 10^6$	40,7	7,88	$5{,}08 \cdot 10^2$	100
$4{,}03 \cdot 10^{-5}$	$9{,}33 \cdot 10^4$	$1{,}4 \cdot 10^6$	30,3	10,0	$3{,}94 \cdot 10^2$	131
$3{,}92 \cdot 10^{-5}$	$1{,}23 \cdot 10^5$	$1{,}3 \cdot 10^6$	18,6	11,3	$2{,}47 \cdot 10^2$	149
$3{,}8 \cdot 10^{-5}$	$1{,}34 \cdot 10^5$	$1{,}1 \cdot 10^6$	10,8	9,23	$1{,}58 \cdot 10^2$	133
$3{,}7 \cdot 10^{-5}$	$1{,}46 \cdot 10^5$	$8{,}3 \cdot 10^5$	6,97	7,63	$1{,}02 \cdot 10^2$	110
$3{,}65 \cdot 10^{-5}$	$1{,}48 \cdot 10^5$	$6{,}5 \cdot 10^5$	4,92	5,9	74,5	89,5

On the Nature of Auroral Dispersing Centers

One of the main problems of auroral physics is connected with explaining the existence of radio reflections in the 30-1000 MHz frequency range from zones of sporadic ionization connected with aurorae and explaining the known characteristics of such radio reflections.

At the present time Booker's theory seems to be the most acceptable [42]. /26 In the opinion of Booker and many other investigators who adhere to his point of view, radar reflections are caused by noncoherent scattering on small, weak ($\Delta n_e/n_e \sim 10^{-3}$-$10^{-4}$) inhomogeneities of auroral ionization, stretched along the magnetic pole. Dimensions of inhomogeneities in the transverse direction (perpendicular to the magnetic field) are on the order of the wavelength of the scattered signal; in the longitudinal direction the dimensions of inhomogeneities do not exceed several tens of wavelengths. Conclusions based on the theoretical results of Booker and his followers are satisfactorily included within the limits of known experimental data, especially in that part of the theory which reflects the electromagnetic side of the question. Evidently the theory of scattering of small, weak inhomogeneities gives a correct concept of the nature of inhomogeneities. However, certain experimental data, with which we will deal below, place one of the basic assumptions of Booker's theory in doubt; namely, the volume scattering from the totality of statistically independent reflectors; i.e., reflectors whose location and velocity are in no way connected functionally.

Meanwhile Seed [70], having performed an analysis of the elementary values of radar signal amplitude as a function of distance, showed that reflections are caused by the totality of radiators, the space distribution of which is more similar to distribution on a certain plane than a homogeneous filling of some volume of space with approximately equal scales along three axes. The results of studying time variations of signals also do not enter the simple scheme originally proposed by Booker.

The amplitude distribution of signal variations, scattered by the totality of statistically independent inhomogeneities, must be a Rayleigh distribution; indeed, it is usually near the "displaced" Gaussian distribution. This indicates that in addition to the noncoherent component there is a coherent component which often prevails. /27 The frequency spectrum of fading analyzed on a sonograph [5] gave a "band" pattern corresponding to the relative motion of several quasistationary scattering structures.

In Figure 5 we see that the fundamental fading frequencies are concentrated in the bands near 2 and 6 KHz; moreover, there are some individual, rather narrow, monochromatic lines in various regions of the spectrum. All of this indicates that in addition to the relatively slow, disordered shift within the scattering struc-

tures, the structures themselves move relative to one another at significant velocities. The presence of monochromatic lines may be explained by

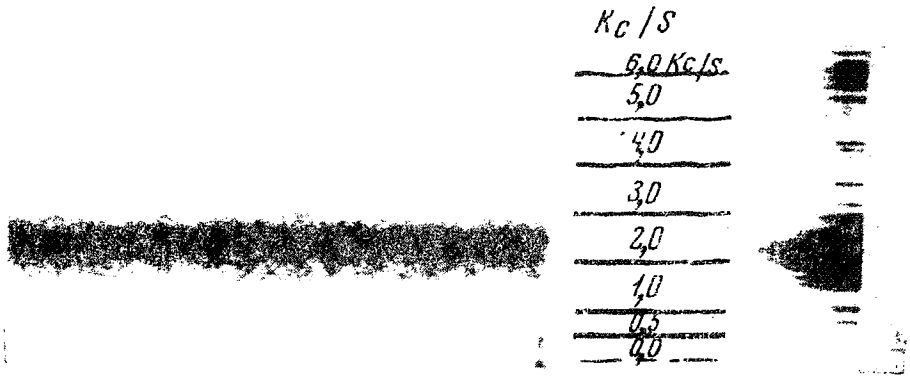

Fig. 5. Sonogram of Auroral Fading of February 23, 1960 (22 hr 45 min Central European Time).

the fact that in this case pairs of quasistationary structures have /28 significant relative velocities. The proposed interpretation of broad bands at 2 and 6 kHz is now unique. Indeed, if reflection takes place from a great accumulation of ordered structures, each of which may be considered stationary but the relative motions of these structures having a certain velocity distribution, we may unite both characteristic-spectral types (band and line) into one model which may be described as follows.

(1) The basic scattering element of the auroral reflecting region is a plane periodic structure with elements extended along force lines, a basic dimension comparable to the wavelength of the sounding pulse and a lifespan much longer than the minimum period of fading.

(2) There is a sufficient number of such plane scattering structures in the auroral reflecting region and their relative velocities may be weakly correlated (quasistable spectrum) or correlated according to individual groups (line spectrum). There are also pairs of structures with effective reflectances sufficient to produce individual lines on a sonogram.

(3) The relative motion of the structures is not connected with the displacement of matter (actually, the frequency 2 kHz at a wavelength of 3 m corresponds to a velocity of 3 km/sec), but is connected with the phase velocity of the motion of small increases in electron concentration.

The proposed model keeps several features of Booker's system; i.e., scattering of small inhomogeneities of electron concentration (almost the entire electrodynamic part of Booker's theory). But we decisively reject the statistical independence of each scattering element; i.e., the hypothesis which arose from the assumption

of a turbulent nature of electron concentration fluctuations. Thus we avoid two difficulties which proved to be insurmountable within the framework of Booker's theory: the non-Rayleigh distribution of amplitudes and the line-band nature of the fading spectrum. It is necessary to note that the very hypothesis of anisotropically-developed turbulence in the auroral plasma is also not lacking critics. The fact of the matter is that at auroral altitudes the density of the neutral atmospheric component is 5-7 orders of magnitude greater than the electron gas density. Due to the mass equilibrium of ions and neutral particles, the pulse-induced exchange between these ionospheric components must be very intense. Consequently, the appearance of turbulence in the electron-ion gas must slowly cause the appearance of turbulent motion even in a neutral gas; i.e., in essence we must accept the hypothesis of the existence of general turbulence in the atmosphere. It is clear that such turbulence will not be anisotropic since the magnetic field does not influence neutral particle motion. Such turbulence is difficult to connect with auroral ionization regions if we assume that sources of turbulence are displaced in neutral gas. If we assume that they are displaced only in the ionized component, then the power density of energy sources for the turbulence must exceed the density of thermal energy in the ionized gas by several orders of magnitude. Actually, in order to create fluctuations of electron concentration on the order of $10^{-3}n_e$ by making the entire atmosphere turbulent, it is necessary to create fluctuations of pressure on the order of 10^{-3} (we consider the temperature to be unchanged) in the atmosphere:

$$\frac{\Delta p_N}{p_N} = \frac{\rho_N (\Delta u)^2}{p_N} = 10^{-3}, \tag{13}$$

i.e., the energy density of the turbulent motion must be /29

$$\rho_N (\Delta u)^2 \sim 10^{-3} p_N .$$

But this energy density is nearly 1000 times greater than the energy density of thermal motion of the ionized component:

$$\frac{\rho_N (\Delta u)^2}{p_i} \sim 10^{-3} \frac{NkT_N}{n_e kT_i} \sim 10^{-3} \frac{N}{n_e}. \tag{14}$$

If we consider that only the electron gas is encompassed by turbulent motion, then the difficulty with very powerful pulse scattering is eliminated due to the transmission of a quantity of motion from the ion gas to the neutral gas, since the great difference in masses between the electron and the "heavy" components makes this process slow. But now the difficulty arises: the existence of density fluctuation of the electron gas alone leads to the appearance of fluctuation of the space discharge, and this in turn causes the appearance of waves in the plasma and individual fluctuations may no longer be considered independent. It is clear that the necessary great relative amplitude of such waves ($\sim 10^{-3}$) may

be expected only when these are quasineutral waves.

If we consider that scattering centers represent bundles of quasineutral waves, then the difficulties which could not be overcome within the limits of Booker's theory are eliminated. Each system of waves may be identified with an ordered scattering structure; such structures (systems of waves) may exist independently, but their phase velocities prove to be statistically connected.

As already mentioned, wave processes may be responsible for the appearance of ionospheric microstructures [54-59]. On the other hand, analysis of the gas discharge theory and of drift instabilities in plasma led to the discovery of various types of oscillations in waves [17].

Below we present a system of equations for a three-component plasma with regard to the following conditions.

(1) Since only quasineutral waves can create a noticeable excess electron-ion concentration, we shall assume that $n_e = n_i$.

(2) We shall consider that a neutral gas is at rest.

(3) Considering heat exchange between the ion gas and the neutral component, we shall assume that the ion temperature is equal to the temperature of the neutral gas and does not undergo variations.

(4) We shall consider phenomena in an altitude range wherein the following condition is satisfied:

$$\frac{e^2 n_e^2 H^2}{c^2 d_{eN}^2} > 1 > \frac{e^2 n_e^2 H^2}{c^2 d_{iN}^2}. \qquad (15)$$

Here e is the discharge of an electron; n_e is electron concentration; H is the magnetic field strength; c is the speed of light. The term $d_{eN} = m_e n_e \nu_{eN}$ is the coefficient of friction between the electron and neutral components of the plasma; $d_{iN} = m_i n_i \nu_{iN}$ is the coefficient of friction between the ion and neutral components of the plasma; ν_{eN} is the number of electron-neutral collisions; ν_{iN} is the number of ion-neutral collisions; m_e, m_i are the electron and ion mass, respectively. The numerical expression (15) corresponds to the inequality

$$2{,}9 \cdot 10^{16} \cdot T_e^{-1/2} > N > 1{,}08 \cdot 10^{14} T_i^{-1/2},$$

i.e., the altitude range from 75 to 110 km.

When (15) is satisfied, we may not consider the influence of the magnetic field on ion motion and, at the same time, we may consider that the electron gas is in a strong magnetic field. Since

up to altitudes of ~120 km the influence of the magnetic field on ion motion will still be relatively small (the approximate and precise value of the coefficient of friction will be distinguished by a factor of 1.5), we shall use the accepted approximation throughout the altitude range investigated (90-120 km). /30

(5) We shall consider that the basic supplier of energy to the auroral plasma is the fast electron stream and energy is basically removed from the plasma by means of gradientless heat transmission to the neutral gas due to collisions of electrons and ions with neutral particles. We shall consider that the electric field is such that the Joule heat liberated with the passage of current is less than the total power of the energy sources connected with dissipation of the fast electron stream.

(6) The degree of ionization is sufficiently small; i.e., $n << N$.

(7) We shall consider processes with a characteristic time $\tau_{char} > \frac{m_{in}}{d_{iN}}$, and this signifies that in the equations of motion of an ion we can ignore inertial force. In the poorest case at the 120 km level, $\tau_{char} > 10^{-2}$.

(8) We shall limit ourselves to consideration of a one-dimensional problem. The x axis is perpendicular to the vector H.

Thus the basic system of equations will have the form:

$$v_e = -\frac{c^2 d_{eN}}{e^2 n^2 H^2}\left(\frac{\partial p_e}{\partial x} + enE + \gamma_\perp \frac{\partial T_e}{\partial x}\right), \tag{16}$$

$$v_i = -\frac{1}{d_{iN}}\left(\frac{\partial p_i}{\partial x} - enE\right), \tag{17}$$

$$\frac{\partial n}{\partial x}(v_e - v_i) + n\left(\frac{\partial v_e}{\partial x} - \frac{\partial v_i}{\partial x}\right) = 0, \tag{18}$$

$$\frac{3}{2}\frac{\partial p_e}{\partial t} + \frac{5}{2}p_e\frac{\partial v_e}{\partial x} + \frac{3}{2}v_e\frac{\partial p_e}{\partial x} - \frac{\partial}{\partial x}\left(\varkappa_{\perp e}\frac{\partial T_e}{\partial x}\right) = w_{se} - w_{re}; \tag{19}$$

Here E is the electric field strength; v_e, v_i are the drift velocity of electrons and ions, respectively; p_e is the electron pressure; $\varkappa_{\perp e}$ is the perpendicular electron heat conductivity; $w_{se} = \alpha n^2 \Delta\varepsilon + (jE)$ is the power density of energy sources for electron gas; j is the electron current density. Finally,

$$w_{re} = \frac{6 d_{eN} k (T_e - T_N)}{m_N}$$

is the power density of energy discharges for the electron gas.

Let this system of equations describe small deviations from

the equilibrium state which are characterized by the conditions:

$$v_{0e} = -\frac{c^2 d_{eN}}{enH^2} E, \tag{20}$$

$$v_{0i} = \frac{en}{d_{iN}} E, \tag{21}$$

$$w_{se} = w_{re}. \tag{22}$$

Whereupon

$$\begin{aligned} v_e &= v_{0e} + u_e, & u_e &\ll v_{0e}; \\ v_i &= v_{0i} + u_i, & u_i &\ll v_{0i}; \\ T_e &= T_{0e} + \tau, & \tau &\ll T_{0e}; \\ n_e &= n_{0e} + \nu, & \nu &\ll n_{0e}. \end{aligned} \tag{23}$$

Small deviations from equilibrium values are coordinate and time functions. We shall consider that they change according to harmonic law; i.e., proportional to the factor $\exp(\beta t + gx)$, for example /31

$$\tau = \tau_0 e^{\beta t + gx}.$$

Substituting (23) into (16-19) and using (20-22), we have (after excluding v_e and v_i):

$$\left[\left(\frac{c^2 d_{eN}}{enH^2} + \frac{en}{d_{iN}}\right) E + \left(\frac{c^2 d_{eN} k T_e}{e^2 n H^2} - \frac{nk T_i}{d_{iN}}\right) g\right] \nu + \frac{c^2 d_{eNk}}{e^2 H^2}\left(\frac{eE}{kT_e} + g\right) \tau = 0; \tag{24}$$

$$\begin{aligned} &\left[(1{,}5\, kT\beta - \alpha n \Delta\varepsilon) - 1{,}5\, \frac{c^2 d_{eN} kTE}{enH^2} g - 2{,}5\, \frac{c^2 d_{eN} k^2 T_e^2}{e^2 n H^2} g^2\right] \nu + \\ &+ \left[\left(1{,}5\, kn\beta + \frac{3k d_{eN} (3T_e - T_i)}{m_i T_e} - \frac{c^2 d_{eN} E^2}{H^2 T_e}\right) - \right. \\ &\left. - \frac{2{,}75\, c^2 d_{eN} kE}{eH^2} g - \left(\varkappa_{e\perp} + 2{,}5\, \frac{c^2 d_{eN} k^2 T}{e^2 H^2}\right) g^2\right] \tau = 0. \end{aligned} \tag{25}$$

In order to simplify the recording we obtain the following symbols:

$$\begin{aligned} \left(\frac{c^2 d_{eN}}{enH^2} + \frac{en}{d_{iN}}\right) E &= a_1; & \left(\frac{c^2 d_{eN} kT_e}{e^2 n H^2} - \frac{nkT_i}{d_{iN}}\right) &= a_2; \\ \frac{c^2 d_{eN} E}{eH^2 T_e} &= a_3; & \frac{c^2 d_{eN} k}{e^2 H^2} &= a_4; \\ (1{,}5\, kT\beta - \alpha n \Delta\varepsilon) &= b_1; & 1{,}5\, \frac{c^2 d_{eN} kT_e E}{enH^2} &= b_2; \\ 2{,}5\, \frac{c^2 d_{eN} k^2 T_e^2}{e^2 n H^2} &= b_3; & \left(1{,}5\, kn\beta + \frac{3k d_{eN} (3T_e - T_i)}{m_i T_e} - \frac{c^2 d_{eN} E^2}{H^2 T_e}\right) &= b_4; \\ 2{,}75\, \frac{c^2 d_{eN} kE}{eH^2} &= b_5; & \left(\varkappa_{\perp e} + 2{,}5\, \frac{c^2 d_{eN} k^2 T_e}{e^2 H^2}\right) &= b_6. \end{aligned} \tag{26}$$

So that the systems in (24) and (25) have a meaningful solution, its determinant must be equated to zero:

$$\begin{vmatrix} (a_1 + a_2 g) & (a_3 + a_4 g) \\ (b_1 - b_2 g - b_3 g^2) & (b_4 - b_5 g - b_6 g^2) \end{vmatrix} = 0 \tag{27}$$

Relative to g, (27) is a cubic equation:

$$(a_4b_3 - a_2b_6)g^3 + (a_3b_3 + a_4b_2 - a_1b_6 - a_1b_5)g^2 + (a_2b_4 - a_1b_5 + a_3b_2 - a_4b_1)g + (a_1b_4 - a_3b_1) = 0. \quad (28)$$

Generally speaking, the values β and g entering (28) may be complex. Depending on the signs and values of the imaginary and real parts β and g, there may exist accumulating or damping waves, oscillations or aperiodic distribution of parameters in the plasma.

If $\mathrm{Im}\beta \neq 0$, $\mathrm{Im}g \neq 0$, then waves exist; if in addition $\mathrm{Re}\beta > 0$, then waves increase with time. The material part g determines the spatial decrement of damping; i.e., the dimensions of the wave system in space. With the aid of (28) it is not only possible to connect two parameters (for example, the imaginary parts β and g), but also the third and fourth parameters remain arbitrary if no physical limitations can be imposed upon them. The spatial decrement of damping in our case interests us least of all, because we shall simply consider that spatial damping is absent. Thus, we designate:

$$g = ik, \quad \beta = \delta + i\omega. \quad (29)$$

Substituting (29) into (28) we obtain two equations: /32

$$\omega = k^3 \frac{(a_3b_3 - a_2b_6)}{1{,}5\,k\,(a_1n - a_3T_e)} - k\,\frac{(a_3b_2 - a_1b_5 - a_4c_1 + a_2c_2)}{1{,}5k\,(a_1n - a_3T_e)}; \quad (30)$$

$$k^4 - k^2\left[\frac{(a_1n - a_3T_e)(a_3b_3 + a_4b_2 - a_1b_6 - a_2b_5)}{(a_4T_e - a_2n)(a_4b_3 - a_2b_6)} + \frac{(a_3b_2 - a_1b_5 - a_4c_1 + a_2c_2)}{a_4b_3 - a_2b_6}\right] + \frac{(a_1c_2 - a_3c_1)(a_1n - a_3T_e)}{(a_4b_3 - a_2b_6)(a_4T_e - a_2n)} = 0, \quad (31)$$

where $c_1 = 1{,}5\,kT_e\delta - \alpha n\Delta\varepsilon$; $c_2 = 1{,}5\,kn\delta + \frac{3kd_{eN}(3T_e - T_i)}{m_iT_e} - \frac{c^2d_{eN}E^2}{H^2T_e}$.

Excluding δ from these equations, we may obtain a connection between k and ω; i.e., a dispersion equation. However, the solutions of (30) and (31) have several peculiarities. Numerical analysis of the coefficients entering here $a_1, a_2, \ldots, a_4$ and $b_1, b_2, \ldots, b_6$ indicates that in the altitude range we are investigating (90-120 km) the coefficients a_3, a_4, b_2, b_3 and b_5 are small and do not essentially influence the solution. Considering this circumstance for (31) we have

$$k^4 + \left[\left(\frac{a_1}{a_2}\right)^2 + \frac{c_2}{b_6}\right]k^2 + \left(\frac{a_1}{a_2}\right)^2\frac{c_2}{b_6} = 0. \quad (32)$$

Consequently,

$$k_{1,2,3,4} = \pm\sqrt{\frac{-\left[\left(\frac{a_1}{a_2}\right)^2 + \frac{c_2}{b_6}\right] \pm \sqrt{\left[\left(\frac{a_1}{a_2}\right)^2 - \frac{c_2}{b_6}\right]^2}}{2}}, \quad (33)$$

i.e.,

$$k_{1,2} = \pm \sqrt{-\frac{c_2}{b_6}}; \quad k_{3,4} = \pm i \left(\frac{a_1}{a_2}\right). \tag{34}$$

In order that our solution describe the space-periodic structure, it is necessary that k be a material number; i.e., $c_2 < 0$. Otherwise the existence condition of space-periodicity has the form:

$$\frac{c^2 d_{eN} E^2}{H^2} > 1{,}5\, nkT_e\delta + \frac{3k d_{eN}(3T_e - T_N)}{m_i}. \tag{35}$$

In (30) we divide the right- and left-hand sides by k. Considering that ω/k is the phase velocity of waves v_{ph} and also the smallness of the coefficients a_3, a_4, b_2, b_3 and b_5 we have

$$v_{ph} = 1{,}83\frac{b_5}{kn} = 1{,}83\frac{c^2 d_{eN}}{enH^2}E. \tag{36}$$

We rewrite (35) in the form

$$\delta < \frac{2c^2 d_{eN} E^2}{3p_e H^2} - \frac{3d_{eN} k(3T_e - T_i)}{p_e m_i}. \tag{37}$$

The behavior of the waves we are considering will depend on the sign δ. Where $\delta > 0$ oscillations will increase; where $\delta < 0$ they will be extinguished. Consequently, the existence condition for increasing oscillations is such that

$$E^2_{min} \geqslant \frac{3k(3T_e - T_i)}{m_i c^2} H^2. \tag{38}$$

Inequality (38) signifies that a certain minimum value of the electric field exists at which the oscillating process begins to increase; this minimum value is such that the power density of Joule heat sources is greater than the power density of energy discharges. This signifies that the electron temperature in the region where increasing oscillations arise must also increase with time. Then /33 the increased decrement δ also determines the characteristic time for temperature increase τ_{therm}

$$\tau_{therm} = \delta^{-1}. \tag{39}$$

We shall conditionally consider that τ_{therm}, i.e., the time after which the temperature of the volume including the inhomogeneities substantially changes, is also the "lifespan" of our system of inhomogeneities (indeed, the latter may even be greater). It is clear that we shall be able to record a signal scattered by a given system of inhomogeneities only in the case where the amplitude of oscillations of electron concentrations in the wave exceeds a certain level. It is customarily considered [9, 48] that for this it is necessary for the ratio $\Delta n_e/n_e$ to exceed $3\cdot10^{-4}$-10^{-3}. In the following discussion we shall use the value 10^{-3} for this ratio. From the system of equations in (24) and (25), the amplitude values

may not be obtained since the system is linear. However, it is possible to evaluate $\Delta n/n$ from simple considerations. Actually, where $\delta > 0$ a "contraction" of the plasma toward the nucleus of an inhomogeneity takes place after a time $\tau_\delta \sim 2\pi/\delta$. The rate of "contraction" is $u \sim l/\tau$, where l is the size of the inhomogeneity. Thus,

$$u = \frac{\delta}{k}. \tag{40}$$

The particle flux toward the center of the inhomogeneity is $\sim nu$. At the same time, due to thermal motion, some of the background particles enter the region of inhomogeneity and their flux is $\sim nv_T$; the rest of the particles leave the region of inhomogeneity and their flux is $-(n + \Delta n)\cdot v_T$; consequently the particle flux leaving the inhomogeneity due to the thermal motion is equal to $\Delta n v_T$.

We shall define the time τ_d as that necessary for reaching the critical value Δn at the moment when the fluxes are equalized. Then

$$\frac{n\delta}{k} \sim \Delta n v_T, \tag{41}$$

and

$$\delta \sim \left(\frac{\Delta n}{n}\right) v_T k, \tag{42}$$

or

$$\left(\frac{\Delta n}{n}\right) \sim \frac{\delta}{v_T k}. \tag{43}$$

For this level of scattering to be reached it is necessary that

$$\tau_{\text{therm}} \geqslant \tau\delta, \tag{44}$$

or

$$\delta \leqslant \left(\frac{\Delta n}{n}\right) v_T k. \tag{45}$$

Conditions (44) or (45) provide us with the possibility of independently evaluating the increment of increase (or the lifespan) of the system of inhomogeneities arising due to "wave instability" of the ionospheric plasma with the passage of electric current through it.

In (45) v_T is the thermal velocity of ions equal to $(8\,kT_N/\pi m_2)^{1/2}$. The relationship in (45) lends a new sense to (34)-(36); i.e., the sign δ proves to be independent of the sign k. But according to (36) the sign depends on field direction; i.e., the system of waves moving in the direction of the electric field increases and the system of waves with a phase velocity directed against the field is damped. For the greater possible value of δ_m we have

$$\delta_m = \left(\frac{\Delta n}{n}\right) v_T k_m.$$

Substituting δ_m in place of δ into (34) and considering that /34

$$\varkappa_{\perp e} = 4{,}66\frac{c^2 d_{eN} k^2 T_e}{e^2 H^2}, \tag{46}$$

for k_m we find

$$k_m = -\frac{0{,}105 P_e \left(\frac{\Delta n}{n}\right) v_\tau e^2 H^2}{(kT_e)^2 c^2 d_{eN}} + \sqrt{\frac{1{,}1\cdot 10^{-2} p_e^2 \left(\frac{\Delta n}{n}\right)^2 v_\tau^2 e^4 H^4}{(kT_e)^4 c^4 d_{eN}^2} + 01{,}4\frac{c^2 E^2}{(kT_e)^2} - \frac{0{,}418 k (3T_e - T_i) e^2 H^2}{(kT_e)^2 m_i c^2}}. \tag{47}$$

In a more compact form it is possible to write:

$$k_m = \frac{0{,}205 n e^2 H^2}{c^2 d_{eN} k T_e}\left[-0{,}515\left(\frac{\Delta n}{n}\right) v_\tau - \sqrt{v_{\text{ph}}^2 - (v_\tau')^2}\right], \tag{48}$$

where

$$(v_\tau')^2 = \left[\frac{10k(3T_e - T_N)}{m_i}\frac{c^2 d_{eN}^2}{n^2 e^2 H^2} - 0{,}264\left(\frac{\Delta n}{n}\right)^2 \frac{8kT_N}{\pi m_i}\right], \tag{49}$$

and v_{ph} is given by (36).

Thus we have found a connection between the phase velocity of a wave and the electric field strength by (36), on the one hand, and between the phase velocity and "dimension of inhomogeneities" on the other. As a "dimension of inhomogeneities" we shall assume the value $z = \frac{\pi}{2}k^{-1}$; i.e., one-fourth of the wavelength for our wave system.

From (45) it is possible to evaluate the effective lifespan of a wave system; i.e., the time during which it scatters a signal at a given frequency with sufficient intensity. Let us arbitrarily consider that the dimension of the inhomogeneity is equal to one-fourth of the wavelength of the scattered radio emission and the effective lifespan to be 0.6 τ_m. Then

$$\tau_s = 0{,}15\frac{\lambda}{v_\tau}\left(\frac{\Delta n}{n}\right)^{-1}. \tag{50}$$

For the level 105-110 km this time totals approximately 1.5-2 sec for λ = 4 m.

If there are few reflecting systems, as occurs in the case of weak ODS-type signals [72], the radar must record well-defined, long-period fadings with $\tau \sim$ 1-2 sec. Actually we noted such fadings during observations at Tiksi in 1958-59, but as a rule, their period was greater (10-15 sec).[5]

On the basis of ray arc models we will perform calculations of

---

[5] Modulation in such cases is usually very deep, at times close to the disappearance of the signal.

the two basic parameters of radio reflecting regions v_{ph} and l as a function of the electric field strength E. But before beginning to describe the calculation, let us make some comments of a general nature.

(1) Conclusions on the basis of a model provide a purely qualitative description of conditions in the auroral ionosphere, and numerical results have only an illustrative significance.

(2) Scattering wave structures arise under essentially nonstationary conditions when the electron temperature increases due to a noncompensated excess of Joule heat. Therefore the above-described models essentially give the physical conditions in the aurora before the appearance of reflections, but with the increase in /35 temperature still greater electric fields are necessary to maintain the same reflection characteristics. If this condition is satisfied (i.e., the electric field increases), then the existence of a scattering structure in the same spatial region may several times exceed the effective lifespan assumed in (50).

(3) All the numerical coefficients and the very nature of the approximation assumed in (32) do not give a basis for relating numerical results to anything other than an illustration of the qualitative theory.

Let us now turn to a calculation of the coefficients in (16) and (19). The coefficients of friction between the electron gas and the neutral component $d_{\perp eN}$ and between the ion gas and the neutral component $d_{\perp iN}$ (with regard to the action of the magnetic field), the coefficient of transverse heat conductivity of the electron gas $\kappa_{\perp e}$ and the coefficient of thermal force $\gamma_{\perp}$ enter here. The coefficient of friction relative to the magnetic field is not difficult to obtain, knowing the expression for these coefficients in the absence of a magnetic field. We shall simply designate them by d_{eN} and d_{iN}, respectively. In [73] equations for d_{ei} are given, and it is easy to generalize them to the case of electron and ion interaction with neutral particles. We have

$$d_{eN} = 0{,}513 m_e n \vartheta_{eN}, \tag{51}$$

$$d_{iN} = 0{,}513 m_i n \vartheta_{iN}. \tag{52}$$

From equations written with regard to conditions where $\tau_{char} > \frac{m_{in}}{d_{in}}$, we have

$$\nabla p_e + en\boldsymbol{E} + d_{eN}\boldsymbol{v}_e + \gamma_{\perp}\nabla T_e + \frac{[\boldsymbol{v}\boldsymbol{H}]en}{c} = 0, \tag{53}$$

$$\nabla p_i - en\boldsymbol{E} + d_{iN}\boldsymbol{v}_i - \frac{[\boldsymbol{v}\boldsymbol{H}]en}{c} = 0. \tag{54}$$

Under the condition that only x-components exist for E, ∇p and ∇T and only z-components for H, we find:

$$\nabla_x p_e + enE_x + \gamma_\perp \nabla_x T_e + d_{\perp eN} v_{ex} = 0, \quad (55)$$

$$\nabla_x p_i - enE_x + d_{\perp iN} v_{ix} = 0, \quad (56)$$

where

$$d_{\perp eN} = d_{eN}\left[1 + \left(\frac{enH_z}{cd_{eN}}\right)^2\right],$$

$$d_{\perp iN} = d_{iN}\left[1 + \left(\frac{enH_z}{cd_{iN}}\right)^2\right].$$

Considering (24) we have

$$d_{\perp eN} = \frac{e^2 n^2 H_z^2}{c^2 d_{eN}}, \quad (57)$$

$$d_{\perp iN} = d_{iN}. \quad (58)$$

According to [73], the coefficient of thermal force has the form:

$$\gamma_\perp = 5{,}1nk\left(\frac{cd_{eN}}{enH}\right)^2. \quad (59)$$

In the altitude range under consideration, $\gamma_\perp$ is negligibly small, since

$$\left(\frac{c^2 d_{eN}}{enH}\right)^2 \ll 1.$$

The accuracy with which most coefficients were calculated evi- /36
dently does not exceed 20%, but in extreme cases it reaches 200%.

Let us now turn to a description of the calculations of the parameters characterizing the system of inhomogeneities responsible for scattering radio waves of the ultrashort wave band.

At first the values of $(v_T')^2$ were calculated; data on temperature, electron concentration and neutral particle concentration were taken from the results of calculating ray arc models. Then values for the critical electric field strength were found from the condition $k_m = 0$, i.e. practically $v_f = v_T'$. Then applying (36), we obtain

$$E_k = 0{,}547\frac{enH^2}{c^2 d_{eN}} v_T'. \quad (60)$$

The condition $k_m = 0$ defines the region of imaginary k, where the space-periodic structure does not exist, from the region of real k where the space-periodic structure, with an amplitude increasing in time, must exist. Consequently the condition $E > E_k$ at the same time is a condition for the appearance of periodic inhomogeneities.

The calculated values of E_k for a ray form of No. 1, 1.5 and 2.5 aurorae are given in Table 5.

For the case $v_{ph} > > v'_T$ we have

$$k_m = 0{,}205 \frac{ne^2H^2}{c^2 d_{eN} kT_e} \cdot v_{ph}. \quad (36)$$

Or, substituting the expression from (36) for v_{ph} we obtain a simple formula

$$k_m = 0{,}375 \frac{eE}{kT_e}. \quad (61)$$

For l_m (the length of a diffusion wave) we have

$$l_m = 16{,}8 \frac{kT}{eE}. \quad (62)$$

Evidently, it is necessary to understand "dimension of inhomogeneity" to mean the dimension of a region adjacent to the antinode of electron concentrations where the electron concentration is still not less than 1/3 of the maximum (in the antinode). The size of such a region amounts to 1/4 l_m. Then we have

$$l = 0{,}25 l_m. \quad (63)$$

By establishing the condition that the size of an elementary inhomogeneity is equal to 1/4 the wavelength of the sounding radio emission, we obtain a condition connecting the temperature T_e, the wavelength λ and the electric field strength E:

$$E = 4{,}8 \cdot 10^{-6} \frac{T_e}{\lambda}. \quad (64)$$

Let us attempt to evaluate the range of radio frequencies effectively scattered by wave systems of inhomogeneity from this condition.

Evidently where $v_{ph} \simeq v'_T$, $k_m \to 0$ the appearance of diffusion waves of any length is possible. However, even small fluctuations of the energy flux of fast electrons easily disturbs the condition in (38); therefore, the solution in the case of $v_{ph} \simeq v'_T$ will be very unstable.

Let the minimum value of the phase velocity be determined by the condition $v_{ph}^{min} = 2v'_T$. This limitation determines the upper limit of possible dimensions of inhomogeneities. The lower limit is somewhat more complicated to evaluate. From physical considerations it is clear that the electric field may not exceed the limit at /37
which ionization by electron impact of plasma electrons accelerated in the electric field begins to arise (i.e., independent discharge begins).

Although it is impossible to completely ignore such a possibility, at the present time a "purely discharge" conception of aurora is obviously little successful. We may also use one more strict physical limitation which indeed is related to the question of the limits of applicability for the theorem. Above we noted that we can ignore the inertial forces of protons:

$$\omega_m = v_{\text{ph}} k_m \ll \frac{2\pi d_{iN}}{m_i n}, \tag{65}$$

i.e., the maximum phase velocity at which (32) remains valid is

$$(v_{\text{ph}} k_m)^{\max} = \frac{2\pi d_{iN}}{m_i n}.$$

Considering (36) and (61), we may find an expression for electric field strength

$$E^{\max} = 3H \left(\frac{d_{iN}}{d_{eN}}\right)^{1/2} \left(\frac{kT_e}{m_i c^2}\right)^{1/2}. \tag{66}$$

Finally, for the maximum phase velocity and the minimum wavelength on the basis of (62), (64), (66) we have convenient calculation formulas:

$$\lambda^{\min} = \frac{4{,}8 \cdot 10^{-6} T_e}{E^{\max}}, \tag{67}$$

$$v_{\text{ph}}^{\max} = 3 \cdot 10^{-6} N T_e^{1/2} E^{\max}. \tag{68}$$

Here it is considered that

$$d_{eN} = 3{,}47 \cdot 10^{-37} N n T_e^{1/2},$$

$$d_{iN} = 7{,}45 \cdot 10^{-35} N n T_i^{1/2}.$$

Finally, it is useful to evaluate the maximum possible value of the fading rate. Fadings will, for example, occur in the case where there is interference of radio waves scattered from two systems of diffusion waves, appearing in two regions with uniform electric fields and equal electron temperatures [the equality $(T_e/E)_1 = (T_e/E)_2$ is important], but with different neutral component concentrations. Then

$$f^{\max} = \frac{2[v_1^{\max} - v_2^{\max}]}{\lambda^{\max}}.$$

As a convenient characteristic of the maximum fading rate we have the value

$$f^{\max} = \frac{2v^{\max}}{\lambda^{\max}}. \tag{69}$$

It is easy to be convinced that this value is a function of neutral

particle concentration.

For No. 1, 1.5 and 2.5 ray arcs the parameters $E^{\max}$, $\lambda^{\min}$, $v_{ph}^{\max}$ /38 and $f^{\max}$ are presented in Table 5, as well as the parameter

$$\lambda_2 = \frac{2.4 \cdot 10^{-6} T_e}{E_k}. \tag{70}$$

The wavelength of radio emission scattered by inhomogeneities at a minimum phase velocity is equal to $v_{ph}^{\min} = 2v_T'$.

Of course all these parameters characterize the reflecting region only qualitatively, since the possibility of obtaining a significant reflective signal depends not only on the dimensions of the inhomogeneities but also on their number, orientation, the absolute value of Δn_e and, certainly, on the fundamental parameters of the equipment. A three-dimensional reflecting inhomogeneity may be conveniently characterized by a triaxial ellipsoid, with one semiaxis parallel to the direction of the magnetic field, another parallel to the direction of the electric field and the third perpendicular to the first two. Let $a \parallel E$, $b \parallel H$ and $(cE) = (cH) = (EH) = 0$, respectively.

Then for the case of backscattering we have:

$$P_{\text{scat}} = \frac{\pi^3 P_t \cdot G^2 \lambda^2}{4R_0^4} \frac{a^2 b^2 c^2}{\lambda_n^4} \left(\frac{\Delta n}{n}\right)^2 \frac{I_1\left(\frac{4\pi a \sin\xi}{\lambda}\right)}{\frac{4\pi a}{\lambda}\sin\xi} \cdot \exp\left[-\frac{8\pi^2}{\lambda^2}(b^2\sin^2\varphi + c^2\sin^2\psi)\right], \tag{71}$$

where P_t is the power of the transmitter; λ is the wavelength of the sounding pulse; G is antenna gain; R_0 is the distance to the target; λ_n is the critical wavelength for the given background electron concentration; P_{scat} is the power of the scattered emission; ξ, ϕ and ψ are the complements of angles between the axes and the wave vector of the radio wave up to 90°.

In the given case $a = L$ is the dimension of the inhomogeneity connected to the length of the diffusion waves in (62), (63). The values b and c are not defined in our problem, since in the case of plane waves it is necessary to assume $b = c = \infty$. However, due to inhomogeneities of the field E in each area of space with the characteristic dimensions

$$B_y = \frac{E_x}{\frac{dE_x}{dy}} \text{ and } c_z = \frac{E_x}{\frac{dE_x}{dz}}, \tag{72}$$

its own system of waves will exist. Consequently it is possible to set $b = B_y$, $c = c_z$. These values will to a certain degree determine

the sensitivity of reflection aspect according to position angle and azimuth, but evidently the sensitivity aspect is a statistical effect to a great degree.

Actually, since $b > > \lambda$ and $a > > \lambda$, the reflection from an elementary reflecting surface (a diffusion wave front) will be almost mirror-like. Since $\xi \approx 90°$ and ϕ and $\psi \approx 0°$, the index of the exponent in (71) may be rewritten as $-\frac{8\pi^2}{\lambda^2}(b^2\phi^2 + a^2\psi^2)$.

Since b and a are much greater than λ, even with small deviations of ϕ and ψ from zero the right-hand side of (71) is near zero. Only for angles of ϕ and ψ near zero does P_{scat} prove to be finite.

All these considerations relate to one elementary reflecting system. Indeed, there are evidently very many such reflecting systems because the vector of the electric field strength of an ionospheric current always has E_y and E_z components which are variable in time and space and not equal to zero. Thus quasiplane reflecting surfaces are positioned in space at very different angles to the x axis and to the wave vector of an incident electromagnetic wave. A certain number of such surfaces will always be "fortunately" located relative to the radar equipment. If the angular distribution of fundamental normals to the reflecting surfaces a is $N(\phi, \psi)$, then considering that /39

$$\lambda_n^4 = \frac{1{,}25 \cdot 10^{26}}{n^2},$$

for P_{scat} we have

$$P_{scat} = 3{,}14 \cdot 10^{-27} \frac{P_t G^2 \lambda^2 (\Delta n)^2}{R_0^4} a^2 b^2 c^2 \frac{\lambda}{4\pi a} I_1\left(\frac{4\pi a}{\lambda}\right) \cdot \iint \exp\left[-\frac{8\pi^2}{\lambda^2}(b^2\varphi^2 + c^2\psi^2)\right] N(\varphi, \psi)\, d\varphi d\psi. \quad (73)$$

If we accept the parameters of the Yakutsk radar as typical values: $\frac{P_{scat}}{P_t} \sim 10^{-18}$; $G = 30$; $\lambda = 4 \cdot 10^2$ cm; $R_0 = 5 \cdot 10^7$ cm, and we give $10^2 \cdot (4 \cdot 10^4) \cdot (4 \cdot 10^4)$ cm as dimensions of the reflecting region then with $\Delta n \sim 10^3$ cm^{-3}, we obtain that $\sim 10^3$-10^4 of oriented reflecting surfaces is properly necessary. In addition, $\phi \sim \psi \sim 10'$.

If we assume that the magnetic field reliably fixes the position of the b axis so that angle $\phi = 0$ and reflecting surfaces are distributed isotropically in space according to the angle ψ, then we find that approximately only 10^{-6} surfaces will be oriented according to ψ; i.e., ψ proves to be less than $10'$ and it will be possible to register reflection from it.

We assume that the region of reflections occupies a volume of $10^7 \cdot 10^7 \cdot 10^6$ cm^3 and is densely filled with reflecting surfaces, then the number of reflections proves to be equal to approximately 10^9.

If they are ideally oriented according to ϕ and disordered according to ψ, then 10^3 of them will reflect in the necessary direction. Indeed, the distribution according to ϕ is not strict but it is usually fixed with an accuracy of up to 1-3°. This decreases the "selection factor" from 10^{-6} to 10^{-7}-10^{-8}; then a certain order must be observed in orientation according to ψ.

Conditionally it is possible to consider that the ψ are isotropically distributed within limits of angles of approximately 30°. Then the "selection factor" increases up to a value of $\sim 10^{-4}$-$5 \cdot 10^{-4}$. And if the radar equipment is appropriately positioned relative to the median direction, around which the position of surfaces varies according to ψ, then the number of effectively-reflecting inhomogeneities increases from 10^3 to 10^5-$5 \cdot 10^5$, and this signifies that for Δn the values 10^2-$3 \cdot 10^2$ cm^{-3} will be sufficient.

All these considerations are too arbitrary to be taken as the basis for quantitative calculations. However, they indicate that the concept of reflecting elements does not cause a crisis in our concepts of the scattering characteristics of sporadic ionization regions known from experiments. The values of Δn (elevation of electron temperature in inhomogeneities above the background) agrees in order of magnitude with those which Booker obtained for cylindrical inhomogeneities ($5 \cdot 10^2$ cm^{-3}). We shall consider that the value $\Delta n \sim 3 \cdot 10^2$ is characteristic of inhomogeneities connected with the appearance of diffusion waves in the lower ionosphere and is sufficient for the appearance of radio reflections with other necessary conditions being satisfied. Considering the earlier-introduced condition $\Delta n/n = 10^{-3}$, we obtain the requirement for electron concentration in the background:

$$n \geqslant 3 \cdot 10^{-5} \text{ см}^{-3}. \qquad (74)$$

The second limitation, which by physical conditions in aurorae /40 is superposed on the possibility of the appearance of scattering inhomogeneities, is connected with the value of the electric field strength. On the one hand, the electric field must even have twice exceeded E_k (the critical value); on the other hand, it must be limited from above by a certain value which corresponds to the maximum possible value of current density. This latter cannot be well-defined, since from observation only the value of the total current in the aurora may be found, while the area of a current cross section remains unknown. Despite this fact, an approximate evaluation may be made. We shall consider that the electric current is uniformly distributed throughout the area of section S. Evidently S is included within the limits of 10^{12}-10^{14} cm^2. The total current in aurorae is evaluated at $3 \cdot 10^3$-10^4 A. Therefore it is conditionally possible to establish that the maximum current density is equal to 10^{-8} A or 30 CGSU.

In the 120-90 km altitude range, the following expressions are

valid for the electron and ion current densities:

$$j_i = 1{,}54 \cdot 10^{14} \frac{n}{N} E, \tag{75}$$

$$j_e = 3{,}13 \cdot 10^{-15} N n T_e^{1/2} E. \tag{76}$$

The maximum and minimum current densities may be calculated according to the maximum and minimum values of E. These data are also presented in Table 5. The maximum possible current density value limits the possible altitude of the appearance of reflections from above, the minimum electron concentration from below.

From this it is apparent that in the case of a No. 1 ray arc reflections may arrive from an altitude of 108 to 99 km, for a 1.5 and 2.5 arc from altitudes of 103 to 95 km and 96 to 93 km, respectively. In the last case the lower limit is set arbitrarily, since calculations were not made for a limit lower than 93 km. Here the maximum radio emission wavelength capable of effectively scattering wave inhomogeneities in No. 1, 1.5 and 2.5 aurorae is equal to approximately 6.5 m; the maximum fading frequencies for these wavelengths are equal to 550, 1000 and 2500 Hz, respectively.

The minimum wavelength of a scattered radio emission is determined from Table 5 with regard to (74) and equals approximately 75 cm.

Based on analysis of Table 5, it is possible to draw the following conclusions.

(1) Scattering inhomogeneities connected with the appearance of diffusion waves arise most rapidly near the lower edge of the aurora on the forward or rear front of a ray arc; i.e., in regions where the electron concentration is sufficient but there is no powerful energy emission connected with the dissipation of electron stream energy.

(2) The more powerful the aurora, the lower the reflection region lies, all other conditions being equal.

(3) Other conditions being equal, the most powerful aurorae yield a greater fading rate for the reflected signal.

(4) The range of wavelengths most effectively scattered by auroral inhomogeneities is included within the 1-7 m range.

(5) Aurorae not connected with magnetic disturbances and especially powerful "superheated" aurorae do not necessarily give radio reflections.

(6) If an aurora remains bright and immobile for a long time, it does not necessarily give prolonged radio reflections (due to

"superheating"); on the contrary, rapidly drifting forms ought to scatter a radio signal better.

Results of Radar Observations of Aurorae in Yakutsk

Systematic radar observations in Yakutsk were begun on December 29, 1963 and conducted according to the IQSY program. Observations were conducted using remodeled P-8 radar equipment. /41

Due to the introduction of supplementary apparatus it was possible to carry out the following types of observations: photographing the PPI at a rate of up to 3 times per minute for the purpose of determining the azimuth, distance and type of radio reflections; visual observations of radio reflections according to the distance-amplitude index and, if necessary, according to the PPI with or without stopping the movie film; recording of the level of reflected signals on an EPP-09 or N-370M recorder; pulse recording of the amplitude and form of reflected signals on an N-102 loop oscillograph for the purpose of investigating slow (10-20 Hz) fadings, amplitude distribution of reflected signals and for calculating the correlation function and coefficient of turbidity.

The use of a well-graduated goniometer permitted us to determine the position angle of radio reflections with an accuracy up to 1° under the conditions that an ODS-type signal fluctuates little and its level on the signal-to-noise scale is not less than 5.

The program of observations may be arbitrarily subdivided into two parts: patrol observations and special observations. Patrol observations provided a circular survey of the sky for one minute every 15 minutes. With the appearance of a reflected signal the radar equipment had to be switched to continuous operation. Here a movie camera had to photograph a PPI for each turn of the antenna. Calculation of the amplitude was specified to be carried out visually on an arbitrary signal-to-noise scale. The transmitter power levels had to be tested daily by a milliameter, and once a week the sensitivity of the receiver was measured by a standard GSS-17 generator.

The receiver sensitivity test was also made daily on the basis of "spot checks". Observational data were recorded in a journal; information on the appearance of reflection was plotted using a special form in a calendar of reflections compiled for each month. Observations were not made from 8 a.m. to 5 p.m.

The program of special observation corresponded to the scientific program of group work and included recording the field level observations with a fixed antenna (in the direction of maximum reflections) and pulse recording of the scattered signal on an N-102 loop oscillograph. Altitude measurement was not carried out in view of the fact that reflections were unstable and the amplitude

small. For conducting special observations the requirements for the capabilities of a radar station were raised. In this connection a typical P-8 radar station underwent substantial modernization (cf. the block-diagram of the station in Fig. 6).

The following changes in the block-diagram of a P-8 state station were conducted. The dc electric motor for rotating the antenna was changed to an ac motor free of interference. The station's power supply was provided by a potential regulator equipped with an electrical lead, controllable by a tracking system for voltage in the grid. The power supply for the receivers and measuring systems was provided by an electronic voltage stabilizer after preparatory stabilization with a ferroresonance stabilizer. This guaranteed high reliability of measurements.

The platform was located 9 km south of the city and reflected signal reception often had to be conducted under conditions of strong interference; therefore the radar station was equipped with a highly effective system for suppressing interference. The operative principle of the system was based on the fact that interference has a rather wide spectrum and may be accepted at a frequency near but not corresponding to the operation frequency of the radar /42 equipment.

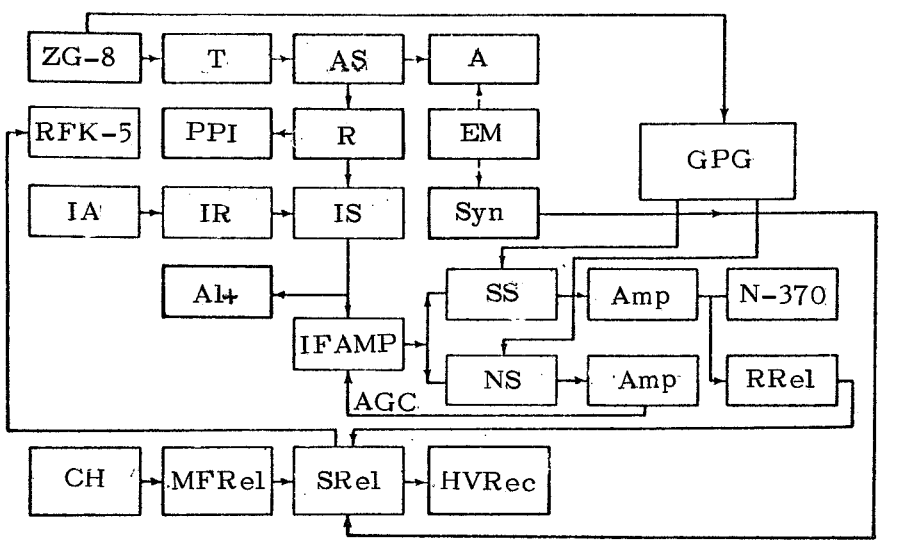

Fig. 6. Block-Diagram of Patrol Radar Surveillance Yakutsk-1. Blocks Making Up the P-8 Radar Station Are Indicated by Heavy Rectangles. Key: T-Transmitter; AS-Antenna Switch; A-Antenna; PPI-Plan Position Indicator; R-Receiver; EM-Electric Motor; GPG-Gating Pulse Generator; IA-Interference Antenna; IR-Interference Receiver; IS-Interference Selector; Syn-Synchro; Alt-Altimeter; SS-Signal Selector; Amp-Amplifier; IFAmp-Intermediate Frequency Amplifier; NS-Noise Selector; RRel-Reflection Relay; AGC-Automatic Gain Control; CH-Contact Hours; MFRel-Mounted Frame Relay; SRel-Slave Relay; HVRec-High-Voltage Rectifier.

Interference was received on a separate antenna; it was amplified by an interference receiver, after which the signal from the interference channel was carried to the interference selector, where an intermediate frequency voltage also arrived from the signal receiver containing both the useful signal and the interference. The selector operated on an anticorrespondence system, and thus interference was excluded. From the interference selector the signal proceeded to the altimeter and the regulating cascade of the gain control.

From the intermediate frequency amplifier the signal proceeded to two selectors controllable by the gating pulse generator which was controlled by the power supply generator of the ZG-8 station. The gating pulse generator provided controlling signals which unlocked the signal channel selector at a delayed time equal to 1 msec (300 km in terms of distance). Thus signals from nearby targets ("spot checks" reflected from airplanes) did not pass through the selector.

Five minutes from transmission time of the sounding pulse, the signal selector was closed and the noise channel selector was opened. It remained open for 4 msec and the signal carried to the amplifier, where it was amplified and integrated. Upon leaving the amplifier, the regulating voltage signal again proceeded to the intermediate frequency amplifier. This allowed maintaining invariable signal tract amplification and excluding the influence of constant interference. The signal from the gating pulse generator was integrated, amplified by the dc amplifier and entered the N-370 (or EPP-09) recorder. The amplifier also had an output to the reflection relay, which through a supplementary relay blocked the antenna and excluded anode feeding by the control relay. Thus, in the case of the appearance of radio reflections the radar automatically switched to continuous operation.

After the disappearance of reflections the transition of the radar from a continuous operation regime to operation from the control hours was delayed for 1-2 turns of the antenna, which served as controls. Simultaneously the reflection relay closed the chain /43 of acoustic and light signalling, informing the operator of the appearance of radio reflection. The control relay also directed the operation of the RFK-5 chamber, photographing the PPI. In order to avoid creating interference by the receiving equipment used in the southern surveillance zone, the anode voltage from the generator lamp could be automatically eliminated for each revolution of the antenna within the limits of this zone.[6]

A very important condition for the reception of qualitative observational material is an exact study of the station parameters.

---

[6]Construction and assembly of the outer blocks of the patrol surveillance was performed by the chief radio technician of the Auroral Laboratory, V.D. Shvetsov.

Measurement of power and traveling-waves in antenna cables was made using a regular thermal ammeter, and control was accomplished by the anode current of generator lamps. Receiver sensitivity was measured by a standard-signal generator and controlled according to the amplitude of "spot checks". Calibration of a recording of a reflected signal level was made in the following way on an N-370 recorder. The transmitter of the radar equipment was excluded; the signal from the GSS-17 was given as an input for the receiver instead of the signal from the antenna, tuned to the carrier frequency. The signal level and modulation on the GSS-17 was advanced with the exclusion of the transmitter. Then the transmitter was included, the interference selector was disconnected and the voltage from its output was replaced by the corresponding constant compensating voltage, selected so that the N-370 instrument indicated an instrumental zero with a completely introduced GSS attenuator. After this the N-370 was calibrated in microvolts.

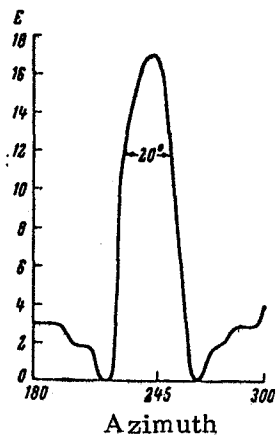

Fig. 7

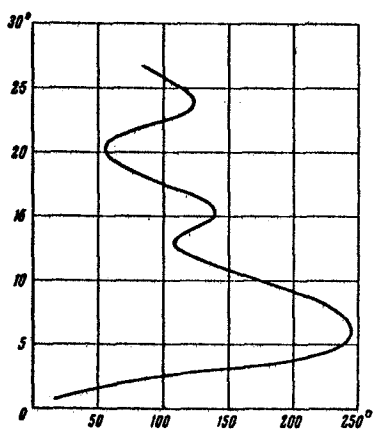

Fig. 8

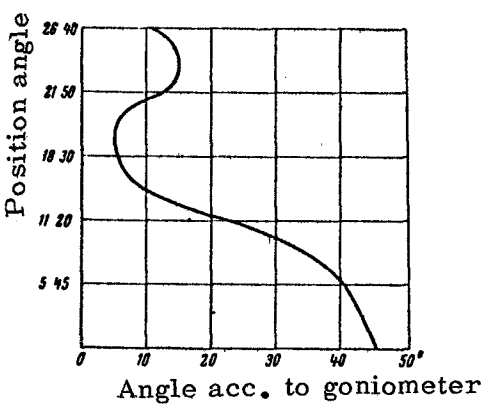

Fig. 9

Fig. 7. Radiation Pattern of the Yakutsk-1 Radar Station Antenna in the Horizontal Plane.

Fig. 8. Radiation Pattern of the Yakutsk-I Radar Station Antenna in the Vertical Plane.

Fig. 9. Calibration Curve of the Yakutsk-1 Radar Station Goniometer.

Measurement of the antenna parameters (radiation pattern in the vertical and horizontal planes) and calibration of the frequency meter was performed by means of a low-power transmitter, capable of being raised to a fixed altitude by a balloon filled with hydrogen. Measurement of the radiation pattern was made in azimuths near the direction of maximum reflection. Moreover, for purposes of control measurement of the radiation pattern in the southern sector a measurement was taken during the passage of the Sun through the main lobe of the antenna. Both methods gave similar results. The goniometer was calibrated in parallel with measurement of the dia- /44

gram. Results of the measurements are presented in Figures 7, 8 and 9.

The daily distribution of the appearance of radio reflections was studied from data of 1964-1965 patrol observations in four seasons; spring (from Feb. 1 to April 30), summer (from May 1 to July 31), autumn (from August 1 to October 30), winter (from Nov. 1 to Jan. 31). As a measurement of *a posteriori* probability of the appearance of reflections, we used the ratio of the number of 15 minute intervals per hour of radio reflection observation to the total number of 15 minute intervals when observations were made. Results of the calculations are presented in Figure 10. Analysis of the graphs leads to the following conclusions. In the spring of 1964 the daily distribution completely repeats that described in [13] for the 1958 observational season (two maxima: the narrowest at 10 p.m. and widest at 3 a.m.), although the total number of recorded reflections evidently was significantly less than in the International Geophysical Year, especially if we consider the difference in instrument sensitivity. The winter season also has the basic features of a typical daily distribution of radio reflections for Yakutsk, although in a less distinct form. In the autumn months of 1964 the daily distribution completely lost the usual evening peak and the night appearance of reflections was characterized by a great disorder. It appears that in this period the normal distribution of ionization began to undergo some anomalies connected with the damping of solar activity. This circumstance was manifested even more clearly in the winter season of 1964-1965 when, instead of the usual increase in auroral echo activity, a strong drop in the probability of the appearance of radio reflections was noticed. Only one daily maximum was noted in each period (daytime observations were not conducted) at 11 p.m. while usually at this time a minimum in the daily course of reflection is noted. Meanwhile, it is difficult to say what caused such a change in the daily course of radio reflections: space-time redistribution of ionization, peculiarities in the behavior of the ionizing agent or combined activity of both factors. For a solution to this problem, broad inclusion of ionospheric and magnetic data are necessary.

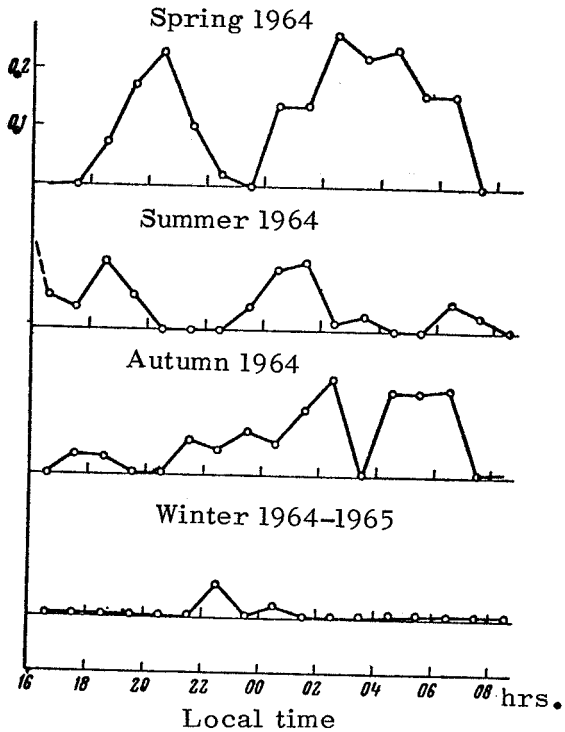

Fig. 10. Daily Distribution of Radio Reflections According to Season.

The investigation of the space distribution of radio reflection

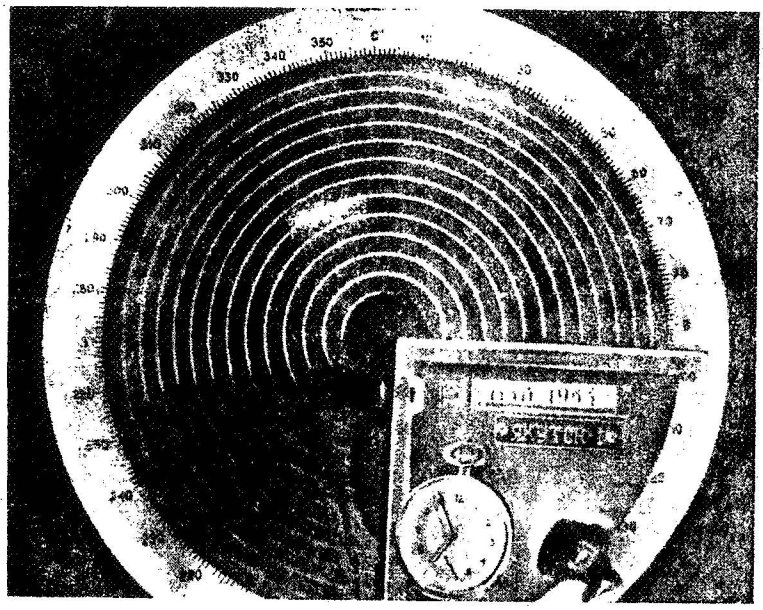

/45

Fig. 11. A Frame of the Recording Movie Film. (SDS-Type Signal)

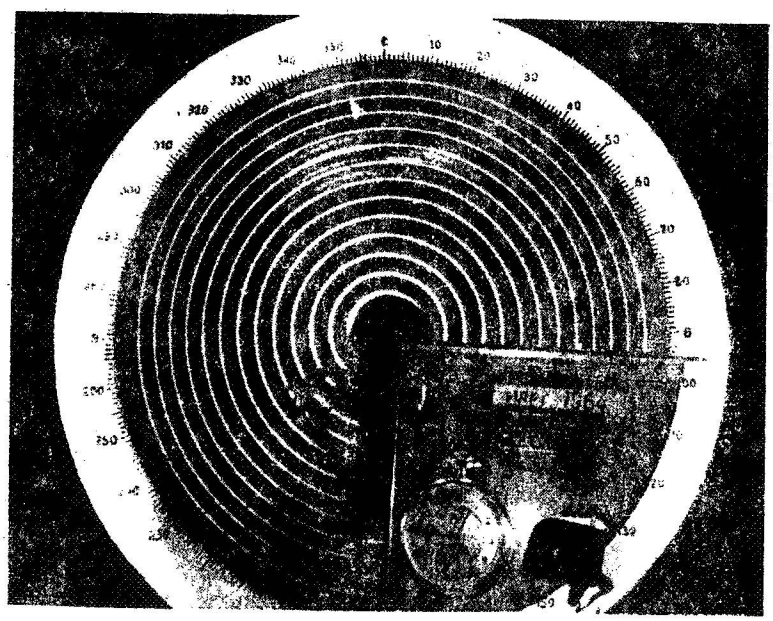

Fig. 12. A Frame of the Recording Movie Film. (GDS-Type Signal).

was also carried out in four seasons, but only for spring 1964 is there sufficient material for qualitative calculations. For summer and autumn, the results of observations do not have the necessary statistical guarantee and are only of an illustrative nature. /46

The data was analyzed in the following way. A plotting board of mm paper in a coordinate system (distance-azimuth) was divided into rectangles (size: 25 X 2.5°); in each rectangle the appearance of a radio reflection center at a given 15 min interval was indicated by a point; i.e., if a center existed from 9 to 17 min, then two points were plotted. If there were several reflection centers or reflections were sufficiently prolonged, points were also plotted in adjacent rectangles. Then the number of points in each rectangle was calculated and isolines were drawn on the plotting board uniting the centers of the rectangles with equal population densities. Calculation of the position of a reflection center was done on movie film containing PPI photographs on a diascope with a X10 magnification, using a spectral graph.

If the duration of the reflection along the azimuth exceeded the width of the radiation pattern, it was considered that there were two reflection centers and that they were located in neighboring rectangles. If the duration of reflections more than twice exceeded the width of the pattern, it was considered that there were three reflection centers, etc. We filled the cells according to distance in exactly the same way.

Typical frames of the recording film are presented in Figure 11 (SDS-type signal) and Figure 12 (GDS-type signal). It is possible to note the following characteristics of the space distribution: the similarity of distribution in general features for all three seasons, and a grouping of the reflections around one basic nucleus. Only in the summer of 1964 did a second activity center appear with coordinates of 500 km and 30° along the azimuth. Relatively large dimensions of the reflection region (550-350 km in distance; 320°-10° in azimuth [according to isochasm of the half-number], 720 km and 350° at the center) were observed in the spring of 1964. In summer of the same year the reflection region was located at a distance of 700-950 km with azimuthal angles of 320°-10°, with a center at 775 km and 345°; finally, in autumn of 1964 the reflection region encompassed a distance range of 750-1000 km and an azimuth range of 340°-25°. Evidently, in Yakutsk, as opposed to other middle latitude stations, the basic reflection center is only the western Chapman locus, and the eastern one is usually suppressed, which may possibly be explained by the influence of the eastern Siberian anomaly [10]. It is necessary to note that most recently (March, 1965) the eastern locus began to manifest great activity.

The question as to which solar activity phenomena are related to the appearance of radio reflections remains open at the present time.

The impression is created that any processes (including tropospheric) causing an increase of ionospheric magnetic disturbance may be responsible for the appearance of radio reflections. A year of minimum solar activity would appear to be a favorable time for testing similar assumptions. With this object in mind we investi-

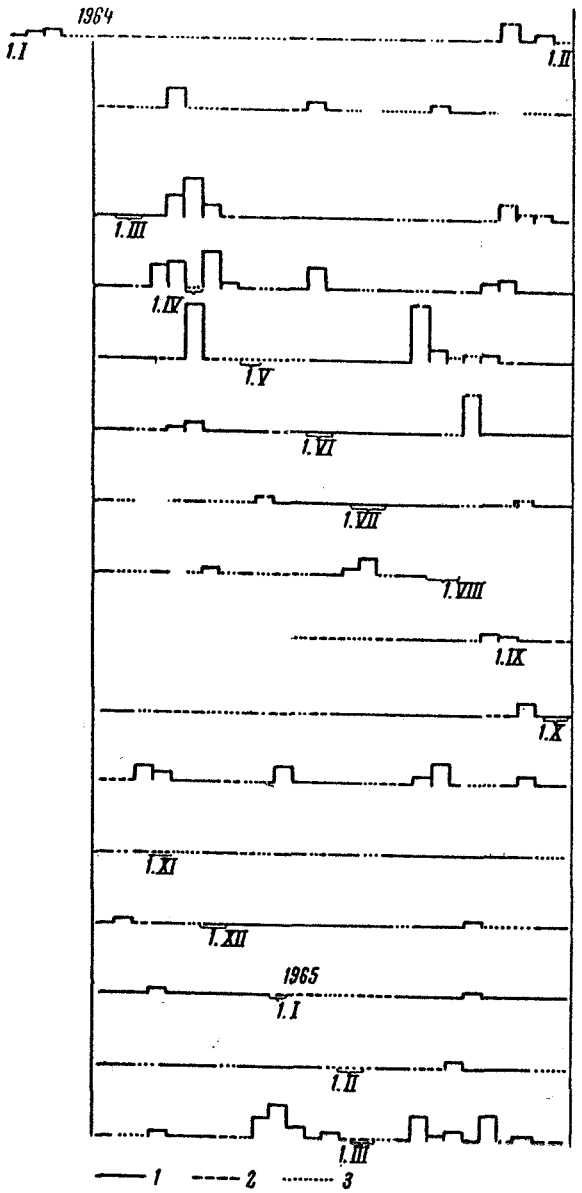

Fig. 13. The Distribution of Radio Reflections for a 27-Day Cycle: (1) Certain; (2) Omitted Hours with Little Probability of Appearance of Reflections; (3) Omitted Hours with Great Probability; the Gap Indicates Complete Omission from Observation.

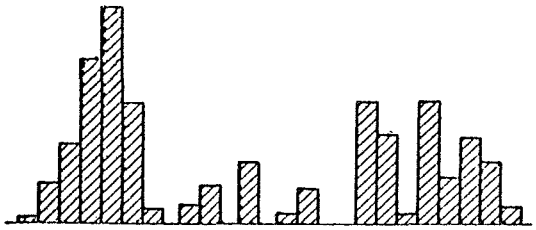

/47

Fig. 14. Total Distribution of Radio Reflections for a 27-Day Cycle (Only for 1964).

/48

gated the 27-day periodicity in the appearance of radio reflections. In order to do this the number of 15 minute intervals in which radio reflections were observed for each day of the 1964-1965 season were calculated; their intensity was expressed by the height of the column on the graphs in Figures 13 and 14. From the graph it is apparent that two independent 27-day cycles and several sporadic bursts of auroral echo activity existed.

The important phenomenological characteristic of radio reflections is their duration; however, in connection with the wise "spacing" of observations (in the USSR, 15 minute intervals were allowed between sessions) the duration distribution of reflections is not well-known for Soviet stations. Despite the known incompleteness of data, we have resolved to present a duration distribution of radio reflections for the 1964 season here. Duration is understood to be the time interval from the detection of a reflected signal to its disappearance in noise (Fig. 15). The number of reflections lasting up to 5 minutes is added in the first column, from 5-10 in the second, etc. From Figure 15 it is apparent that most often reflections of short duration (up to 5 minutes) are observed.

Analysis of the results also leads to the conclusion that even in the case where, for technical reasons, there are no gaps in the observational session, given the contemporary method of recording, we may observe only 37% of all reflections which could be recorded with constant operation of the radar equipment. This involves primarily low-amplitude reflections.

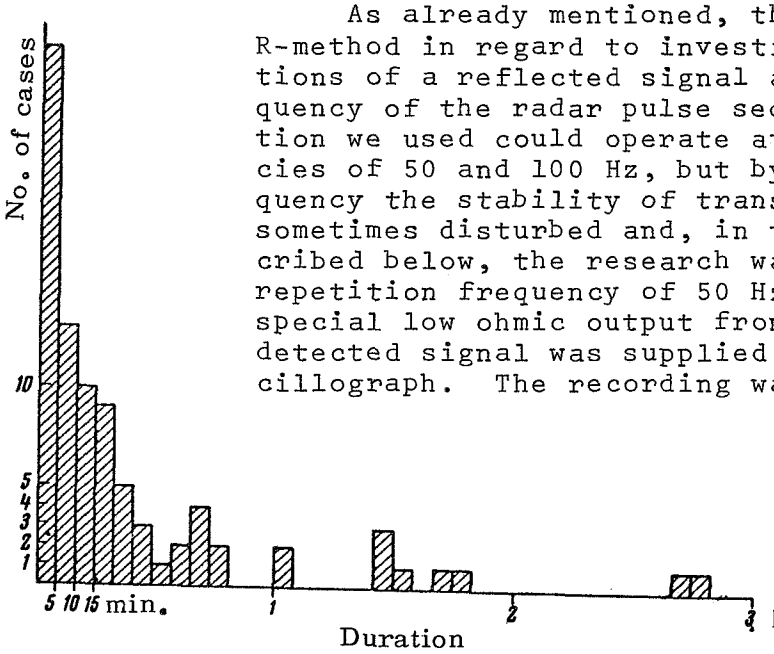

Fig. 15. Duration Distribution of Radio Reflections.

As already mentioned, the capabilities of the R-method in regard to investigations of time variations of a reflected signal are limited by the frequency of the radar pulse sequence. The radar station we used could operate at transmitting frequencies of 50 and 100 Hz, but by using the higher frequency the stability of transmitter operation was sometimes disturbed and, in the experiments described below, the research was carried out at a repetition frequency of 50 Hz. The station had a special low ohmic output from which a preliminarily-detected signal was supplied to the N-102 loop oscillograph. The recording was made with an immobile antenna oriented in the direction of maximum reflections onto a 3 kHz loop. The tracing speed was usually 500 mm/min. A model of such a recording is shown in Figure 16. The narrow, high peak of the sounding pulse and the wider peak of the scattered signal appears quite clearly here. The amplitude of the reflected signal was calculated from the lower level of the background. Measurements were conducted on a diascope with an X10 magnification. The accuracy of the calculation reached several percent and evidently was less than the error introduced by the instability of instrument operation.

In order to evaluate the long-period variations of the amplitude of the reflected signal, it proved convenient to record the amplitude on an N-370M recorder (in this case it was not necessary to fix the antenna so that the possibility for simultaneous PPI photography be maintained). Here the amplitude recording appears in the form of a number of individual peaks on the diagram tape. An example of such simultaneous recording of the signal and the position of radio reflecting regions according to the PPI is presented in Figure 17.

In the case of an analysis of echo signal recording on a loop oscillograph and interpretation of the results, the assumption was

/49

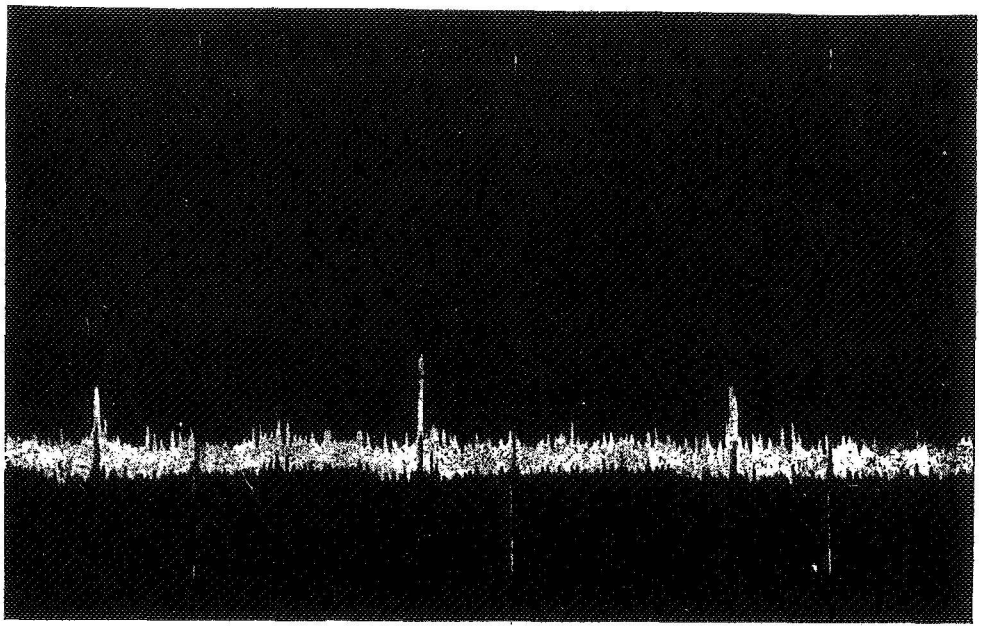

Fig. 16. Model of a Loop Oscillograph Recording of a Signal Scattered by an Auroral Reflecting Region.

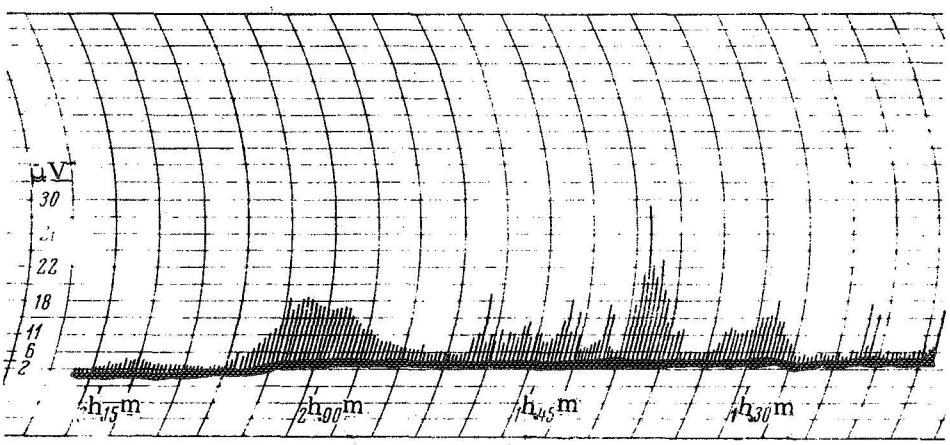

Fig. 17. Model of a Recording of a Scattered Signal Level on an N-370 Recorder with Antenna Rotation (the PPI Is Filmed Simultaneously).

introduced that we were dealing with a stationary random process. /50
Also, the parameters of reflected signals such as the amplitude distribution, $w(R_i)$ and the turbidity index β were investigated. Calculations of the parameters were made in the following way: a table of the values of R_i (pulse amplitude) was compiled in the order of their sequence (i is the number of the pulse); then a selection was

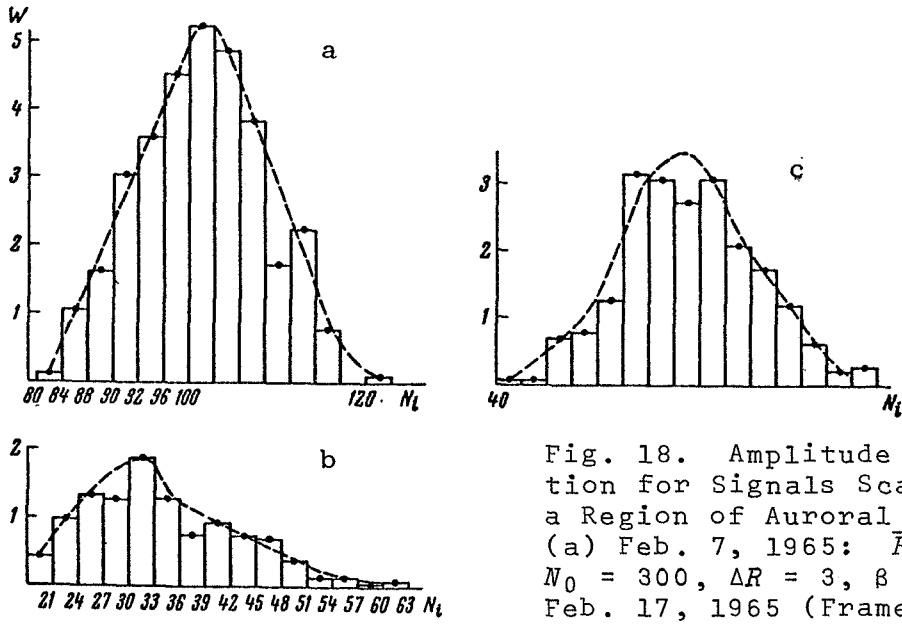

Fig. 18. Amplitude Distribution for Signals Scattered by a Region of Auroral Ionization. (a) Feb. 7, 1965: $\bar{R}_i$ = 100.5, N_0 = 300, ΔR = 3, β = 10; (b) Feb. 17, 1965 (Frame 1): $\bar{R}_i$ = 33, N_0 = 300, ΔR = 3, β = 2.5; (c) Feb. 17, 1965 (Frame 2): $\bar{R}_i$ = 62.4, N_0 = 300, ΔR = 3, β = 5.36.

made and on that basis the values /51

$$\bar{R}^2 = \frac{1}{N}\sum_i^N R_i^2 \tag{77}$$

and

$$(\bar{R})^2 = \bar{R}^2 = \left(\frac{1}{N}\sum_i^N R_i\right)^2 \tag{78}$$

were found. Here N is the number of reflected pulses in the selection. Hence, using the relationship from [74]

$$\frac{\bar{R}^2}{\bar{R}^2} = \frac{4(1+\beta^2)\exp\beta^2}{\pi\left[(1+\beta^2)I_0\left(\frac{\beta^2}{2}\right)+\beta^2 I_1\left(\frac{\beta^2}{2}\right)\right]^2}, \tag{79}$$

we find β. The amplitude distribution of the signals is determined according to

$$w(R_i) = \frac{N_i(\Delta R_i)}{\Delta R_i N}, \tag{80}$$

where $N_i(\Delta R_i)$ indicates the number of pulses in the selection with amplitudes included in the interval from R_i to $R_i + \Delta R_i$; N is the total number of pulses in the selection.

The distribution of amplitudes of the signal $w(R_i)$, calculated according to (80) is given in Figure 18. It is apparent that in two of the three cases the distribution is almost Gaussian, and in one case it approximates a Rayleigh distribution. This indicates that in two of the three cases scattering was nearly coherent; i.e., part of the signal scattered by noncorrelated, randomly-moving inhomogeneities is small. In the case when Booker's system is valid, scattering must always have a coherent nature, and $w(R_i)$ is described by a pure Rayleigh function. With the analysis of β this circumstance is manifested even more clearly.

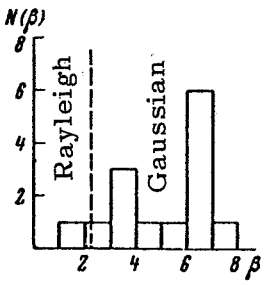

Fig. 19. Distribution of the Degree of Turbidity Index According to Frequency of Cases.

It is possible to consider that where $\beta^2 \geq 4.5\, w(R_i)$ the distribution is already indistinguishable from a Gaussian one. The measured distribution of β according to the number of cases is given in Figure 19. From 14 measured values of β only one corresponds relatively well to the case of incoherent scattering (β = 1.7); most frequently the value of β is found to be around 6. It is necessary to note that with a drop in reflections when the scattered signal begins to decrease, β also decreases. On the other hand, near the reflection maximum β is usually large and increases with an increase in mean signal strength. A model of the time-dependence of the signal from pulse to pulse is shown in Figure 20. It is evident that low-frequency fluctuations are small.

Conclusion

The physical conditions in an aurorae rather sharply differ from conditions in a quiet ionosphere. Therefore, before formulating the necessary and sufficient requirements for "background" upon which radio reflecting regions are formed, we had to investigate the question of electron stream interaction with the ionosphere, chiefly from the standpoint of balance of energy and ionization.

With simple assumptions relative to the distribution of energy dissipating from the electron stream between radiation and heat, a connection was successfully established between the energy parameters of the current and the parameters of the auroral ionosphere: the power density of energy sources, the electron temperature and the electron concentration.

After determining the basic parameters of the "background" upon which inhomogeneities responsible for the scattering of ultrashort wave signals are formed, on the basis of critical comments on Booker's theory, requirements for the physical characteristics of auroral inhomogeneities were formulated and a physical model was

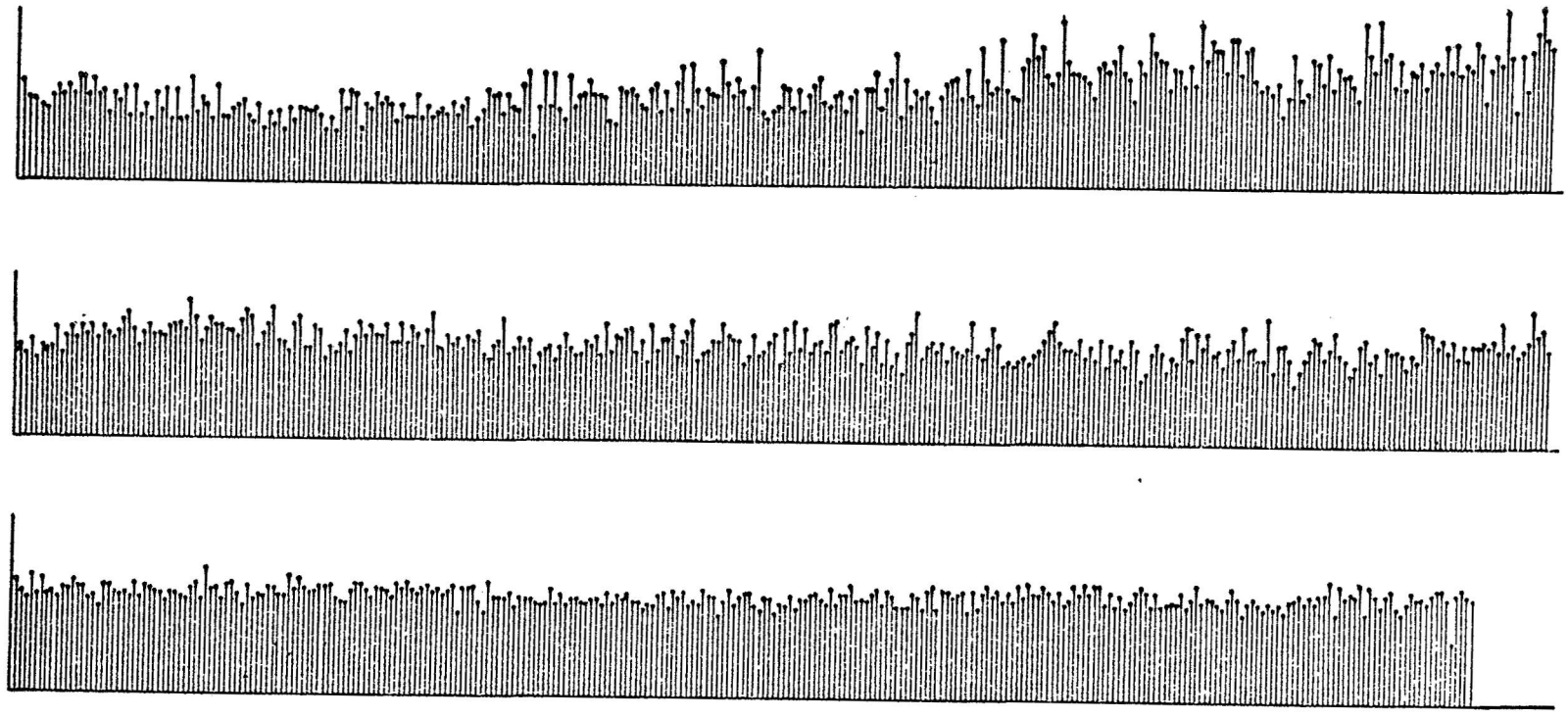

Fig. 20. Example of the Time-Dependence of Signal Amplitudes Scattered by a Region of Auroral Ionization. Interval Between Vertical Lines: 1/50 sec.

selected: diffusion of quasineutral waves in plasma. This model /53
was considered from the point of view of the correspondence to conditions in the auroral plasma and stability. Then its characteristics as a scatterer of ultrashort wave signals were considered.

The basic results of the given division may be reduced to the following.

(1) Fast electrons are the basic energy source and ionization source in an aurora. Energy is introduced into the ionosphere by an electron stream sufficient for the creation of luminescence and maintenance of a high electron temperature in the aurora. If intense intrusion of electrons continues in the same ionospheric region, it may cause a significant increase in the temperature of the "heavy gas" (ions + neutrals). The critical time usually amounts to 10^2-10^3 sec.

(2) Assuming that ray arcs of different intensity are caused by electron streams of equal spectral compositions but different intensities, with simplifying assumptions of "light output" the ionization and energy balance in a ray arc and the curve of electron temperature were calculated on the assumption that the heavy component of the plasma acts as a thermostat.

(3) Several difficulties are indicated which remain undefined within the limits of Booker's theory; the conclusion is drawn that scattering inhomogeneities are connected with wave processes in the auroral plasma.

(4) The process of the formation of quasineutral diffusion waves was considered as a possible wave process causing the appearance of small-scale, unidimensionally-ordered inhomogeneities in the ionosphere.

(5) A semiqualitative analysis of the conditions for the ap- /54
pearance of diffusion waves was conducted on the basis of calculated physical conditions in ray arcs of different intensity. Their characteristics as scatterers of radio signals for cases of radar sounding were considered qualitatively. It was shown that the assumption of diffusion waves as scatterers of ultrashort waves does not contradict the existing observational data.

(6) The automatic interference-free equipment for radar investigations of aurorae is described; results are presented of analysis of the space-time distribution of radio reflections; it was shown that during a period of minimum solar activity the space distribution of radio reflections maintains the basic features of the distribution found by the IGY. At the same time, unusual activity of the eastern Chapman locus (spring, 1965) was discovered. The time distribution undergoes significant changes in the period of transition to the minimum solar activity; the daily distribution of *a posteriori* probability of the appearance of radio reflections

for autumn 1964 had an important distinguishing characteristic: it lost the usual evening peak.

It was shown that given the existing program of observations (15 minute "spacing") only 37% of radio reflections were observed due to gaps in the reflections of short duration.

On the basis of an analysis of the results obtained from amplitude recordings of the reflected signal on a loop oscillograph, an amplitude distribution of radio reflections was found which, in the majority of cases, proved to be Gaussian. This circumstance and also the value of the turbidity index are usually cited as evidence of the quasicoherent nature of scattering on auroral inhomogeneities.

III. STUDY OF CONTINUOUS ULTRALOW FREQUENCY EMISSION IN THE AURORAL ZONE

The characteristic radio emission of the Earth's upper atmosphere occupies a band from a single Hz to several hundred MHz. At the present time a large amount of observational material has already been accumulated on the recording of characteristic radio emission in the ULF band (it is considered that the ULF band includes frequencies from 1-30 kHz), the majority of observations being made in the acoustic range. Observations of frequencies of several hundred MHz were conducted only in individual cases [32, 76-78]. /55

The broadest category of ULF emission are "whistlers". The cause of their appearance has been determined: they are thunderstorm discharges. In the presence of a discharge, spherics are emitted with an amplitude having a quasiequilibrium frequency distribution. Then propagating along force lines of the geomagnetic fields in the ionized region, the spherics undergo scattering, and at the point of observation this is heard as a whistle. Whistles were classified on the basis of the change in their spectral nature with time. In case of whistles, at each separate moment of time a low frequency band is observed. Therefore such emission is called discrete.

The cause of other types of ULF emission and the mechanism of their generation is not known; therefore the overwhelming majority of investigations dedicated to the phenomena are of descriptive nature. At the present time continuous emission ("hiss" and discrete emission; "dawn chorus") has not been satisfactorily explained (at least there is no single explanation).[7] It was established that "hiss" agrees well with geomagnetic disturbances. In the presence of constant recording, "hiss" is viewed as a series of individual broad band pulses lasting as long as an hour and sometimes repeating over the course of tens of hours.

The basic difference between "dawn chorus" and "hiss" consists in the fact that the former clearly shows short discrete lines ("musical tones") on spectrograms with a high resolution time. The ear perceives them as "bird chirping". "Dawn chorus" is observed basically at geomagnetic latitudes between 45 and 65°. There is an

[7]In the literature, continuous emission is also called "noise", "geomagnetic noise" and "auroral hiss".

interesting dependence between the time of its appearance and the latitude. At low latitudes "choruses" appear in the early morning hours (hence the name "dawn chorus") and at high latitudes the maximum probability of their appearance is shifted toward noon. As in the case of "hiss", "dawn chorus" shows good agreement with geomagnetic activities.

In our opinion, the constant ULF emission may be divided into three basic types distinguished by a time envelope: (1) "hiss" connected with aurorae; (2) isolated noise pulses and noise storm; and (3) elevated background of noise emission.

Some General Results of Observations of Ultralow Frequency Emission

As a result of terrestrial measurements it was found that the /56
flux density of continuous ULF emission lies within the range of $6 \cdot 10^{-18}$ W/m^2·Hz to 10^{-14} W/m^2·Hz. The greatest flux density corresponds to the low frequency. Many investigators (for example [79]) consider that the flux of an emission source has a smooth spectral curve and in the immediate vicinity of a source a value of 10^{-10} W/m^2·Hz. Variations of the frequency-amplitude pattern are caused, in their opinion, by absorption in the ionosphere and by peculiarities of the propagation of ULF in the Earth-ionosphere waveguide.

From observations of whistling atmospheres, Chapman and Macario [80] found that the absorption coefficient at a frequency of 5 kHz for a path in the Earth-ionosphere waveguide by day amounts to 8 dB at 1000 km, and by night it totals 4 dB at 1000 km. From similar observations at a frequency of 5 kHz in the case of signal propagation above the ocean, Taylor [81] obtained an absorption coefficient in the range of 5-11 dB at 1000 km. Special measurements of the absorption coefficient in the ionosphere were conducted on the "Lofti 1" [82] satellite. For frequencies of 8 kHz absorption fluctuated: 33-45 dB by day and 4-29 dB by night. Rocket measurements at a frequency of 512 kHz [83] indicated that the passage of a signal through the ionosphere at night weakens it by approximately 40 decibels. During geomagnetic disturbances, absorption sharply increases.

On the basis of data on the absorption of ULF waves, Australian investigators [84] undertook an attempt to determine the position of an emission source by observations at four points. They succeeded in making only a rough evaluation. ULF sources have an oval shape around 500 km in diameter and are located somewhere in the auroral zone.

According to data obtained on the satellite "Injun 3" [85], sources have diameters of several wavelengths; i.e., on the order of 3° or greater in width since an evaluation of the diameters was made at a height around 300 km, and the source was assumed to be located at the upper boundary of the magnetosphere. There is still no clear concept of the position of the source.

From measurements of ULF emission connected with aurorae by "Injun 3", the magnetic spectral emission density at frequencies lower than 10 KHz exceeds the terrestrial value by 10^6 times and amounts to $3.6 \cdot 10^{-7}$ γ^2/Hz. The maximum energy flux calculated for these frequencies amounts to $8.0 \cdot 10^{-7}$ erg/cm^2·sec, if at an altitude of 300 km the electron concentration is assumed to be equal to $5 \cdot 10^5$ cm^{-3}. Measurements of the energy flux of electrons $\geq$ 10 keV conducted simultaneously gave a value of 10.0 erg/cm^2·sec. Therefore the authors [85] put Kellogg's point of view [86] in doubt, considering that ULF emission may cause acceleration of electrons, producing aurorae.

A large volume of observational material on the recording of noise storms and isolated flashes, which we relate to the second type of continuous ULF emission, was studied by Australian investigators [84,87]. Noise storms usually appear at the time of geomagnetic storms and several hours afterwards. These isolated flashes as a rule are observed during the magnetically quiet period. Noise storms encompass the entire ULF range, being grouped in several broad bands. A maximum of the lower band (around 3 kHz) undergoes significant variations in amplitude and frequency depending on the level of variation of the geomagnetic field. The maximum amplitude of isolated flashes is distinuished by its good stability and usually lies at a frequency of 2-3 kHz. Sound storms sometimes last for tens of hours; the duration of isolated bursts is usually less than an hour.

According to the results of Ellis's investigations [88], /57
noise storms have a tendency to be repeated after an average of 23.5 hours relative to the original burst, and bursts on adjacent days almost repeat the amplitude variations. In the case of simultaneous observations at 4 points spaced in longitude, it appeared that individual bursts of noise storms and noise storms at western stations appear later than at eastern stations. Ellis explains this by the fact that the ULF source is not completely expended during one revolution of the Earth and remains constantly located in a position of straight ascent.

After noise storms and significant geomagnetic disturbances, an elevated background of noise emission is frequently observed. But there also exists a regular elevation of the noise background in night hours. The background level at each frequency of the ULF band does not reach a maximum at the same time. Information on the investigation by other authors of the regular elevated noise background with a smooth time envelope is not known to us.

On the Theories of Ultralow Frequency Emission Generation

The only possible means for the transfer of ULF emission energy from the exosphere to the Earth's surface is by means of whistles (along geomagnetic force lines). For usual waves of the

ULF band, in the case of a quasilongitudinal distribution the coefficient of refraction is determined with a sufficient degree of accuracy [89] by the expression

$$n^2 = 1 + \frac{v}{\sqrt{u}\cos\alpha - 1 - \frac{u}{2v}\sin^2\alpha + is}, \tag{81}$$

where $v = \omega_0^2/\omega^2$; $u = \omega_n^2/\omega^2$ where ω is the angular frequency of a wave; $\omega_0^2 = 4\pi e^2 N/m$ is the plasmatic (Langmuir) frequency N is the electron concentration; α is the angle between the direction of the waves and the magnetic force lines; $s = \nu/\omega$; ν is the frequency of collisions.

Ignoring collisions and excluding very small values of cos α and rather high frequencies when $\sqrt{u}\cos\alpha \approx 1$, there results that propagation of the usual waves is possible only under the condition

$$\sqrt{u}\cos\alpha \equiv \frac{w_n \cos\alpha}{w} > 1. \tag{82}$$

This signifies that only waves whose frequencies do not exceed the minimum value of the gyrofrequency on the propagation path may pass through the ionosphere.

Where $\omega = \omega_n$, the refraction coefficient becomes indeterminate and absorption very great. For extraordinary low frequency waves n^2 is always less than zero; i.e., propagation is forbidden.

It is necessary to note that the possibility of propagation of ULF waves through the ionosphere to the Earth's surface is created by the interaction of normal waves. In a magnetoactive heterogeneous plasma such as the upper atmosphere, ordinary waves are propagated. In the region of interaction where $v \approx 1$, they are transformed into extraordinary waves. For the ULF band this band is located at altitudes of 20-70 km.

Cyclotron emission is caused by a flux of nonrelativistic charged particles. In the presence of cyclotron excitation, the frequency of a generated wave in a frame of reference connected with the flux is equal to the gyrofrequency of particle flux. For electrons with $\omega = \omega_n$, propagation by means of whistles is forbidden due to the indefiniteness of the refraction index. But with regard to the Doppler frequency shift it is possible to explain noise in the 750 Hz band and even certain types of discrete emissions by cyclotron emission. The frequency of the emittable wave /58 in this case is

$$\omega = \frac{\Omega_n}{1 - \beta n}, \tag{83}$$

where $\beta = v/c$ and n is the refraction index of the emitted frequency. For energy protons it is possible to choose the value n such that ω will not be comparable to Ω_n. But the power of the gyroproton emission may be sufficient to be detected on the surface of the Earth in the case when protons emit coherently.

Synchrotron emission of electrons is more effective that that of protons since the emissivity is inversely proportional to the square of the particle mass. Synchrotron emission is excited at frequencies of multiples of the electron gyrofrequency. But in contrast to cyclotron mechanisms, emission is caused by relativistic electrons. Therefore the radiated frequency is

$$\omega = \omega_n(1-\beta^2)^{1/2}. \tag{84}$$

This type of emission evidently may exist only in rare cases, since the observable emissivity may only provide electrons with minimum energies from 0.5 to 1 MeV.

It is possible to assume the presence of synchrotron emission caused by relativistic protons. However, according to available experimental data, such protons are insufficient to explain the observed emission intensity, even if most of the energy of these protons were transformed into ULF emission.

Plasma oscillations are excited by hard particles at frequencies $\omega_0^2 = 4\pi e^2 N/m$, where N is the particle concentration. Alcock [90] considers that the mechanism of plasma oscillations may explain "dawn chorus". Clouds of intruding hard particles will excite oscillations at successively lower levels. For an observer on Earth the oscillations will appear as a series of rising tones. It is considered that such a process may be caused by the third type of solar radio flares.

The excitation of proton plasma oscillations is also possible, the conditions for their propagation being favorable for the entire frequency range greater than 500 Hz. But such a "proton" process may not provide an unusual intensity of emission.

The mechanism of Čerenkov radiation was assumed by Ellis [91] as the explanation of broad band ULF noises of the exosphere. Čerenkov radiation of a relativistic electron originates at a frequency ω for which

$$1-\beta_{\parallel} n(\omega x)\cos\alpha = 0. \tag{85}$$

Excitation of waves takes place only if the condition $v_0 \geq v_{ph} = \omega/k_{II}$ is satisfied, where v_0 is the velocity of electron flux;

is the projection of the wave vector k onto the direction of flux motion (it is considered that a flux moves at a small angle to the geomagnetic force lines). Moreover, it is assumed that an equilibrium function of particle flux distribution is isotropic in a reference system connected with a flux. The refraction index may with a sufficient degree of accuracy [cf. (81) and (82) where $\alpha = 0$] be written in the form

$$n = \frac{v}{\sqrt{u} - 1}. \qquad (86)$$

It will be great near the gyrofrequency (the value $|\omega_n - \omega|$ is small). Therefore ULF emission will be observed even for relatively slow electrons ($v_0 \sim 0.1c$). Emission will be broad band with a sharp cutoff at the higher frequencies. If we assume the flux velocity of the electrons be equal to 10^9 cm/sec, the flux density on the order of 10 cm^{-3} and the interaction distance 2000 km, then for the frequency 5 KHz the emission flux will be 10^{-19} $V/m^2 \cdot Hz$. This value is significantly lower than that observed. But if we consider that small (diameters $< \lambda$) and rather close bundles of electrons radiate coherently, then a comparatively small number of such bundles is sufficient to explain the observed intensity of emission. /59

The mechanism of Čerenkov radiation was originally applied for studying laboratory plasma. But the terrestrial exosphere is a highly anisotropic and scattering medium; therefore, the emission mechanism in it evidently is more complicated, since this mechanism cannot explain many characteristics of broad band ULF noise.

Gallet and Helliwell [92] assume that in the case of ULF wave generation a mechanism in the exosphere acts similar to amplification in a traveling-wave tube. In a traveling-wave tube an electron bundle and an electromagnetic wave are propagated along the axis of the tube. The weak wave structure reduces the phase velocity of a wave to a value significantly lower than the velocity in free space. In addition, there is interaction of the longitudinal component of the electric field of a wave with electrons of the bundle. If a magnetic focusing is used in the tube, then with equality of the longitudinal component of the electron velocity and the phase velocity of the wave, electrons will transmit energy to the wave. The wave amplitude begins to increase exponentially.

In the exosphere, electron streams and ULF waves are propagated in the tubes of force of the geomagnetic field. The inhibiting structure of the laboratory traveling-wave tube is replaced by the increasing component of refraction index by means of whistles. Therefore the longitudinal component of an electric field of a wave will interact with the electron stream. The amplification of ULF waves originates at a frequency ω, for which the electron velocity βc is equal to the phase velocity of the wave c/n.

With the condition $n\beta = 1$ and assuming $n^2 >> 1$, from (81) it is possible to find:

$$\omega_{1,2} = \frac{\omega_n}{1}\left\{1 \pm \left[1 - \left(2\frac{\omega_0}{\omega_n}\frac{v}{c}\right)^2\right]^{1/2}\right\}. \qquad (87)$$

From this it is apparent that in the longitudinal direction there are two frequencies: ω_1 and ω_2, the value of which depends on ω_0, ω_n and the bundle velocity v.

The condition for the existence of Čerenkov radiation is $n\beta > 1$. Therefore radiation takes place in the tube frequency ranges from 0 to ω_1 and from ω_2 to ω_n. If it is considered that radiation is possible only along a force line, then there will only be two emitted frequencies: ω_1 and ω_2.

If the electron stream consists of monochromatic electrons and the stream length is on the order of several hundred km, then at each given moment of time two narrow frequency bands will be amplified. For an observer on Earth these bands will be seen as varying tones. Gallet and Helliwell indicated that the time-dependence of the frequency of one of these bands will be near the observed discrete type ("hooks" and quasiconstant tomes), since the frequency $\omega_1 = (v/c)^2\ \omega_0^2/\omega_n$ is almost constant while the stream is in the exosphere and will swiftly increase when the stream enters the upper ionosphere.

One insufficiency of this theory is specifically that good agreement with experiments is only obtained for spectrograms in the form of "hooks".

For an explanation of the mechanism generating steady ULF emission in the upper atmosphere, laboratory investigations of the /60
interaction between originally nonmodulated beams of charged particles and plasma are very valuable in our opinion. As a result of these investigations, around 20 different types of convective instabilities [95] were detected. At the basis of these instabilities lie three elementary processes; the Vavilov-Čerenkov effect, the anomalous and the normal Doppler effect. The condition of cyclotron excitation of electromagnetic oscillations in the case of an anomalous Doppler effect may be written:

$$\omega = \frac{\omega_{res}}{v_0/v_\phi - 1}, \qquad (88)$$

where v_0 is the beam velocity; ω_{res} is the Larmer or the Langmuir frequency of the beam. The excitation of waves, as in the case of Čerenkov radiation occurring with the equilibrium distribution function of beam particles of low density, is isotropic in a reference system connected with the bundle and $v_0 \geq v_{ph} = \omega/k$. The transition of beam particles into oscillators and emission takes place due to the energy of longitudinal motion.

In the case of a normal Doppler effect, emission always occurs if beam particles have an initial transverse energy. Emission arises where $v_0 < v_{ph}$ and even where $v_0 = 0$. The only condition for the existence of the effect is the space and phase grouping of particles in the field of an electromagnetic wave. More bundle particles must be concentrated in the region of phases where particles give off energy to the electromagnetic field than that where the particles absorb it. In the case of isotropic distribution of beam particles, under the conditions of a normal Doppler effect cyclotron wave damping takes place.

In the theoretical interpretation of laboratory investigations of gas discharge plasma at low pressures, several difficulties arise [93]. These difficulties are connected with determination of one of the most important characteristics: the amplitude of oscillations, for which it is necessary to know the energy spectrum of the initial noise and thermal fluctuations of the particles in the beam; consideration of the reverse action of excited oscillations on the distribution function of beam electrons (with an increase in the amplitude of oscillations, the synchronism between beam and field is disturbed); investigation of transition from linear to nonlinear oscillations and determination of the amplitude of steady oscillations. In application to ULF generation in the upper atmosphere, it is important to investigate the question of coherent radiation intensity of electron bundles with nonlinear interaction with the ionospheric plasma.

Laboratory investigations of electron bundle-plasma interaction in the magnetic field permitted determining the spectrum of excitable oscillations, the increments of their increase [93] and energy losses of a beam. In [94] it is shown that in the case of beam-plasma interaction in a quasilinear approximation the beam loses up to 75% of its own kinetic energy (30% of these are expended on plasma heating, 30% on excitation of transverse electromagnetic radiation and longitudinal waves of discharge density, 15% on beam heating).

In [95] it was established that the appearance of high-frequency oscillations is always accompanied by evidence of low-frequency ones, and there is a definite connection between them:

$$\omega_e = \omega \sqrt{M/m}, \qquad (89)$$

where ω is the observable low frequency; m is the electron mass; M is the ion mass; ω_e is the electron plasma frequency. It is also established that the amplitude modulation of low-frequency oscillations is a function of pressure. With an increase in plasma pressure from $5 \cdot 10^{-6}$ to $3 \cdot 10^{-5}$ mm Hg the modulation period decreases from 10 to 10^{-5} sec. With a pressure drop (to 10^{-7} mm Hg) oscillation becomes instable; with a pressure increase to $3 \cdot 10^{-5}$ mm Hg /61 the amplitude of low-frequency oscillations drops sharply to zero.

It is interesting to note that this pressure threshold corresponds to the pressure in the upper atmosphere at an altitude of approximately 120 km.

Equipment

Observations of ULF radiation of the upper atmosphere were conducted with the aid of equipment prepared in the Auroral Laboratory of the IKFIA Yakutsk Division, Siberian Department of the Academy of Sciences, USSR. Observations were made in experimental conditions in the region of Tiksi Bay.

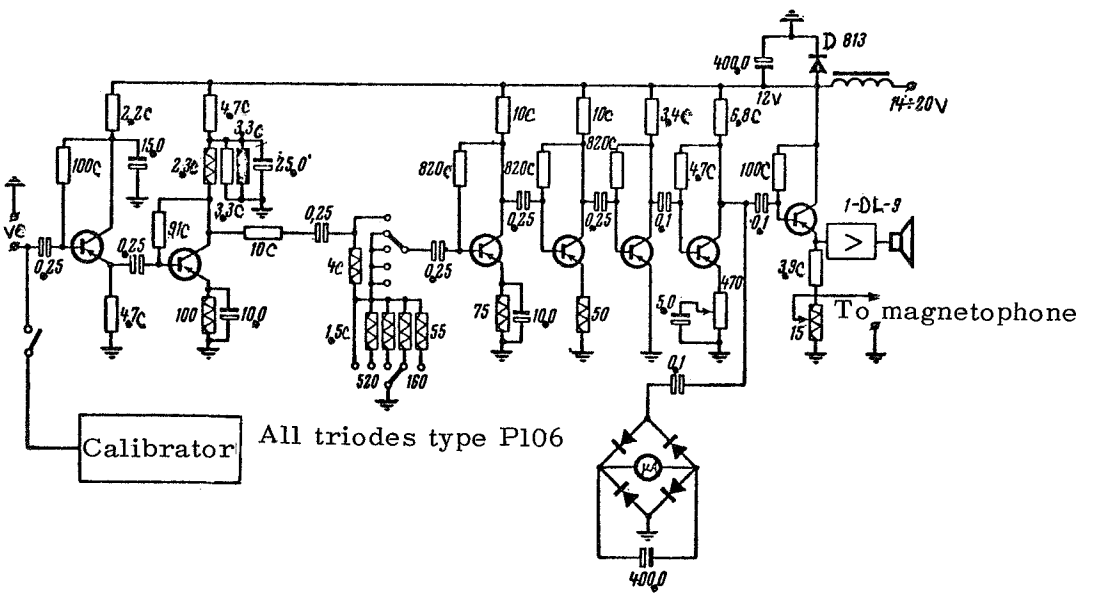

Fig. 21. Fundamental Plan for a Broad Band Amplifier of ULF Emission.

In 1962 ULF emission was recorded using equipment which is described briefly in [96]. To receive the magnetic component of the ULF signal a horizontally located framework antenna was used. The broad band preamplifier, filters, and output instruments were made on electron tubes. The equipment was intended for recording ULF signals on photographic film from an oscillograph screen on 12 channels in the range 40 Hz to 14 kHz. The signal was recorded continuously at a frequency of 11 kHz with recording on a diagram film N-370M. The remaining channels were observed by periodically photographing the signal on the oscillograph screen, since the measures undertaken to eliminate interference (feeding the filaments of the preamplifier tubes from accumulator batteries, noise filters, screening) did not give the necessary results.

In 1963 an attempt to record ULF radiation connected with aurorae in the band 450 Hz to 11 kHz was accomplished on a magneto-

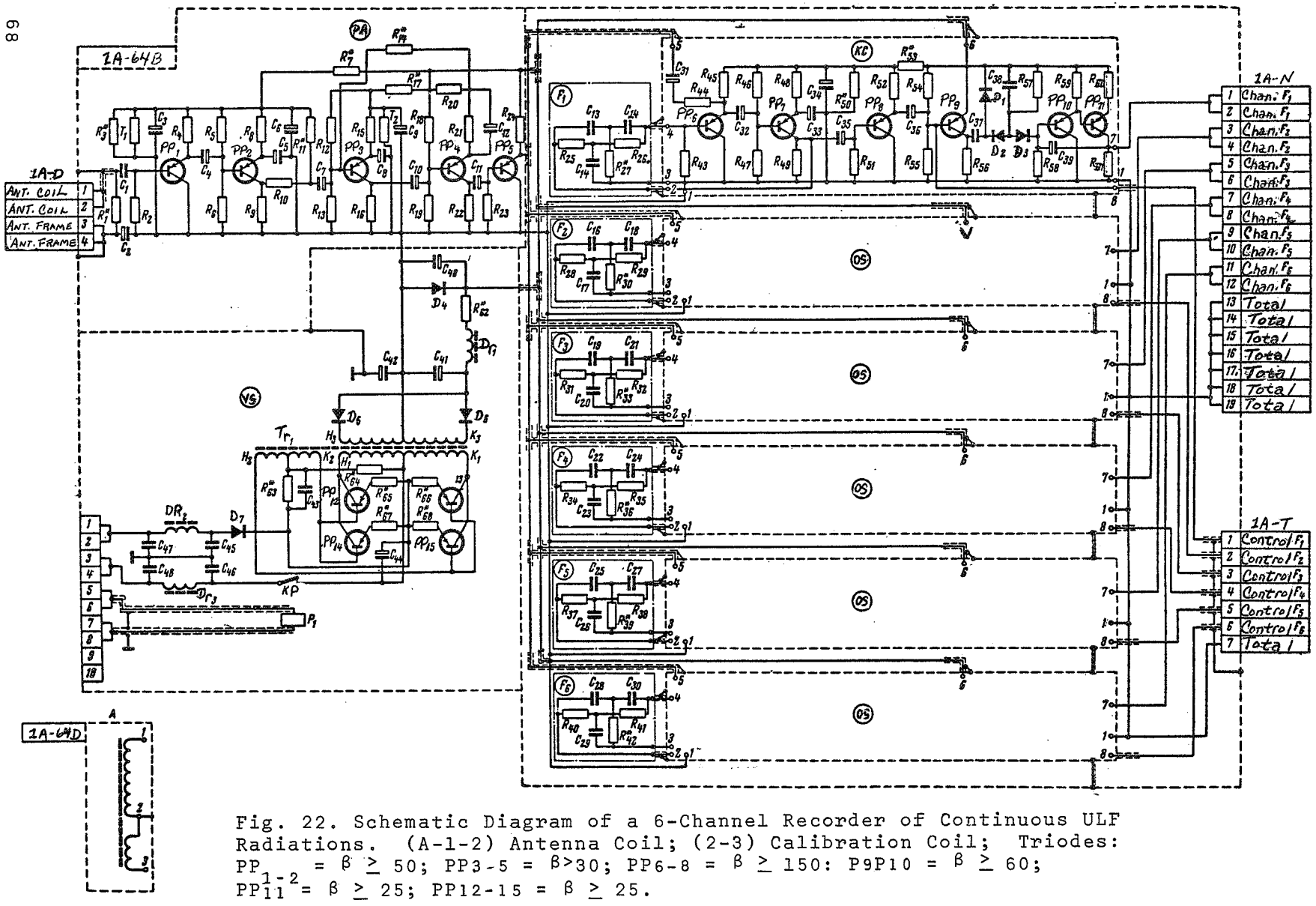

Fig. 22. Schematic Diagram of a 6-Channel Recorder of Continuous ULF Radiations. (A-1-2) Antenna Coil; (2-3) Calibration Coil; Triodes: $PP_{1-2} = \beta \geq 50$; PP3-5 = $\beta > 30$; PP6-8 = $\beta \geq 150$: P9P10 = $\beta \geq 60$; $PP_{11} = \beta \geq 25$; PP12-15 = $\beta \geq 25$.

phone. A ferrite rod with a 2450-turn coil was used as the receiving antenna. The length of the rod was 30 cm, the cross sectional area 4 cm^2. A five-cascade transistor amplifier with an emitter repeater at the input (Fig. 21) was used as a ULF receiver. The signal levels were tested by an arrow indicator. Simultaneously an auditory test was conducted. Signal recording at selected moments of time was accomplished by means of a "Reporter-3" magnetophone. Accumulator batteries were used as power sources. Observations were made in field conditions 35 km from sources of grid interference. /62 A substantial shortcoming of the observations conducted was the absence of operative data on the state of the ionosphere and the geomagnetic field.

A transistorized 6-channel recorder of ULF radiation was prepared for the 1954 observation season with an AC recording coulometer N-370M. The power supply of the receiving instrument was directly provided by accumulators and the power supply of the N-370M motors by a transistor voltage transformer.

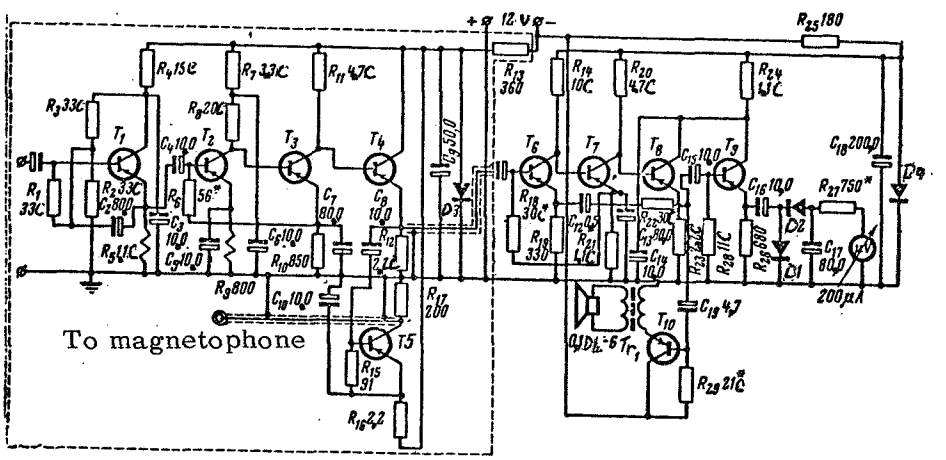

Fig. 23. Schematic Diagram of Broad Band Linear ULF Amplifier with a Low Inherent Noise Level.
T_1-T_9: P416B-Type Transistors, β_{ave} = 70; T_{10}: P25A-Type; D_{1_2}: D9B-Type; D_{3_4}: D808-Type; Tr_1- ω_1= 400 V, Ø 0.21; ω_2 = 100 V, Ø 0.33.

A permalloy rod (μ_0 = 20,000) 80 cm long with diameter d = 0.83 cm served as an antenna for the recorder. The antenna coil (2000 turns) was broken into three sections and located in the middle of the rod. The antenna parameters were calculated by the method described in [97]. The effective antenna area was $\mu^* Sn$ = 200 m^2; the calibrated coil was wound uniformly along the entire length of the rod. The antenna was continuously oriented with the axis approximately along the magnetic meridian.

TABLE 6

Frequency, kHz	Δf_{eff}, Hz	Equivalent Input Resistance of Recorder, kΩ	Antenna Sensitivity, μV/mγ	Inherent Noise Level of Recorder, $W/m^2 \cdot Hz \cdot 10^{-18}$
0,77	267	2,5	0,72	258
2,49	667	5,5	1,67	72
4,17	1070	11	3,30	3,3
5,51	1330	18,5	5,65	3,0
8,15	1500	23	6,80	2,4
11,65	1450	12	3,40	3,5
14,16	1500	8,7	2,30	4,1

The input of the receiving equipment is asymmetrical, constructed based on an emitter repeater system. The input resistance in the working range is not less than 20 kΩ. After three preamplifier cascades a broad band signal reaches the buffer cascade; at its output there are two-cascade, narrow-band active filters, set at frequencies of 2.4, 4.2, 5.6, 8.2, 11.0 and 14.0 kHz. After supplementary amplification the signal proceeds to the N-370M recorder. /63

With the appearance of a ULF signal of sufficient amplitude on the 6-channel recorder, a broad band signal was periodically recorded on a "Reporter-3"-type magnetophone. A ferrite antenna was used for signal reception.

The continuous ULF radiation was recorded at Muosty Island, 40 km away from sources of great interference.

In 1964-1965, the 6-channel recorder system was perfected. In order to eliminate pulse interference a system for one-directional signal integration was used. A supplementary channel at 800 Hz was introduced. The transmission bands of the filters were approximately equal and, at a level of 0.5, contributed 3% of the frequency of each channel. A schematic of the 1964 variant of such a recorder is presented in Figure 22. The fundamental parameters of the 1965 variant using a broad band antenna are represented in Table 6.

For recording a broad band signal, a transistor line amplifier with a low inherent noise level was prepared. The amplifier sensitivity in the band 50 Hz to 20 kHz is 1.5 μV. The input resistance

throughout the range is 50 kΩ. A schematic diagram of the amplifier is given in Figure 23. The receiving antenna for the broad band recorder is 120 cm long, with a diameter of 1.33 cm, μ* = 2800 and 1500 turns ($n\mu^*S$ = 420 m^2).

With the aim of improving receiver antenna efficiency for a 7-channel ULF recorder, the plate assembly of the rods was enlarged to d = 1.13 cm. The effective area of the antenna became $n\mu^*S$ = 360 m^2. The antenna coil had 2400 turns.

In order to conduct simultaneous patrol observations of continuous ULF radiation at several points, 1-channel recorders at a frequency of 4.0 kHz were developed and prepared. A schematic drawing of such recorder is presented in Figure 24. The bandwidth of the active filter at the 0.5 level amounts to 200 Hz. Antennas were prepared from layers of transformer steel μ_0 = 10,000. The length of the antenna is 100 cm, d = 1.6 cm, μ^*S = 2000; the working coil has 3600 turns, the calibration coil 200 turns. The construction of antennas for all recorders is similar to that of the induction detectors described in [97]. The antennas are connected to the recorder imputs by types RK-1 and RK-101 coaxial cables 7-12 m long (selection of the cable length was partially determined by the requirements of the antenna frequency characteristics).

The comparatively low inherent noise level of the equipment was reached by use of semiconductors with a large amplification coefficient (β ≈ 100-150) at the input and with a small current of 1 kΩ, the selection of an optimal input resistance and low voltage supply of the input cascades. The preamplifier system with a direct connection and normal emitter proved to be very effective with regard to noises. The introduction of thermocondensation allowed ignoring correction for temperature in the 15-30°C range. The same power supply stabilization ensures a constant amplification coefficient of the recorders and voltage

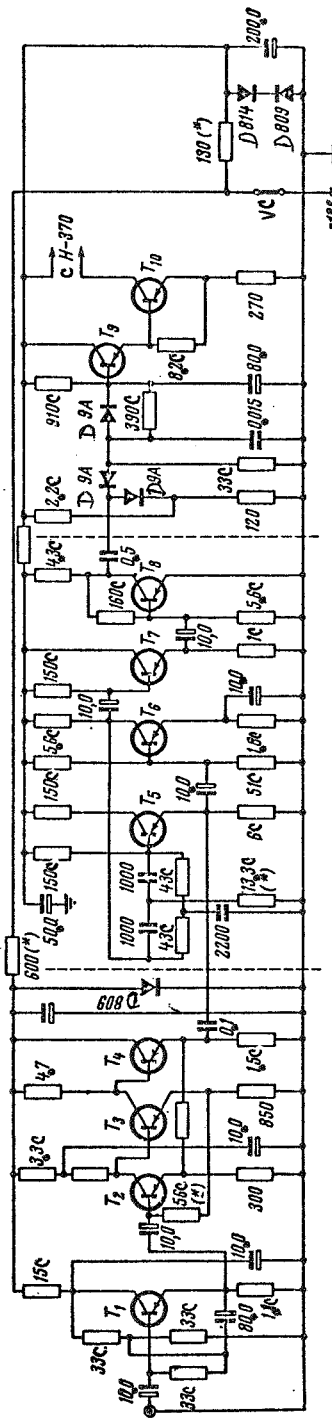

Fig. 24. Schematic Diagram of the Patrol ULF Recorder: f = 3950 Hz, Δf = 200 Hz.

/64

variation within limits of 16-20 V. The normal voltage of the power supply is 18 V. Recordings of the ULF signal on 7-channel and patrol recorders was made on a dc N-370M on scales of 5 and 15 mA.

Measurement Methods of the Intensity of Ultralow Frequency Emission Flux

The absolute intensity of the flux and spectral densities of continuous ULF emission were measured in the following way. In the usual case the spectral intensity of a ULF flux may be determined according to the formula

$$J = \frac{EH}{\Delta f} = \left(\frac{u \cdot 12{,}56 \cdot 10^{-3}}{w}\right)^2 \frac{z}{\Delta f}, \qquad (90)$$

where E is the electrical component of the voltage of the ULF field in V/m; H is the magnetic component, A/m; u is the emf of the signal, μV; w is antenna sensitivity, μV/mγ; Z is the impedance of free space, equal to 120 π Ω; Δf is the transmission band of the recorder filter at the 0.7 Hz level.

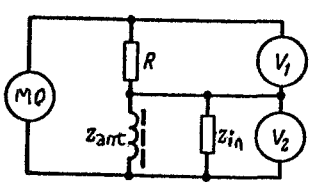

Fig. 25

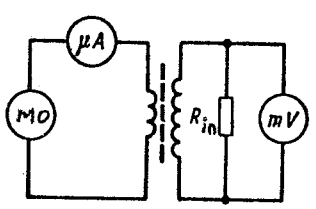

Fig. 26

The spectral intensity of the flux may also be determined by the ULF emf induced in the antenna, knowing the effective area of the antenna, the sensitivity and the equivalent input incidence of the recorder:

$$J = \frac{u^2 \cdot k(f)}{R_{e.in}\, \Delta f S_{eff.}}, \qquad (91)$$

where u is the emf of the signal in μV; $k(f)$ is a coefficient inversely proportional to the sensitivity of the antenna. The measurement of $R_{e.in}$ as a function of frequency was performed according to the method shown in Figure 25. According to this method $R_{e.in}(f) = \frac{u_2}{u_1} R$. The value of R was 35-40 kΩ.

Antenna sensitivitiy w in μV/mγ was measured according to the system in Figure 26. A signal from an audio frequency oscillator MO-10 (SG-2) was supplied to the calibration coil of the antenna. /65

The current in the calibration coil (200-100 μA) was measured by a T133 thermal microammeter. The emf of the signal on the antenna output was measured by a tube millivoltmeter connected by the working cable to the recorder input. The magnetic field of the voltage, creating an emf measurable at the recorder input, was determined by the well-known formula

$$H = 0{,}4\pi wI/l \ a/cм,$$

where w is the number of turns of the calibration coil; l is its length; I is the current in A. The sensitivity of the broad band antenna at the working frequencies of the recorder is presented in Table 6.

The recorder is calibrated by a low-frequency noise generator G2-1. The noise signal was supplied from this generator through a supplementary attenuator at 60 dB directly on the output of the recorder.

The following measures proved to be most effective in combating interference while recording continuous ULF emission:

(a) application of a magnetic antenna, permitting the use of a deep minimum in the radiation pattern for decreasing the amplitude of local interference by 2-3 times; blizzard interference, arising due to the magnetostriction effect, was practically reduced to zero (a wind of 25-30 m/sec did not influence ULF recording); in order to do this quilted sacks were put on the antennas and they were dug into the snow;

(b) removal from sources of network and industrial interference by a distance of 30-40 km;

(c) application of a system of one-directional signal integration, cutting pulse interference and discrete types of emission;

(d) auditory control of the broad band signal; a radio station in the ultralong wave band during the period while observations were being conducted was not listened to; time signals were usually given from ordinary contact clocks for the recorder input.

Observation Results of Continuous Ultralow Frequency Emission in the Auroral Zone

The first experiment on recording continuous ULF emission was conducted in March and April 1963 at Tiksi Bay. As a result of the observations made, data were obtained on the connection between ULF noises and the state of the ionosphere, the behavior of the H-components of the geomagnetic pole, a change in the total flux of optical luminescence of aurorae according to electrophotometer data on the entire sky and with visual observations of aurorae.

In a majority of cases a ULF emission maximum at 11 kHz corresponded to a maximum of the integral light flux from aurorae, but no detailed connection between them was observed. With analysis

of simultaneous visual observations, a closer connection appeared between the ULF signal and auroral activity. An increase in signal amplitude accompanies an elevation of auroral activity but then the signal drops sharply. The most probable cause of this is an increase in ionospheric absorption, since during complete absorption of radio sounding waves a signal appeared on the recording only during great disturbances of the geomagnetic field (variations of the H-component > 400 γ). Evidently this explains the fact that during active ray forms of aurorae [96] the signal was small within the limits of the frequency band of the recorder.

Moreover, it was established that with the appearance of an E_S layer in the ionosphere there is always a signal on the ULF recorder. In the case of homogeneous and pulsing forms of aurorae, ULF noise was detected at all frequencies but, unfortunately, a quantitative evaluation of the signal amplitude could only be done at a frequency of 11 kHz. /66

Observations of ULF emission in a broad band frequency with recording onto a magnetophone provided an explanation of several spectral regularities of radio emission connected with aurorae.

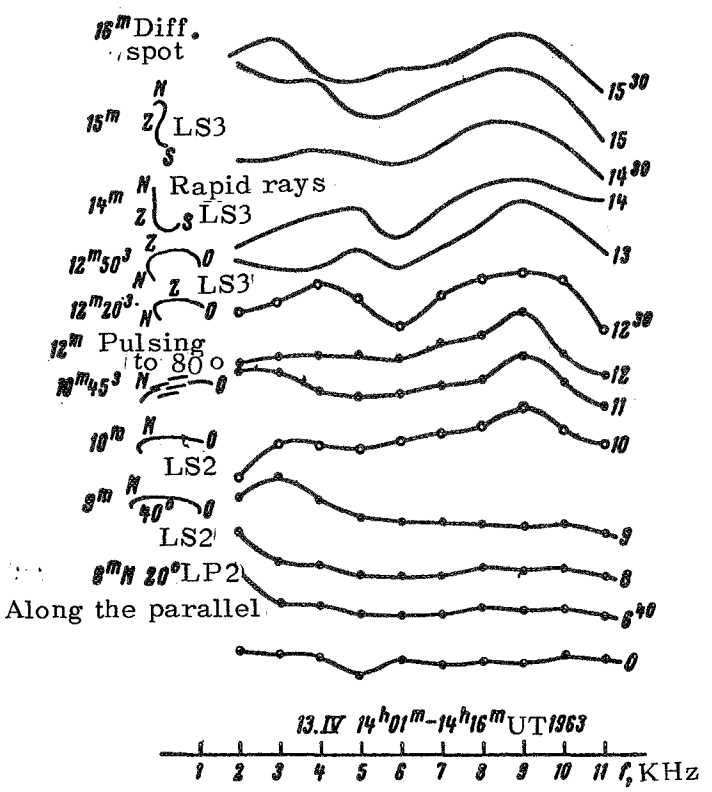

Fig. 27. The Relative Distribution of Signal Amplitude According to Spectrum. Data from Observations of Aurorae are given at Left.

Due to the lack of instruments necessary for calibration, a qualitative analysis of the obtained magnetophone recording was performed. With each reproduction the signal was recorded on one of the consecutively selected frequencies with an 8% band. Calculation of the amplitude was performed relative to the quiet signal level recorded in a period of complete atmospheric absorption. Then correction was considered on nonequilibrium of the C4-7 analyzer characteristics. As a result we obtained a relative distribution of amplitudes according to spectrum and its variation with time (Figs. 27,28).

As a result of recording analysis it was established that ULF emission connected with aurorae is grouped into two cross bands. The maximum of one of them

varies within the range from 2-5 kHz. Here the increase in amplitude of variations of the *H*-component of the geomagnetic field corresponds to the increase in maximum frequency. Bursts of amplitude of the ULF signal also correspond to abrupt changes in the *H*-component.

The second maximum is more stable and lies in a frequency range from 7-11 kHz. During one aurora the maximum does not shift by more than 0.5 kHz. Amplitude variations in this band are small in comparison with the lower one, but the maximum amplitude is usually less. /67

Comparison of the results of spectral analysis of ULF emission with visual observations also permits drawing the conclusion that the increase in signal amplitude throughout the recorded range and the shift of the maximum of the lower band toward the higher frequencies (up to 5 kHz) correspond to an increase in auroral activity.

The auditory test which was simultaneously conducted allowed interference to be fixed. For the entire period of night observations from April 2-15, 1963, no instances of the appearance of atmospherics were observed. Thirty-nine magnetophone tapes were recorded and analyzed (15 min).

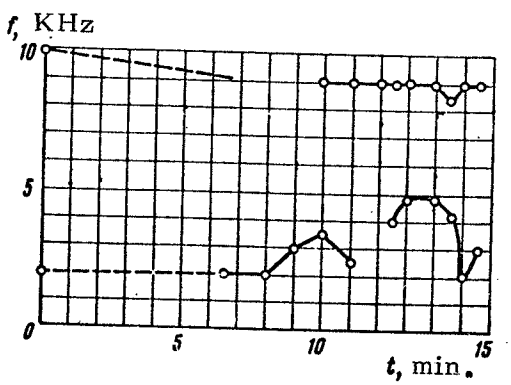

Fig. 28. Shift of the Maximum Frequency in the Spectrum with Time.

From February 28 to April 3, 1964, recording of continuous ULF emission was taken on 6 fixed frequencies. A total of 573 hours of recordings were made. Where possible recording was made continuously (the recorder was switched on during the time of accumulator discharges). Before beginning and at completion of observations, the recorder was calibrated and its amplitude characteristics were taken depending on the supply voltage. The temperature stabilization of the recorder ensured a constant coefficient of amplification and temperature range from 15-25°C. Therefore correction for temperature change was not considered in analyzing the results. A tracing speed of the diagram tape on the recorders of 180 mm/hr was selected, which permitted a detailed analysis to be made of the time changes of the amplitude-frequency curve of the signal. Change in the antenna parameters (sensitivity in the measurement range and frequency curves), the input resistance of the recorder and the bandwidth of individual channels (at the 0.5 level) made it possible to determine the absolute spectral densities of the ULF emission flux.

As a result of preliminary analysis of the obtained data three

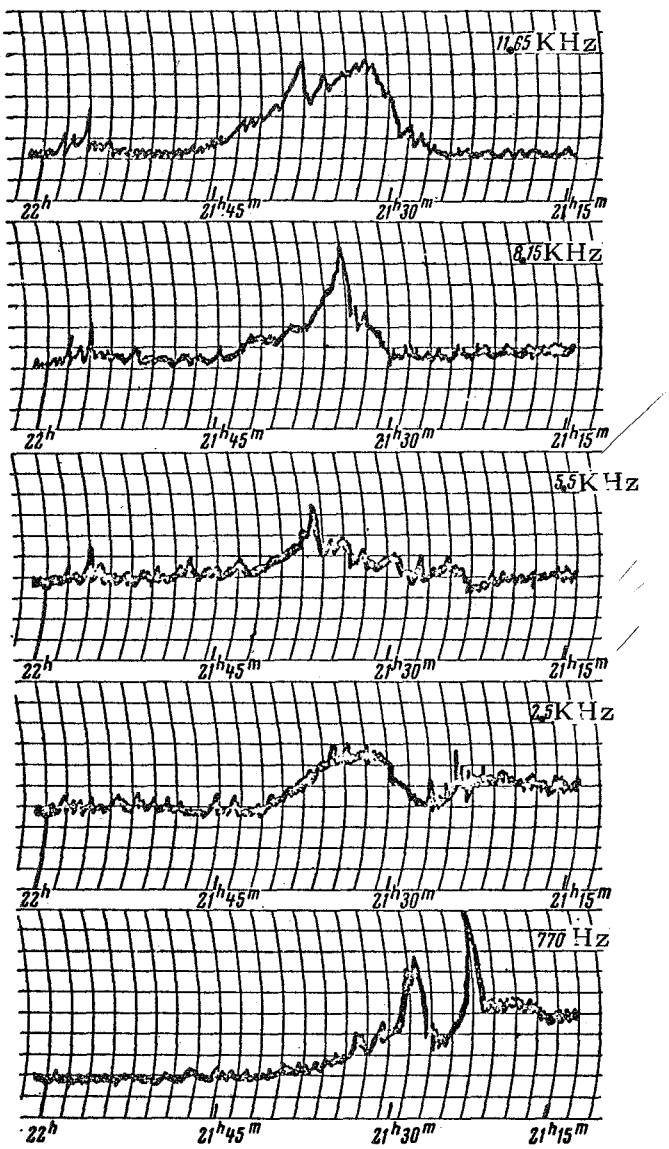

Fig. 29. Typical Recordings of the Auroral ULF Signal on March 5, 1965; Time 135° E.

types of continuous ULF emission of the upper atmosphere were separated and absolute values of electric and magnetic spectral intensities of the flux were determined. With the analysis of recordings of ULF emission on 6 fixed frequencies for comparison and the establishment of the connection with other geophysical phenomena, the following data were used: data on the recording of variations of *H*-, *D*-, and *Z*- components of the geomagnetic field obtained at the point ULF recording; data on vertical radial sounding of the ionosphere; data on the absorption of cosmic radio noises at a frequency of 30 MHz and data on visual observations of the aurorae. Moreover, there are data on simultaneous observations of the integral light flux from aurorae obtained on an electrophotometer of the entire sky; data on photographic observations on a C-180° chamber; data on the recording of terrestrial currents and radar observations of aurorae at the Yakutsk-1 station. However, these data have not yet been analyzed.

The first type of ULF emission of the upper atmosphere revealed a close connection with auroral phenomena and the E_s layer. The appearance of traces of ULF emission, usually on all channels of the recorder, corresponds to the appearance of a homogeneous arc of luminescence at the horizon. With further development of the aurora and an increase in its activity, the amplitude of the ULF signal sharply increases and undergoes strong variations in frequency and amplitude. It is characteristic that rapid variations in amplitude at various frequencies are divided in time (units of seconds), but envelope changes of it after several minutes at various frequencies are similar. A typical recording of ULF signal on 5 frequencies is presented in Figure 29. As indicated above, the amplitude-frequency curve of ULF noises connected with aurora has a double-hump distribution. This distribution is almost always maintained, but the maximum amplitude of the lower band is often shifted toward the higher frequencies when auroral activity appears. The recorded maximum frequency was 6 kHz. The curve of spectral variations is given in Figure 28. The characteristic distribution of spectral flux density in relative units is presented in Figure 30. The spectral flux density in the lower band is almost higher than in the upper band. Individual cases are an exception.

/68

/69

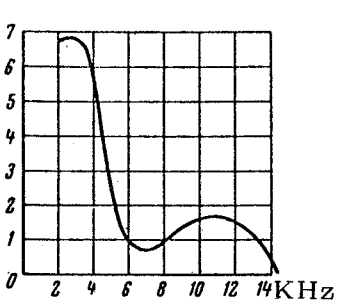

Fig. 30. Distribution of ULF Spectral Density According to Frequency.

With the further development of the aurora, when very active ray forms appear at the zenith, the signal usually disappears at all frequencies and appears only in the case of very great geomagnetic disturbances, even with complete absorption of the waves of vertical radio sounding (for example, March 31, 1964 at 16 h 49 m GMT). After the auroral disintegration phase, the ULF signal usually disappears, although

visually individual rays, fragments or ray arcs and a veil are still evident. This fragment may be explained by the increase in absorption in the lower layers of the ionosphere.

Then with the appearance of aurorae in the form of pulsating spots, the signal reappears, the pulse frequency of this amplitude corresponding to the pulse frequency of visual optical illumination. Additional experiments on synchronized recording of ULF and luminescence of aurorae in resolved lines permit establishing a detailed connection between them. The maximum intensity of the ULF emission flux connected with aurorae throughout the band does not exceed the value $3 \cdot 10^{-16}$ W/m^2·Hz in our experiments (March 17, 1964, 15^h20^m GMT). A typical distribution of ULF emission according to spectrum is presented in Table 7.

TABLE 7

Date, Local Time	Frequency, kHz	Signal Amplitude, μV	Spectral Density μV/m·Hz$^{\frac{1}{2}}$	Spectral Density A/m·Hz$^{\frac{1}{2}}$ ·10	Flux Intensity W/m^2·Hz
3/4/65 01^h10^m	0,77	0,065	0,51	4,42	$2,6 \cdot 10^{-15}$
	2,49	0,4	0,62	7,4	$1,1 \cdot 10^{-15}$
	4,17	0,8	0,58	5,9	$3,2 \cdot 10^{-15}$
	5,51	1,1	0,54	4,3	$2,2 \cdot 10^{-15}$
	8,15	1,3	0,41	3,9	$1,6 \cdot 10^{-15}$
	11,65	0,65	0,15	4,0	$5,8 \cdot 10^{-16}$
	14,16	0,47	0,09	4,2	$3,6 \cdot 10^{-16}$
3/4/64 23^h35^m	0,77	—	—	—	—
	2,49	0,24	0,37	4,4	$1,7 \cdot 10^{-15}$
	4,17	0,32	0,23	5,2	$5,6 \cdot 10^{-16}$
	5,51	0,7	0,34	2,7	$8,6 \cdot 10^{-16}$
	8,15	1,2	0,38	3,6	$1,3 \cdot 10^{-15}$
	11,65	0,75	0,17	4,6	$7,8 \cdot 10^{-16}$
	14,16	0,37	0,07	3,3	$2,3 \cdot 10^{-16}$

For determining the connection between ULF emission of the upper atmosphere and visually observable aurorae, a standard distribution of their appearance in time was constructed. Histograms of this distribution are shown in Figure 31. From the figure it is apparent that in both cases there are three clearly-defined maxima which correspond in time. The evening maximum occurs at 11 pm local time, the night maximum at 1 am and the morning at 4 am. The imprecise correspondence between evening and morning maxima may evidently be explained by unfavorable conditions for visual observations (haze and solar illumination of the upper layers of the atmosphere). Moreover, without detailed spectral analysis it is not always possible to reliably separate the first type of noise from the third type. /70

During the operation of the 6-channel recorder, the broad band

signal was constantly controlled by ear. This made it possible to determine sources of interference and to record them in the log book. At especially interesting moments, the broad band signal was recorded on magnetic tape. But analysis of the tape is hindered at the present time by the technical imperfections of the analyzer. Moreover, due to insufficient sensitivity of the receiving antenna at high frequencies and characteristics of the "Reporter-3" magnetophones, the signal is weak at these frequencies. The nature of the noise in the lower frequency band is seen on a photograph of the noise during an aurora (Fig. 32) obtained on IZMIRAN[8] equipment, intended for analysis of whistling atmospherics.

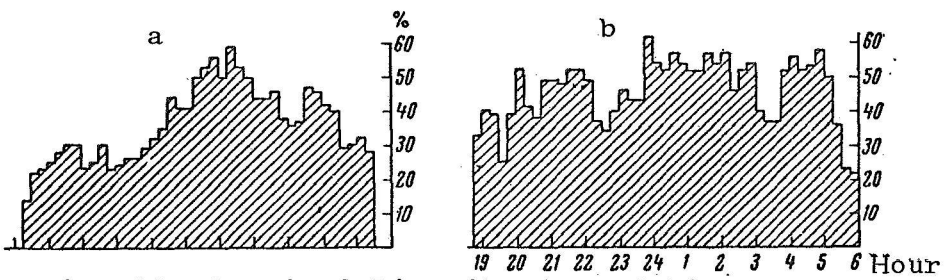

Fig. 31. Standard Distribution of Visually Observable Aurorae (March 1964) (a) and a Standard Distribution of the ULF Signal at a Frequency of 8 kHz for the Entire Period (b).

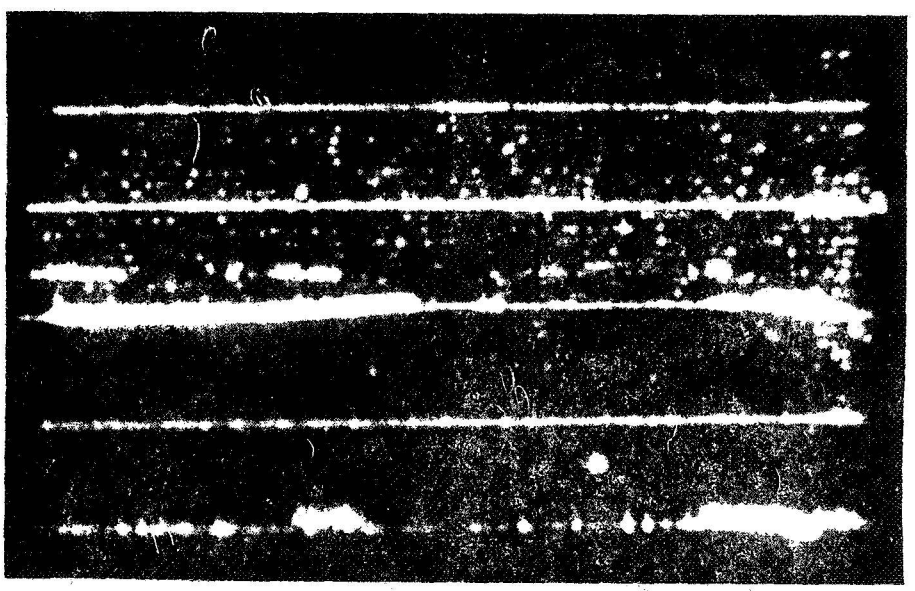

Fig. 32. Sonogram of Auroral ULF Emission.

For the entire 1964 observational period, 6 noise storms and 22 isolated bursts were recorded. The spectral density of the second type of ULF noise is always higher than in the case of aurorae. A typical recording of the noise storm is shown in Figure 33. /71

According to our observations, isolated bursts appear in the morning and evening twilight when the altitude of the shadow above the Earth is less than 300 km. From analysis of the data on the state of the ionosphere at the moment isolated bursts appear, it was discovered that sharp oscillations of minimum and critical frequencies

[8]Institute of Terrestrial Magnetism, the Ionosphere and Radio Wave Propagation of the Academy of Sciences, USSR (Translator's note).

of the F_2 layer and its altitudes correspond to the bursts. In several cases total transparency was observed on ionograms, and sometimes the E_s layer also appeared. As a rule, in the F_2 layer there is strong diffusion.

One more characteristic peculiarity of ionized bursts is that they are observed in the case of a quasiquiet geomagnetic field. At this time the H-component undergoes slight variations with an amplitude of 10-30 γ and a quasiperiod of 5-20 min. In recordings of terrestrial currents no peculiarities were observed. A characteristic example of the appearance of isolated bursts, variations of the H-component of the geomagnetic field and oscillations of frequencies of the F_2 layer and its altitudes are shown in Figure 34. On a riometer (32 MHz) there are not even traces of absorption.

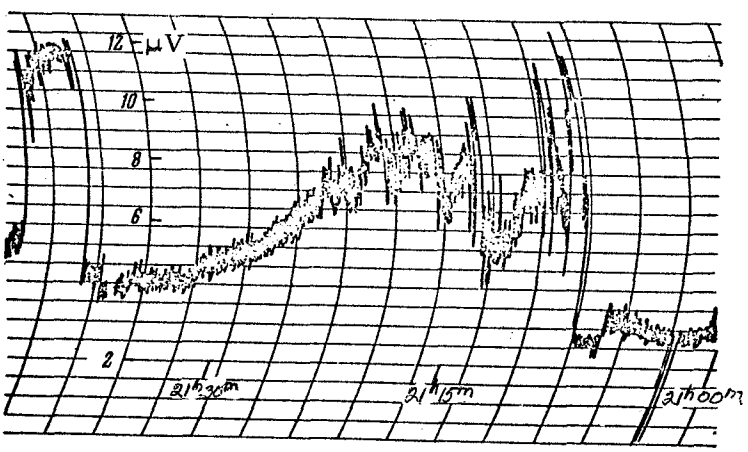

Fig. 33. Fragment of a Noise Storm Recording at a Frequency of 8 kHz.

On various oscillation frequencies, noise amplitudes are not synchronized, but the shapes of the bursts are very similar on all frequencies. Moreover, the shape of the original burst is often reproduced with great accuracy in several hours. Sometimes short, sharp peaks at equal time intervals (5, 7 or 12 min) precede bursts lasting 15-30 min. Low frequency "wheezes" are intensely emitted during bursts. The distribution of signal amplitudes according to duration is shown in Figure 35.

Noise storms appear at any time of the day and are accompanied by significant geomagnetic disturbances. The distribution of amplitude according to spectrum has two humps, but the amplitude in frequency undergoes rapid variations. With an increase in ionospheric absorption, recorded by the ion-sounding station and riometer, the amplitude of noise always drops sharply but does not completely disappear. Values of the spectral density of noises and flux intensity for isolated bursts and noise storms are on the same order.

Noise storms continue for tens of hours; isolated bursts usually less than an hour. The maximum amplitude of the lower band, depending on the level of the magnetic disturbance, is shifted as with signals accompanying aurorae. In the case of isolated bursts, no visually observable aurorae are noted, even with favorable meteorological

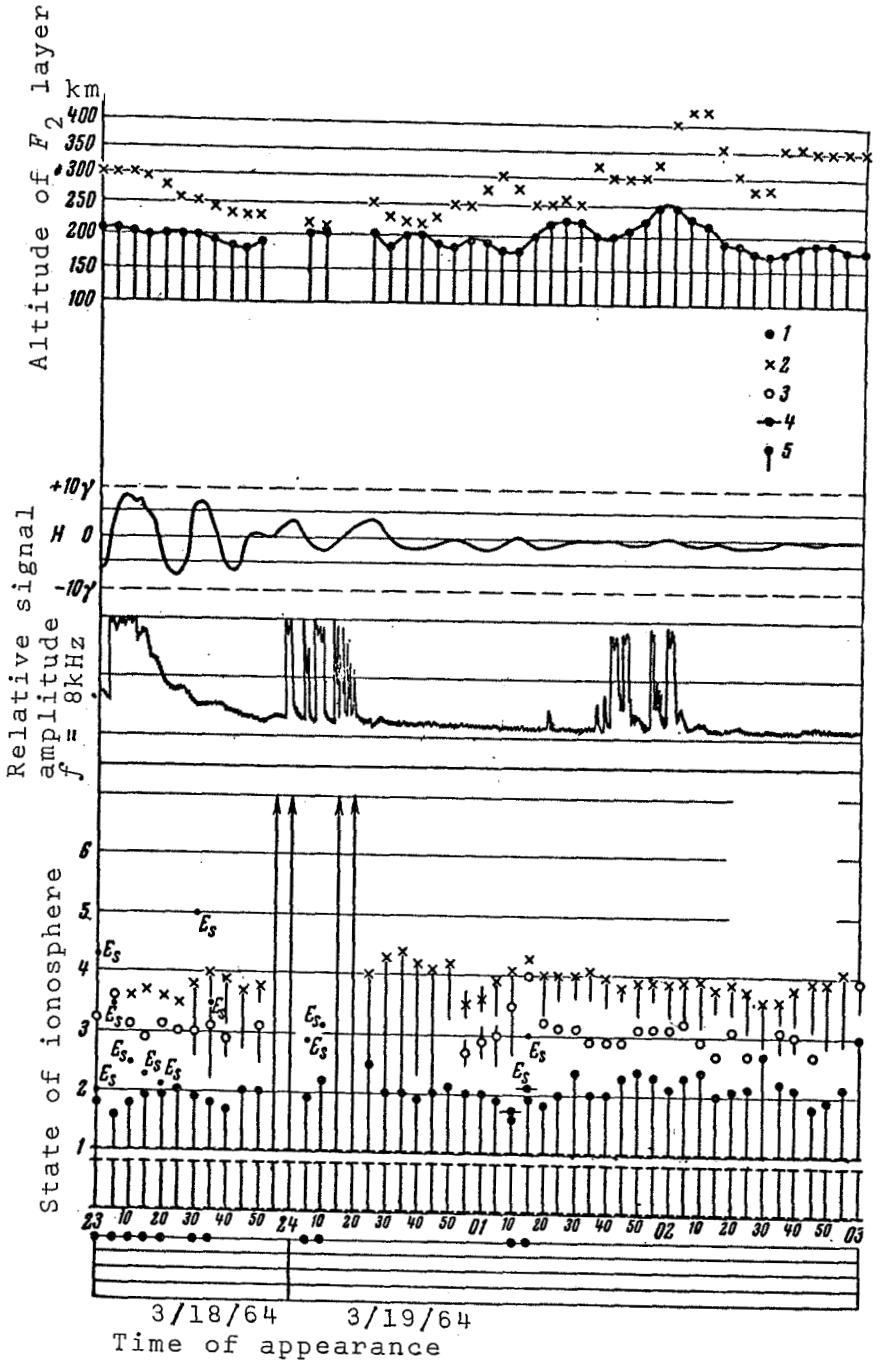

Fig. 34. Connection between the Appearance of Isolated Noise Bursts and the State of the Ionosphere and Variations of the *H*-Component of the Geomagnetic Field.

/72

conditions. During noise storms at night, aurorae are usually noted. /73

Despite the clear difference between the natures of noise storm processes and isolated noise bursts as well as the physical phenomena accompanying them, both these and others evidently are produced by one cause and have a similar generation mechanism.

We conducted an analysis of the time of appearance of 55 noise storms and isolated bursts from the data of Australian investigators [84, 98]. It proved to be the case that their appearance is controlled by a 27-day solar cycle. This periodicity is clearly apparent in Figure 36. After 27 days, not only is the appearance of isolated bursts and noise storms repeated, but also the nature of their time envelope is reproduced.

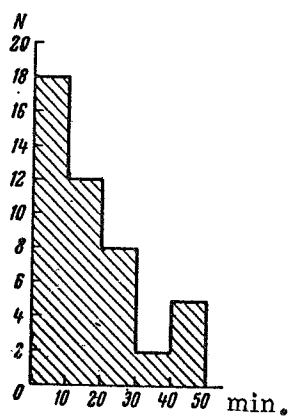

Fig. 35.

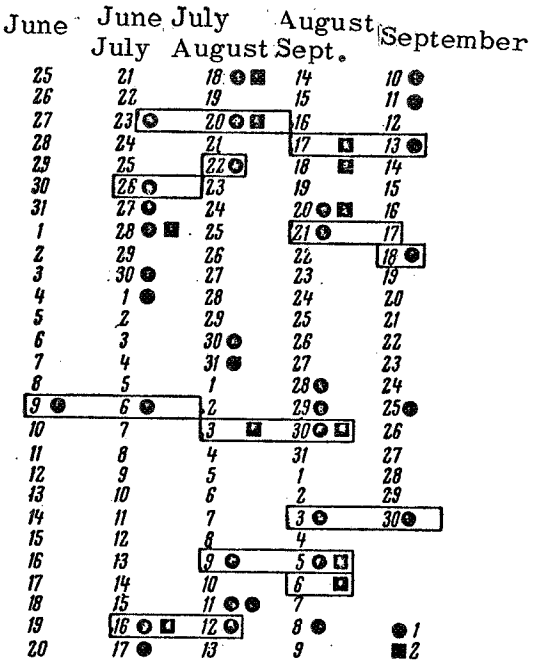

Fig. 36. 27-Day Cycle of the Appearance of Isolated Noise Bursts (1) and Noise Storms (2) (According to Observational Results [88]).

The daily curve of the appearance of isolated bursts drawn on the basis of these data has three maxima (Fig. 37). The morning maximum occurs at 5-6 am, the day maximum at 1 pm and the evening maximum at 10-11 pm local time. The daily maximum evidently is caused by the maximum probability of the appearance of noise storms, and isolated bursts appear at the peak portion of a noise storm which has not completely ended due to the intense absorption in the day ionosphere.

In our opinion, one of the possible causes for the appearance

of noise storms and isolated bursts in the morning, day and evening may be soft X-ray solar radiation in the 3-8 Å range. This ionizing radiation may be the source of electrons with energies of 1.5-4.2 keV at altitudes above 120 km. The flux of solar X-ray emission /74 in this range during No. 2 bursts amounts to 0.02 erg·cm^{-2}·sec^{-1} [99]. According to observations on the "Injun-3" [85], the energy flux of ULF emission at frequencies below 10 kHz amounts to $8 \cdot 10^{-7}$ erg·cm^{-2}·sec^{-1}.

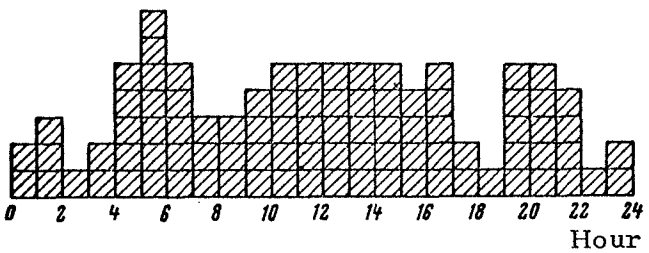

Fig. 37. Daily Distribution of the Appearance of Isolated Noise Bursts (According to the Observations of [84] and [98]).

Very valuable from this point of view is the discovery by the "Kosmos-5" satellite of electrons with energies of 40 eV-5 keV in the light upper atmosphere [100]. When the satellite entered the Earth's shadow, the number of electrons recorded abruptly decreased and after several minutes before beginning the lighted part of the orbit. An absence of rapid variations in intensity of the softest electrons was noted (for 8 sec of continuous recording, the change in intensity did not exceed 50%). The harder electrons underwent strong modulation during rotation of the satellite.

A tendency for soft electrons to increase in intensity with altitude was also noted. For altitudes below 500 km, the signal on the average amounted to 10^8 el·cm^{-2}·sec^{-1}·sterad^{-1}, and for altitudes exceeding 1000 km it was $4 \cdot 10^8$ el·cm^{-2}·sec^{-1}·sterad^{-1}. The C-index at the time of observation did not exceed 3. During No. 2 bursts no clear change in intensity was observed. Mulyarchik [100] assumed that atmospheric photoelectrons which do not successfully come into equilibrium with the surrounding medium are recorded on lighted portions of a satellite's orbit. From the standpoint of energy, a soft electron stream recorded experimentally is completely sufficient for providing the intensity of the second ULF type observable on Earth.

The third type of continuous ULF (elevated noise background) is observed after noise and geomagnetic storms. On the basis of observations in March 1965, it was established that there is a regular increase in the noise background with a smooth time envelope during the night hours which does not depend on the state of geomagnetic

disturbance. A typical recording of the noise background at a frequency of 11 kHz is given on Figure 38. In our observations, the /75

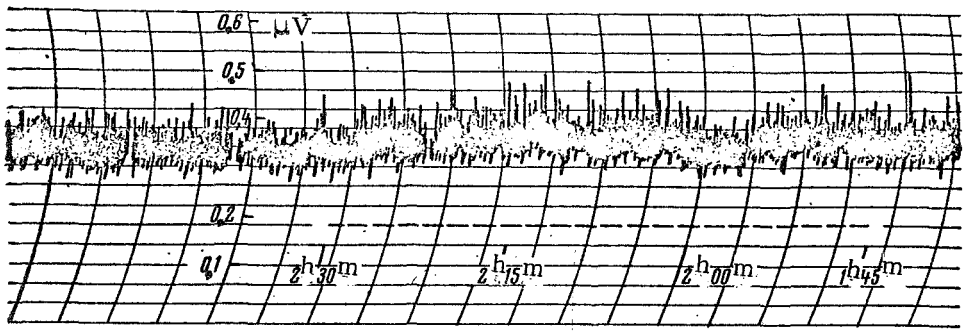

Fig. 38. Fragment of the Recording of an Elevated Background of Noisy ULF Emission at a Frequency of 11 kHz on March 5, 1965.

The Normal Noise Level Is Indicated by Dotted Line; Calibration Marks Are from an SG-2.

maximum noise intensity at a frequency of 11 kHz had a value of $4.4 \cdot 10^{-16}$ W/m^2·Hz (March 15, 1965, 0^h45^m, time 135° E), the minimum background value is usually observed by day and amounts to $1.6 \cdot 10^{-17}$ W/m^2·Hz.

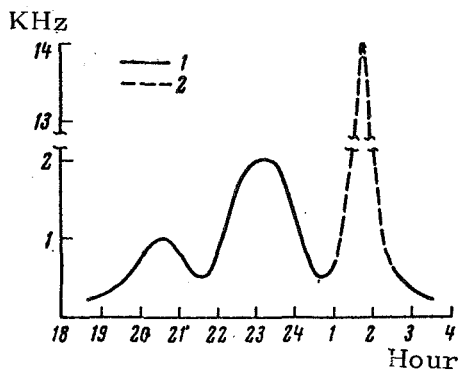

Fig. 39. Daily Curve of Bursts of the Auroral ULF Signal at a Frequency of 11 kHz (1) and a Regular Elevated ULF Background in March, 1965 (2).

Figure 39 shows the daily curve of ULF bursts at a frequency of 11 kHz relative to aurorae. Along the ordinate axis the number of bursts is plotted in relative units for March, 1965; along the abscissa the time 135° E. From 1 AM to 2:30 AM auroral bursts were not observed. During this period (1:45) the maximum amplitude of the regular noise background occurs at a frequency of 11 kHz. Evidently this is not an accidental event. Despite the fact that for several days of observations there were admittedly no aurora and the geomagnetic field was quiet, an elevation of the noise background was observed each night. On recordings the noise appears as a "platform" on which the ULF bursts relative to aurorae appear. After bursts from aurorae an insignificant decrease in the background level is usually observed.

Analysis of the recordings of the noise level on other fre-

quencies showed that the noise background at various frequencies reaches a maximum at different times; i.e., each frequency shows its own daily curve shifted from that of the neighboring frequency by a time measured in tens of minutes. At low frequencies the maximum background level is reached earlier than at high frequencies. Absorption bays on a riometer (32 MHz) during the night hours are only slightly reflected in the behavior of the ULF noise background. In the morning hours the increase in the ULF level corresponds to absorption bays, but nonsimultaneous.

Analysis of magnetophone recordings of a broad band signal in a frequency range from 700-900 Hz leads to the detection of one or more maxima of ULF radio emission. In [101, 102] the hypothesis is advanced that cyclotron proton emission is excited at these frequencies. In further experiments we hope to test this hypothesis.

Conclusion

Experimental study of continuous ULF emission of the upper atmosphere and aurorae was begun quite recently and to date it has been sporadic to a certain extent. In contrast to many other types of research, in this region there is still nothing similar to service coordinated on a world-wide scale. The volume of accumulated information is insufficient for detailed scientific analysis, and the nature of available theories is still hypothetical. Therefore, our basic task has been to create the proper, reliably-operating equipment to develop a method and to make observations with the object of explaining the characteristics of the emission itself, and especially to establish causal connections with more thoroughly studied geophysical phenomena. Achievements along these lines may be completely summarized as follows. /76

(1) Three types of recording equipment were planned, constructed and operationally tested:

(a) A multiband instrument permitting signal recording with a high degree of accuracy in amplitude at several frequencies; this apparatus produces a high sensitivity and stability but low time resolution and gives only an approximate idea of the spectrum of a broad band signal;

(b) A broad band instrument for magnetophone recording with subsequent laboratory analysis does not make it possible to simply evaluate the absolute values of the signals, has a high time resolution, permits obtaining accurate data on the spectrum, but has the substantial drawback that it cannot operate continuously;

(c) A patrol instrument representing a single-band receiver at 4 kHz with a recorder; it is simple and reliable in use and provides a true concept of the level of ULF disturbance.

(2) The conditions under which observations may be made are clarified; the influence of network, spark-like and blizzard interference and interference from longwave radio stations is studied; a means for decreasing their influence is found.

3. A classification of continuous ULF was made, basically corresponding with that commonly accepted by other authors.

4. It was found that one of the types of radio emission is a combination of short bursts, often with a smooth increase in the amplitude of maxima in the night, evening and pre-dawn hours. It is connected with the presence and activity of aurorae with a moderate small absorption in the ionosphere. Amplitudes are small and moderate.

Another type is characterized by great amplitude values and has a smoother envelope. The so-called isolated bursts and noise spots are referred to here. Isolated bursts have a clear tendency to appear at altitudes of 120-250 km at the time of sunrise or sunset when the magnetic field is quiet and there is no ionospheric absorption. Amplitudes of isolated bursts have approximately equal /77
levels and always show a sudden increase in the signal, then an almost even plateau and a smooth decrease to the undisturbed level. Noise storms have different amplitudes and different durations (up to days), but are observed with a disturbed magnetic field and often with the presence of substantial ionospheric absorption.

The third type is an elevation of the normal background level; usually it is observed as the consequence of intense noise storms or magneto-ionospheric disturbances, and they last from several hours to several days. Also, a regular elevation of the background with a maximum in the night hours exists. The envelope is completely smooth and the amplitude comparatively small; it is observed under conditions of moderate or low absorption according to riometer data.

(5) In our opinion, the first stage is connected with the emission of fast electrons producing aurorae. The region and mechanism of generation are unclear.

The second type is connected, in our opinion, with photoelectrons which are formed by solar ray emission. Isolated bursts are evidently formed under the action of X-ray emission from high-temperature regions of the solar corona under conditions of an undisturbed, weakly absorbing ionosphere at sunrise and sunset at ionospheric altitudes and noise storms by X-ray emission from bursts.

Under conditions of a quiet field, photoelectrons may exist several days as captured radiation above the same region of the Earth's surface, since their azimuthal drift is very small (energy 2-4 keV). Isolated bursts may also be the result of microbursts not causing substantial disturbances in the ionosphere and magnet-

ic field.

To give any explanation to the third type of emission is still difficult; however, it is clear that this is not thermal emission of the ionosphere heated during strong disturbances. The difference in the time of appearance of the maximum amplitude of the regular background noise at various frequencies may evidently be explained by the course in time of the change in hardness of electrons responsible for excitation of this type of emission.

Ultralow frequency emission is closely connected with processes of energy exchange between electrons and collisionless plazma, and therefore after this is studied, it may be converted into a powerful instrument for the investigation of phenomena in the upper atmosphere of the Earth.

References

1. Nauchnyy otchet po teme "Issledovaniya polyarnykh siyaniy radiometodami" (Scientific Report on the Subject "Investigation of Aurorae by Radio Means"). Fondy Yakutsk Division, Siberian Dept. of the Academy of Sciences USSR, 1965. /79
2. Yarin, V. I.: In: "Spektral'nyye, elektrofometricheskiye i radiolokatsionnyye issledovaniya polyarnykh siyaniy i svecheniya nochnogo neba" ("Spectral, Electrophotometric and Radar Investigation of Aurorae and Luminescence of the Night Sky"). Seriya "Rezul'taty MGG", Academy of Sciences USSR Press, No. 5, p. 56, 1961.
3. Ponomarev, Ye. A.: Sbornik rabot po MGG (Collection of Studies on the IGY), No. 1, Kiev University Press, 1961.
4. Dovger, V. I.: In: "Spektral'nyye, elektrofotometricheskiye i radiolokatsionnyye issledovaniya polyarnykh siyaniy i svecheniya nochnogo neba" ("Spectral, Electrophotometric and Radar Investigation of Aurorae and Luminescence of the Night Sky"). Seriya "Rezul'taty MGG", Academy of Sciences USSR Press, No. 7, p. 7, 1961.
5. Egeland, A.: Arkiv Geofys., Vol. 4, p. 103, 1963.
6. Forsyth, P. A. and E. L. Vogan: J. Atm. Terr. Phys., Vol. 10, p. 215, 1957.
7. Collins, C., P. A. Forsyth: J. Atm. Terr. Phys., Vol. 13, p. 315, 1959.
8. Curre, B. W., P. A. Forsyth, F. E. Vawater: J. Geophys. Res., Vol. 58, pp. 178-200, 1953.
9. Bagaryatskiy, B. A.: Uspekhi fizicheskikh nauk, Vol. 73, No. 2, p. 197, 1961.
10. Bagaryatskiy, B. A. and Ya. I. Fel'dshteyn: Osobennosti avroral'nykh radiootrazheniy i svyan' ikh s postoyannym magnitnym polem i ionosfernymi tokami (Peculiarities of Auroral Radio Reflections and Their Connection with the Constant Magnetic Field and Ionospheric Currents). Seriya "Rezul'taty MGG", No. 12, Nauka Press, 1965.
11. Gadsden, N.: Ann. Geophys., Vol. 15, p. 396, 1959.
12. Harrison, D. R. and C. D. Watkins: Nature, Vol. 182, p. 43, 1958.
13. Yarin, V. I.: In: "Spektral'nyye, elektrofotometricheskiye i radiolokatsionnyye issledovaniya polyarnykh siyaniy i svecheniya nochnogo neba" ("Spectral, Electrophotometric and Radar Investigation of Aurorae and Luminescence of the Night Sky"). Seriya Rezul'taty MGG", Academy of Sciences USSR Press, No. 2-3, p. 37, 1960.
14. Pogorelov, V. I.: Izvestiya Academy of Sciences, USSR, Seriya geofiz., No. 6, p. 1082, 1960.
15. Vershinin, Ye. F.: Geomagnetizm i aeronomiya, Vol. 2, p. 289, 1962.
16. Harang, L.: J. Troim. Planet. Space Sci., Vol 5, p. 33, 1961.
17. Pogorelov, V. I.: Geomagnetizm i aeronomiya, Vol. 1, p. 687, 1961.

18. Zaborshikov, F. Ya. and N. I. Fedyakina: Problemy arktiki i antarktiki, No. 2, p. 149, 1957.
19. Fel'dshteyn, Ya. I.: Sb. "Issledovaniya polyarnykh siyaniy", Academy of Sciences USSR Press, No. 4, p. 61, 1960.
20. Matsushita, S.: Sporadic Ionospherics. E. Oxford, Pergamon Press.
21. Fizika verkhney atmosfery (Physics of the Upper Atmosphere). Edited by: J. A. Ratcliff, translated from the English under the Editorship of Ya. I. Likhter, Fizmatgiz, 1963, p. 319.
22. Dzyubenko, V. I. and Yu. A. Nadubovich: Geomagnetizm i aeronomiya, No. 1, No. 4, p. 621, 1961.
23. Moore, R. K.: J. Geophys. Res., Vol. 56, p. 97, 1951.
24. Bowles, K. L.: J. Geophys. Res., Vol. 57, p. 191, 1952.
25. Bowles, K. L.: J. Geophys. Res., Vol. 59, p. 553, 1954.
26. Bailey, D. R., R. Bateman and R. C. Kirby: Proc. IRE, Vol. 43, p. 1181, 1955.
27. Havatum, H. and T. Orhang: XII Gen. Assembly of URSI, No. 178, p. 4, 1957.
28. Little, C. G., W. M. Rayton and R. R. Roof: Proc. IRE, Vol. 44, p. 992, 1956.
29. Harang, L., V. Landmark: J. Atmos. Terr. Phys., Vol. 4, p. 332, 1954.
30. Weisbrood, S. and L. Colin: Nature, Vol. 184, p. 57, 1959.
31. Guided Waves in the Troposphere. J. Res. Nat. Bur. Standards, D68, No. 5, p. 563, 1964.
32. Chamberlain, J.: Fizika polyarnykh siyaniy i izlucheniye verkhney atmosfery (Physics of Aurorae and Upper Atmosphere Radiation). Foreign Literature, 1963.
33. Mularchik, T. M. and P. V. Shcheglov: Planet. Space Sci., Vol. 10, p. 219, 1963.
34. Duquesne Sci. Counselor "Unusual Recording of Infrasonic Disturbances in the Atmosphere", Vol. 27, No. 1, p. 6, 1964.
35. Maeda, K., and T. Watanabe: J. Atm. Sci., Vol. 21, p. 15, 1964.
36. Maeda, K: Meteorol. Abhandl. Inst. Meteorol. and Geophys., Freien Univ., Berlin, Vol. 36, p. 451, 1963.
37. Maeda, K.: NASA Technical Report, NASA TR-R-141, 1962.
38. Krasovskiy, V. I.: Kosmicheskiye issledovaniya, No. 2, p. 219, 1964. /80
39. Hirao, K. and T. Muraoka: Proc. 4th Intern. Sympos. Space Technol. and Sce., Vol. 469, Tokyo, 1962.
40. Serbu, G. P. and E. J. Maier: Proc. 4th Intern. Sympos. Space Technol. and Sce., Vol. 469, 1962.
41. Ivanov-Kholodnyy, G. S.: Geomagnetizm i aeronomiya, Vol. 4, p. 417, 1964.
42. Booker, H. G.: J. Atm. Terr. Phys., Vol. 8, p. 204, 1956.
43. Pogorelov, V. I.: Geomagnetizm i aeronomiya, Vol. 2, p. 168, 1962.
44. Wickersham, A. F.: J. Geophys. Res., Vol. 69, p. 457, 1964.
45. Korotin, A. B. and M. I. Pudovkin: In: "Spektral'nyye, elektrofotometricheskiye i radiolokatsionnyye issledovaniya

polyarnykh siyaniy i svecheniya nochnogo neba" ("Spectral, Electrophotometric and Radar Investigation of Aurorae and Luminescence of the Night Sky"). Seriya "Rezul'taty MGG", Academy of Sciences USSR Press, No. 6, p. 37, 1960.
46. Biondi, M. A.: Ann. Geophys., Vo. 20, p. 34, 1964.
47. Mitra, A. P.: J. Geophys. Res., Vol. 69, p. 4067, 1964.
48. Pogorelov, V. I.: Candidates Dissertation, Institute of Physica of the Atmosphere, Academy of Sciences USSR, 1963.
49. Starkov, G. V.: Geomagnetizm i aeronomiya, No. 5, p. 177, 1965.
50. Villars, F. and H. Feshbach: J. Geophys. Res., Vol. 68, p. 1303, 1963.
51. Whitehead, J. D.: J. Atmos. and Terr. Phys., Vol. 25, p. 167, 1963.
52. Buneman, O.: Phys. Rev. Letters, Vol. 10, p. 285, 1963.
53. Vedenov, A. A., Ye. P. Velikhov and R. Z. Sagdeyev: Uspekhi fizicheskikh nauk, Vol. 53, p. 701, 1961.
54. Maeda, K., T. Tsuda and H. Maeda: Rept. Ionosphere and Space Res., Vol. 17, p. 147, Japan, 1963.
55. Farley, D. T., Jr.: J. Geophys. Res., Vol. 68, p. 6083, 1963.
56. Maeda, K., T. Tsuda and H. Maeda: Phys. Rev. Letters, Vol. 11, p. 406, 1963.
57. Gershman, B. N.: Geomagnetizm i aeronomiya, Vol. 3, p. 878, 1963.
58. Farly, D. T.: Phys. Rev. Letters, Vol. 10, p. 279, 1963.
59. Knox, F. B.: J. Atm. Terr. Phys., Vol. 26, p. 239, 1964.
60. McIlvaine, K.: Pryamye izmereniya chastits, vyzyvayushchikh vidimyye polyarnyye siyania (Direct Measurement of Particles Causing Visible Aurorae). In the Collection "Issledovaniya verkhney atmosfery s pomoshch'yu raket i sputnikov" (Investigation of the Upper Atmosphere with the Aid of Rockets and Satellites), Edited by G. A. Ivanov-Kholodnyy, Foreign Literature, 1961.
61. Massey, G. and Ye. Barhop: Elektronnyye i ionnyye stolknoveniya (Electron and Ion Collisions). Foreign Literature Press, 1959.
62. Gambosh, G.: Statisticheskaya teoriya atoma i yeye primeneniye (Statistical Theory of the Atom and Its Application). Foreign Literature Press, 1951.
63. Hartz, T. R.: Canad. J. Phys., Vol. 36, p. 667, 1958.
64. Nicols, B.: Proc. IRE, Vol. 47, p. 245, 1959.
65. Presnell, R. J., R. L. Leadebrand, A. M. Peterson, R. B. Dyce, J. C. Schbbohm and M. R. Berg: J. Geophys. Res., Vol. 64, p. 1179, 1959.
66. Flood, W. A.: J. Geophys. Res., Vol. 65, p. 2261, 1960.
67. Owren, L.: High Latitude Radio Aurora. XIII Gen. Assembly of URSI, Commission III, London, 1960.
68. Harang, L. and J. Troim: Planet. Space Sci., Vol. 5, p. 33, 1961.
69. Leonard, R. S.: Sci. Rept., No. 9, College, Alaska, 1961.
70. Seed, T. J.: J. Geophys. Res., Vol. 63, p. 517, 1958.
71. Prudkovskaya, O. V.: Doklady Academy of Sciences USSR, Vol. 117, No. 4, p. 601. 1967.

72. Birfelb, Ya. G.: Izvestiya Academy of Sciences USSR, Seriya geofiz., No. 4, p. 543, 1957.
73. "Voprosy teorii plazmy" (Problems of Plasma Theory). Collection Edited by M. A. Leontovich, Gosatomizdat, 1963, p. 221.
74. Alpert, Ya. L.: Rasprostraneniye radiovoln i ionosfera (Propagation of Radio Waves and the Ionosphere). Academy of Sciences USSR Press, 1960.
75. Vlasov, A. A.: "Teoriya mnogikh chastits" (Theory of Many Particles). State Technical and Theoretical Press, 1950.
76. Chivers, H. J. A. and H. W. Wells: Nature, Vol. 183, No. 4669, 1959.
77. Forsyth, P. A., Wm. Petrie and B. W. Currie: Nature, Vol. 164, p. 453, 1949.
78. Hartz, T. R.: Canad. J. Phys., Vol. 36, No. 6, pp. 677-682, 1958.
79. Dowden, R. L.: Austral. J. Phys., Vol. 15, No. 1, pp. 114-119, 1962.
80. Chapman, F. W. and R. C. V. Macario: Nature, Vol. 177, p. 930, 1956.
81. Taylor, W. L.: J. Geophys. Res., Vol. 65, pp. 1933-1938, 1960.
82. Leiphart, J. P., R. W. Zeek, L. S. Breace and E. Toth: Proc. Inst. Radio Engrs., Vol. 50, pp. 6-17, 1962.
83. Mechtly, E. A. and S. A. Bowhill: J. Geophys. Res., Vol. 65, p. 3501, 1960.
84. Ellis, G. R. A.: J. Geophys. Res., Vol. 66, pp. 19-23, 1961.
85. Gurnett, D. A. and B. J. O'Brien: J. Geophys. Res., Vol. 69, pp. 65-89, 1964.
86. Kellog, P.: Planet. Space Sci., Vol. 10, p. 165, 1963.
87. Ellis, G. R. A., D. C. Cartwright, J. R. V. Croves: Nature, Vol. 84, p. 1391, 1959.
88. Ellis, G. R. A.: Planet. Space Sci., Vol. 1, pp. 253-258, 1959.
89. Gershman, B. N. and V. A. Ugarov: Rasprostraneniye i generatsiya nizkochastotnykh elektromagnitnykh voln v verkhney atmosfere (Propagation and Generation of Low-Frequency Electromagnetic Waves in the Upper Atmosphere). Uspekhi fizicheskikh nauk, Vol. 22, No. 2, pp. 235-270, 1960.
90. Allcock, G. McK.: Austral. J. Phys., Vol. 10, pp. 286-298, 1957.
91. Ellis, G. R. A.: J. Atmos. Terr. Phys., Vol. 10, pp. 302-306, 1957.
92. Gallet, R. M., R. A. Helliwell: J. Res. NBS, Vol. 63D, pp. 21-27, 1959. /81
93. Faynberg, Ya. B.: Vzaimodeystviye puchkov zaryazhennykh chastits s plazmoy (Interaction of Bundles of Charged Particles with Plasma). In the Collection: "Fizika plazmy i problemy upravlyayemogo termoyadernogo sinteza" (Plasma Physics and Problems of Controllable Thermonuclear Synthesis), Academy of Sciences Ukrainian SSR Press, No. 2, p. 88, 1963.
94. Shapiro, V. D.: Zhurnal experimental'noy i teoreticheskoy fiziki, Vol. 44, p. 613, 1963.

95. Fedorchenko, V. D., B. N. Rutkevich, V. I. Muratov and B. M. Chernyy: In the Collection: "Fizika plazmy i problemy upravlyayemogo termoyadernogo sinteza" (Plasma Physics and Problems of Controllable Thermo-Nuclear Synthesis). Academy of Sciences Ukrainian SSR Press, No. 2, p. 133, 1963.
96. Ponomarev, Ye. A. and Ye. F. Vershinin: Ob ul'tranizkochastotnom izluchenii polyarnykh siyaniy (Concerning Ultralow Frequency Emission of Aurorae). Vol. 3, No. 3, 1963.
97. Kolmakov, M. V. and I. A. Zelentsov: O konstruktsii induktsionnykh datchikov dlya magnitotellurichеskikh issledovaniy (The Construction of Induction Detectors for Magneto-Telluric Investigation). Izvestiya Academy of Sciences USSR, Seriya geofiz., No. 10, pp. 1381-1396, 1962.
98. Dowden, R. L.: Ionospheric Prediction Service Research Report, 1963.
99. Ratcliff, J. A.: Fizika verkhney atmosfery (Physics of the Upper Atmosphere). Translated from the English, Edited by Ya. I. Lakhter, Fizmatgiz, 1963.
100. Mulyarchik, T. M.: Kosmicheskiye issledovaniya, Vol. 2, No. 2, p. 266, 1964.
101. Gustafsson, G., A. Egeland and J. Aarons: J. Geophys. Res., Vol. 65, pp. 2749-2758, 1960.
102. Aarons, J., G. Gustafsson and A. Egeland: Nature, Vol. 185, pp. 148-151, 1960.

Translated for the National Aeronautics and Space Administration by:
Aztec School of Languages, Inc.
Research Translation Division (708)
Maynard, Massachusetts and McLean, Virginia
NASW-1692

NASA-Langley, 1970 —— 13 F-618

NATIONAL AERONAUTICS AND SPACE ADMINISTRATION
WASHINGTON, D.C. 20546

OFFICIAL BUSINESS

FIRST CLASS MAIL

POSTAGE AND FEES PAID
NATIONAL AERONAUTICS A
SPACE ADMINISTRATION

POSTMASTER: If Undeliverable (Section 15
Postal Manual) Do Not Reu

"The aeronautical and space activities of the United States shall be conducted so as to contribute . . . to the expansion of human knowledge of phenomena in the atmosphere and space. The Administration shall provide for the widest practicable and appropriate dissemination of information concerning its activities and the results thereof."

—NATIONAL AERONAUTICS AND SPACE ACT OF 1958

NASA SCIENTIFIC AND TECHNICAL PUBLICATIONS

TECHNICAL REPORTS: Scientific and technical information considered important, complete, and a lasting contribution to existing knowledge.

TECHNICAL NOTES: Information less broad in scope but nevertheless of importance as a contribution to existing knowledge.

TECHNICAL MEMORANDUMS: Information receiving limited distribution because of preliminary data, security classification, or other reasons.

CONTRACTOR REPORTS: Scientific and technical information generated under a NASA contract or grant and considered an important contribution to existing knowledge.

TECHNICAL TRANSLATIONS: Information published in a foreign language considered to merit NASA distribution in English.

SPECIAL PUBLICATIONS: Information derived from or of value to NASA activities. Publications include conference proceedings, monographs, data compilations, handbooks, sourcebooks, and special bibliographies.

TECHNOLOGY UTILIZATION PUBLICATIONS: Information on technology used by NASA that may be of particular interest in commercial and other non-aerospace applications. Publications include Tech Briefs, Technology Utilization Reports and Notes, and Technology Surveys.

Details on the availability of these publications may be obtained from:

SCIENTIFIC AND TECHNICAL INFORMATION DIVISION

NATIONAL AERONAUTICS AND SPACE ADMINISTRATION

Washington, D.C. 20546